FOREWORD

This report was prepared by the Engineering Experiment Station of the Georgia Institute of Technology, 225 North Avenue, N. W., Atlanta 13, Georgia, under USAF Contract No. AF 33(616)-6028 and Supplemental Agreement No. 3(59-1432). This contract was initiated under Project No. 8-(8-4150), Task No. 41709. The work was administered under the direction of the Advanced Solid State Section, Electronic Technology Laboratory, Wright Air Development Division, with Mr. John M. Blasingame, Jr., as project engineer. This research is a part of the Composite Molecular Circuits and Systems Research Program.

This report covers work conducted between 1 October 1959 and 30 September 1960, and is related to WADC TR 59-737 which also contains a compilation of technical articles on the same program.

This project was directed by Dr. Edwin J. Scheibner, Research Professor of Physics. Others who have participated in the conduct of this work are Dr. Vernon Crawford, Head, Physics Branch, and Professor of Physics; Mr. Frederick B. Dyer, Research Assistant; Dr. James R. Stevenson, Research Associate, Associate Professor of Physics; Dr. William C. Simpson, Research Associate, Associate Professor of Physics; Mr. C. Robert Meissner, Research Engineer; Mr. Robert M. Nicklow, Graduate Research Assistant; and Mr. L. W. Ross, Assistant Research Engineer.

ABSTRACT

The investigation of various solid-state phenomena and effects which might have an application in electronic systems was continued. In the 11 technical articles presented in this report 14 phenomena and effects are discussed. An ultra-high vacuum system designed for the deposition of high-purity thin films is described. One hundred and fifty-seven annotated articles on various solid-state phenomena and effects are included.

PUBLICATION REVIEW

The content of this report represents the scientific findings of an Air Force sponsored program. It does not direct any specific application thereof. The report is approved for publication to achieve an exchange and stimulation of ideas.

FOR THE COMMANDER:

Robert D. Larson

ROBERT D. LARSON
Chief, Advanced Techniques Branch
Electronic Technology Laboratory

TABLE OF CONTENTS

LIST OF FIGURES

SECTION I

INTRODUCTION

Under Contract No. AF 33(616)-6028 and Supplemental Agreement No. 3(59-1432), the Georgia Institute of Technology has been participating in the Composite Molecular Circuits and Systems Research Program of the Wright Air Development Division. During the period from July 1, 1958, to September 1, 1959, a research team was engaged at Georgia Institute of Technology in surveying various solid state phenomena and effects. WADC Technical Report No. 59-737 of October 1959 contains a compilation of technical articles on a large number of effects.

Since October 1959, the effort has continued, in general, the previous work. The specific objectives were:

(1) To provide a comprehensive literature survey to point out pertinent articles of interest to researchers working on composite molecular circuits.

(2) To continue the survey and investigation of all known solid-state physical phenomena and effects, placing special emphasis on the less known effects.

(3) To conduct a general theoretical analysis of properties of solid-state materials to focus attention on the possibilities of yet undiscovered phenomena in new materials.

In addition, after discussions with the sponsor, it was agreed that experimental work on some of the effects could be performed in order to clarify information on known effects or to obtain information on new ones.

Section II contains 11 discussions on specific solid-state effects. The articles on the thermoelectric effects and the Zener effect supplement those of the same title appearing in WADC Technical Report No. 59-737. The others are on effects not previously discussed.

An ultra-high vacuum system for the preparation and testing of high-purity thin films at vacua of the order of 10^{-8} Torr. is described in Section III. The material of this section was presented at the Sixth National Vacuum Symposium, October 12-14, 1960, and will be published in the transactions of that meeting.

One hundred and fifty-seven annotated articles comprise Section IV. These articles are arranged according to various groups of solid state effects for maximum utility. Adequate cross-referencing is included to relate articles which may belong to more than one group.

Manuscript released by the authors October 1960 for publication as a WADD Technical Report.

SECTION I
TECHNICAL ARTICLES

1. EXTRAORDINARY HALL EFFECT

In ferromagnetic materials the Hall effect depends not only on the applied magnetic field but also on the magnetization of the sample. Below saturation the Hall voltage is proportional to the magnetization while above saturation the Hall voltage continues to increase slightly with applied field. This behavior suggests an empirical relation of the following form:

$$e_y = R_o H + R_1 M \tag{1.1}$$

where e_y is the Hall field per unit current density in the x-direction, H is the applied magnetic field in the z-direction, and M is the magnetization of the sample in the z-direction. R_o and R_1 are, respectively, the ordinary and extraordinary Hall coefficients. The extraordinary effect is often much larger than the ordinary effect, and it depends strongly on temperature or composition of the ferromagnetic sample.

Pugh and Rostoker[1] have reviewed the experimental data on the Hall effect in iron, nickel, cobalt and alloys of nickel with cobalt or copper. In analyzing the data they have assumed that the Hall effect in ferromagnetic metals may be considered similar to that in other metals if one replaces the external field by an "effective" field.

$$H_{eff} = H + 4\pi M\alpha \tag{1.2}$$

where α is an arbitrary parameter. With data available on the temperature dependence of the Hall effect in nickel, Pugh and Rostoker were able to plot the behavior of the parameter α as a function of temperature as shown in Figure 1.

Any proposed theory for the extraordinary effect then has to explain the large magnitude of α at the Curie point and the temperature dependence of α.

Smit[6] also tabulated data on the Hall effect in ferromagnetic metals and alloys; from measurements at different temperatures, he suggested that the effect is closely related to the resistivity of the material. Actually, recent theoretical studies[2,3,4] have shown that the extraordinary Hall coefficient contains a factor equal to the square of the ordinary resistivity in good agreement with experimental results. It is of interest to note that the resistivity of ferromagnetic metals below the Curie point behaves differently with temperature than the resistivity of non-ferromagnetic metals.

Wilson[5] discusses the question of the resistivity of ferromagnetic metals in relation to a theory for the conductivity of the transition elements. The transition elements have their valence electrons divided between a broad s-band and a narrow, high-level density, d-band, but, because of the large effective mass of the d-electrons, only the s-electrons contribute to the

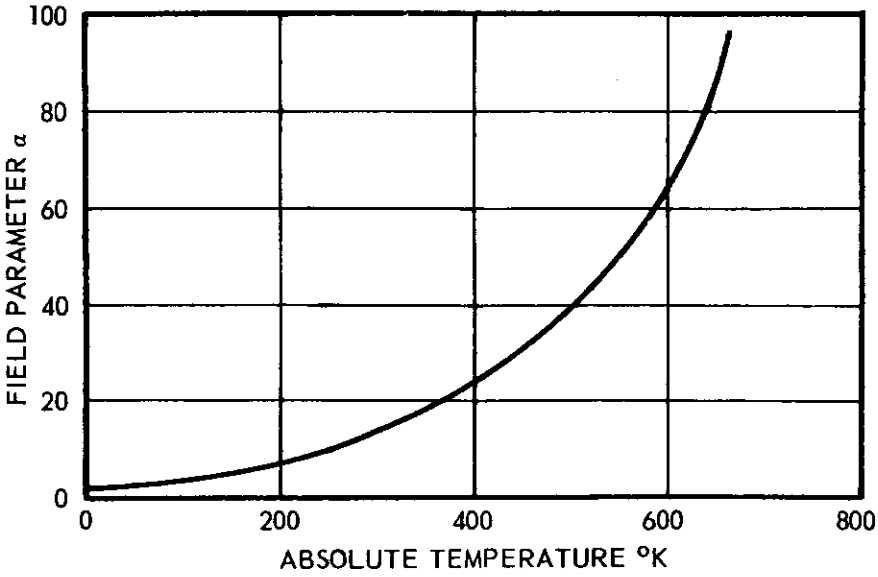

Figure 1. Temperature Dependence of the Field Parameter α, for Nickel.

conductivity. The vacant levels in the d-band provide energy levels into which the s-electrons can be scattered (s-d transitions), where normally only the scattering into s-levels (s-s transitions) need be considered. In a simplified version of the theory Wilson assumes that the energy bands for the transition elements have the form shown in Figure 2 and described by the following equations:

$$E_s(\vec{k}) = 1/2\hbar^2 |\vec{k}|/m_s, \qquad E_d(\vec{k}) = A - 1/2\hbar^2 |\vec{k}|^2/m_d \ (A>0) \qquad (1.3)$$

where $\hbar$ is Plank's constant divided by 2π, k is the wave number of an energy state and m_s and m_d are effective masses of s- and d-electrons respectively.

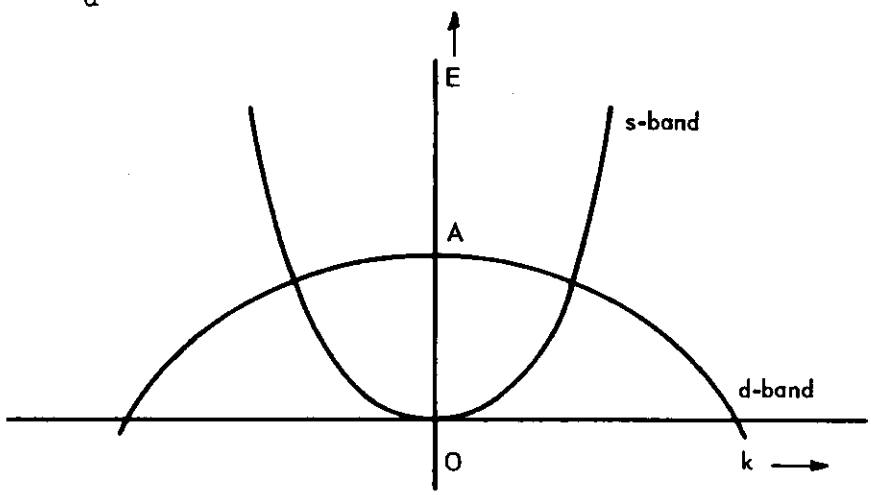

Figure 2. Energy Band Model for Transition Elements.

The calculations show that the transition probability for an s-electron being scattered into the d-band is about ten times the normal probability. This additional scattering accounts roughly for the poor conductivity of the transition elements at room temperature. For the ferromagnetic metals it is assumed that the resistance above the Curie point is also due mainly to s-d transitions. Below the Curie point, however, spontaneous magnetization occurs and the number of vacant d-levels change with temperature. The dependence of the s-d transition probability on temperature depends on the distribution of the d-electrons in the levels. For example, if the spin is not changed during a scattering process then only half of the s-electrons can be scattered into d-levels when all the d-levels of one spin are occupied. Therefore, one would expect the resistance to decrease with decreasing temperature.

The extraordinary Hall coefficient varies as the square of the ordinary resistivity for many ferromagnetic metals and alloys. Karplus and Luttinger[2] presented a theory based on spin-orbit interactions in which just such a resistivity dependence was predicted. They show that a transverse current results which is perpendicular to both the electric field and the magnetization and which vanishes in the absence of spin-orbit coupling. If we write this current as

$$J_y = r\, M_z\, E_x \tag{1.4}$$

where r is intricately connected with the Bloch functions of electrons in a ferromagnetic material, then the Hall field which prevents current flow in the y-direction is

$$E_y = -\rho\, J_y \tag{1.5}$$

or the Hall field per unit current density in the x-direction is

$$e_y = E_y/J_x = -\rho r\, M_z\, E_x/J_x = -\rho^2\, r\, M_z \quad . \tag{1.6}$$

The Karplus and Luttinger theory was criticized by Smit[6] who pointed out that additional scattering effects should be considered. Subsequently, Luttinger[7] re-examined the theory of the effect and, because of the questions raised on the earlier work, treated the case of impurity scattering rigorously according to the transport theory of Kohn and Luttinger.[8] At the sacrifice of simple assumptions such as a slowly varying scattering potential, a simple band, and very few conduction electrons, he arrived at an explanation for the effect but found that the extraordinary coefficient should vary as the resistivity and not as the resistivity squared. More recently, Adams,[9] in a critical review of the theories of the extraordinary Hall effect, indicated that if the important scattering interaction were phonon scattering, then the coefficient would vary as the square of the resistivity (this conclusion was also obtained by Smit[3]). For alloys, however, the scattering interaction would be more complicated and one could not predict the exact dependence on resistivity without further theoretical work.

The Hall effect has also been observed in thin ferromagnetic films.[10,11,12] In the paper by Coren and Juretschke, for instance, data are presented which show that the ρ^2 dependence of the extraordinary coefficient is observed just as for the bulk material.

E. J. Scheibner

REFERENCES

1. E. M. Pugh and N. Rostoker, "Hall Effect in Ferromagnetic Materials," Rev. Mod. Phys. 25, 151 (1953).

2. R. Karplus and J. M. Luttinger, "Hall Effect in Ferromagnetics," Physical Review 95, 1154 (1954).

3. J. Smit, "The Spontaneous Hall Effect in Ferromagnetics. II.," Physica 24, 39 (1958).

4. C. Strachan and A. M. Murray, "Spin-Orbit Coupling and the Extraordinary Hall Effect," Nature 181, 1260 (1958); Prac. Phys. Soc. Land 73, 433 (1959).

5. A. H. Wilson, "The Theory of Metals," Cambridge University Press, London 273 (1953).

6. J. Smit, "The Spontaneous Hall Effect in Ferromagnetics. I.," Physica 21, 877 (1955).

7. J. M. Luttinger, "Theory of the Hall Effect in Ferromagnetic Substances," Physical Review 112, 739 (1958).

8. W. Kohn and J. M. Luttinger, "Quantum Theory of Electrical Transport Phenomena," Physical Review 108, 590 (1957).

9. E. N. Adams and E. I. Blount, "Energy Bands in the Presence of an External Force Field. II. Anomalous Velocities," J. Phys. Chem. Solids 10, 286 (1959).

10. G. Goureaux, P. Huet, and A. Colombani, "Thin Ferromagnetic Films. Hall Effect in Thin Films of Nickel," Comptes Rendus 247, 189 (1958).

11. L. Reimer, "Measurements of the Hall Effect on Ferromagnetic Nickel Layers," Z. Physik 150, 277 (1958).

12. R. Coren and H. J. Juretschke, "Hall Effect and Ferromagnetism of Very Thin Nickel Films," J. Appl. Phys. 28, 806 (1957).

2. MAGNETO-OPTIC EFFECTS

In our Technical Report of October 1959, articles were presented on the cyclotron resonance effect and the de Haas-van Alphen effect. These articles provide the introduction to two related effects, the interband magneto-optic (IMO) effect and the impurity magneto-optic (IPMO) effect.

A. Interband Magneto-Optic (IMO) Effects

The IMO effect is the difference caused by a magnetic field in the interband optical absorption of a semiconductor or insulator. To understand the process, Figure 16 of our Technical Report of October 1959 is reproduced as Figure 3 of this report. Figure 3(a) shows some parameters useful in describing the spherical conduction band of a solid. No magnetic field is present in Figure 3(a). The distribution of allowable energy states increases as the one-half power of the energy above the bottom of the conduction band. The allowable energy states above the bottom of the conduction band are given by equation (2.1),

$$E_c(k) = \frac{\hbar^2}{2m_c^*}(k_x^2 + k_y^2 + k_z^2), \tag{2.1}$$

where $\hbar$ is Planck's constant divided by 2π

m_c^* is the effective mass of the charge carriers in the conduction band

k_x, k_y, and k_z are the components of the propagation vectors of the charge carriers in the conduction band and

$\hbar k_x$ is the component of crystal momentum of a charge carrier in the x-direction. As seen from equation (2.1), the curve of E vs k_x, k_y, or k_z is a parabola as shown in Figure 3(a).

If a magnetic field is applied in the z-direction, the momentum of the charge carriers in the z-direction will not be changed. The component of angular momentum along the z-axis will be quantized[1,2,3] and for a given value of linear momentum in the z-direction, a discreteness in energies allowed to the charge carriers will appear. Since the total number of allowed states is not changed, the discrete levels associated with a given value of linear momentum in the z-direction are highly degenerate. These allowed energy states for a given value of linear momentum in the z-direction are spaced at intervals of energy, ΔE, given by equation (2.2),

$$\Delta E = \frac{hBe}{m_c^*} = \hbar\omega_c, \tag{2.2}$$

where B is the magnetic induction

e is the electronic charge

ω_c is the cyclotron resonance angular frequency for charge carriers in the conduction band. For a given value of linear momentum in the z-direction

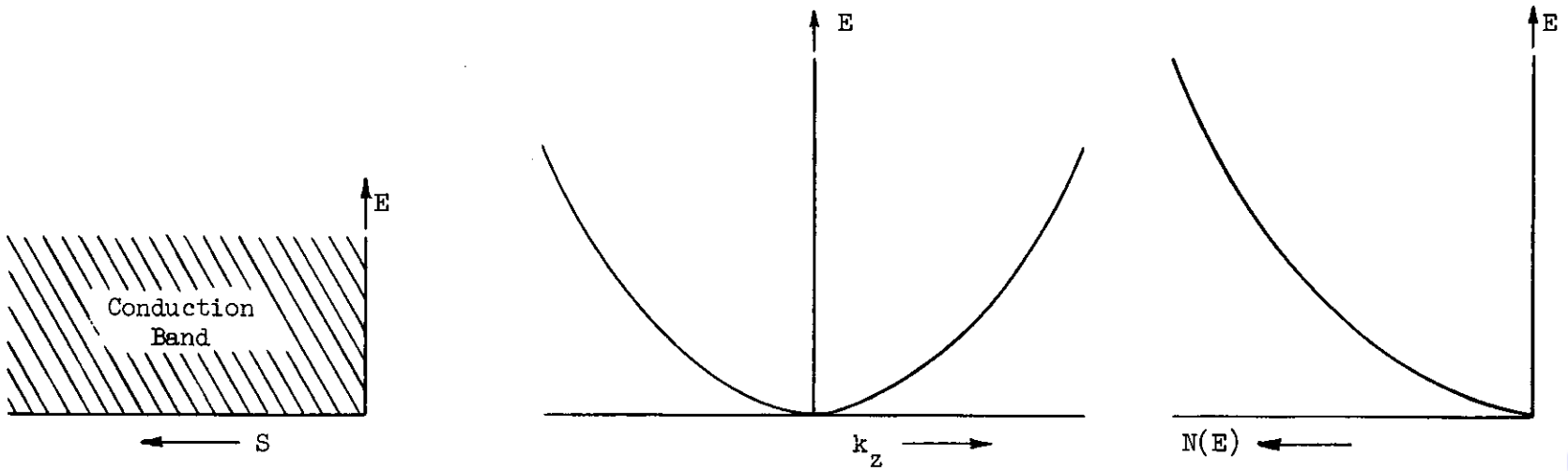

Figure 16 (a)

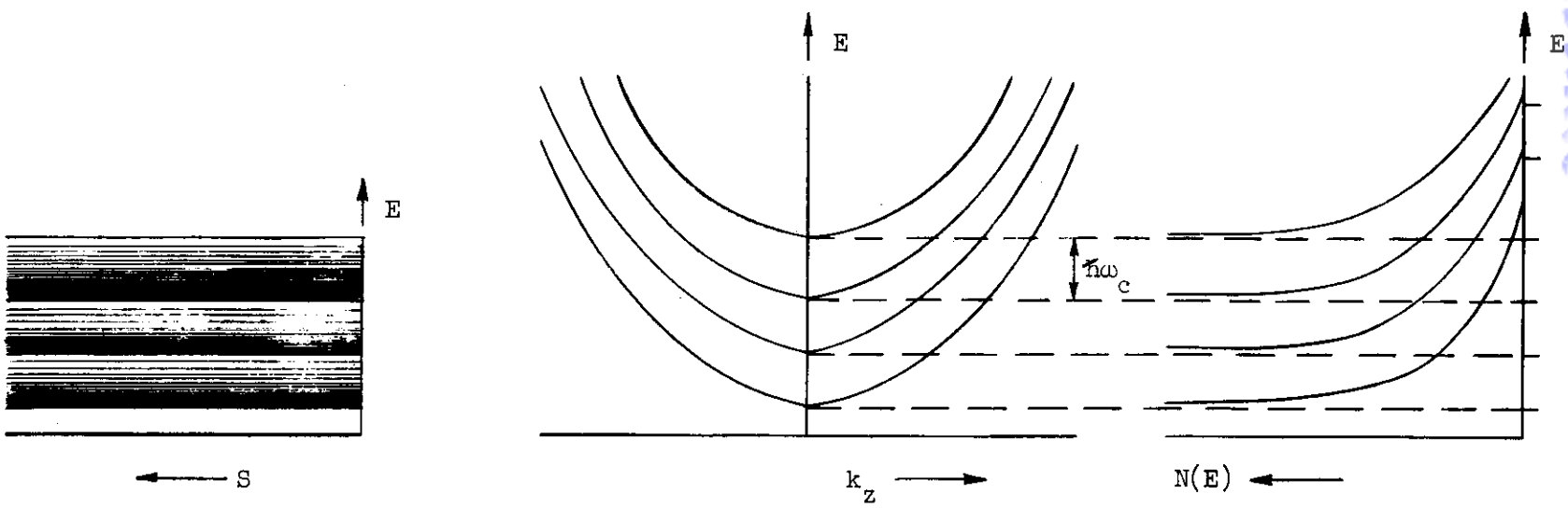

Figure 3. The Effect of a Magnetic Field in the z-Direction on a Spherical Conduction Band of a Solid.

the density of states decreases as $E^{-1/2}$ instead of increasing as $E^{1/2}$. Figure 3(b) shows the effect of the magnetic field on the parameters shown in Figure 3(a).

If the valance band of a semiconductor or insulator is also assumed to be spherical, the magnetic field will have the same effect as outlined above except that the charge carriers are now holes instead of electrons. Figure 4 shows the energy versus k_z curves for both the conduction bands and the valance bands of the same solid. Since the effective mass of the charge carriers in the valence band will be different than the effective mass in the conduction band the cyclotron resonance frequency will be different and the separation between energy levels for a given magnetic field will be different. The allowable energy states[4,5,6] in the conduction band for a magnetic field along the z-direction are given by equation (2.3),

$$E_c\ (k_z,\ l_c) = E_{cv} + \hbar\omega_c\ (l_c + \tfrac{1}{2}) + \frac{\hbar^2 k_z^2}{2m_c^*}\ , \qquad (2.3)$$

where E_c is the energy above the top of the valence band, E_{cv} is the energy gap between valence band and conduction band in the absence of a magnetic field, l_c is the Landau magnetic quantum number and is a positive integer or zero, and the other quantities have the same significance as in equation (2.1). The allowed energy states[4,5,6] in the valence band are given by equation (2.4),

$$E_v(k_z,\ l_v) = \hbar\omega_v(l_v + \tfrac{1}{2}) - \frac{\hbar^2\ k_z^2}{2m_v^*}\ , \qquad (2.4)$$

in which E_v is energy measured relative to the top of the valence band for zero magnetic field, m_v^* is the effective mass of the charge carriers in the valence band, and ω_v differs from ω_c because of the difference in the effective mass in the two bands.

For the case of the simple spherical bands considered, the optical transitions in the case of zero magnetic field should begin to take place for $k_z = k_x = k_y = 0$ whenever electromagnetic energy equal to $E_c - E_v = E_{cv}$ is incident on the material. When a magnetic field is applied the threshold of absorption is given by $k_z = 0$ and $l_c = 0$ which leads to equation (2.5),

$$E_c - E_v = E_{cv} + \frac{1}{2}\hbar\omega_c + \frac{1}{2}\hbar\omega_v . \qquad (2.5)$$

because of the quantization introduced by the magnetic field, optical transitions between the valence band and the conduction band will be subject to particular selection rules. The rules for the simple case outlined above are $\Delta l = 0$, and $\Delta k_z = 0$. In addition, another quantum number specifying the component of angular momentum along the direction of the applied magnetic field is introduced. This quantum number, M_J, is subject to selection rules which

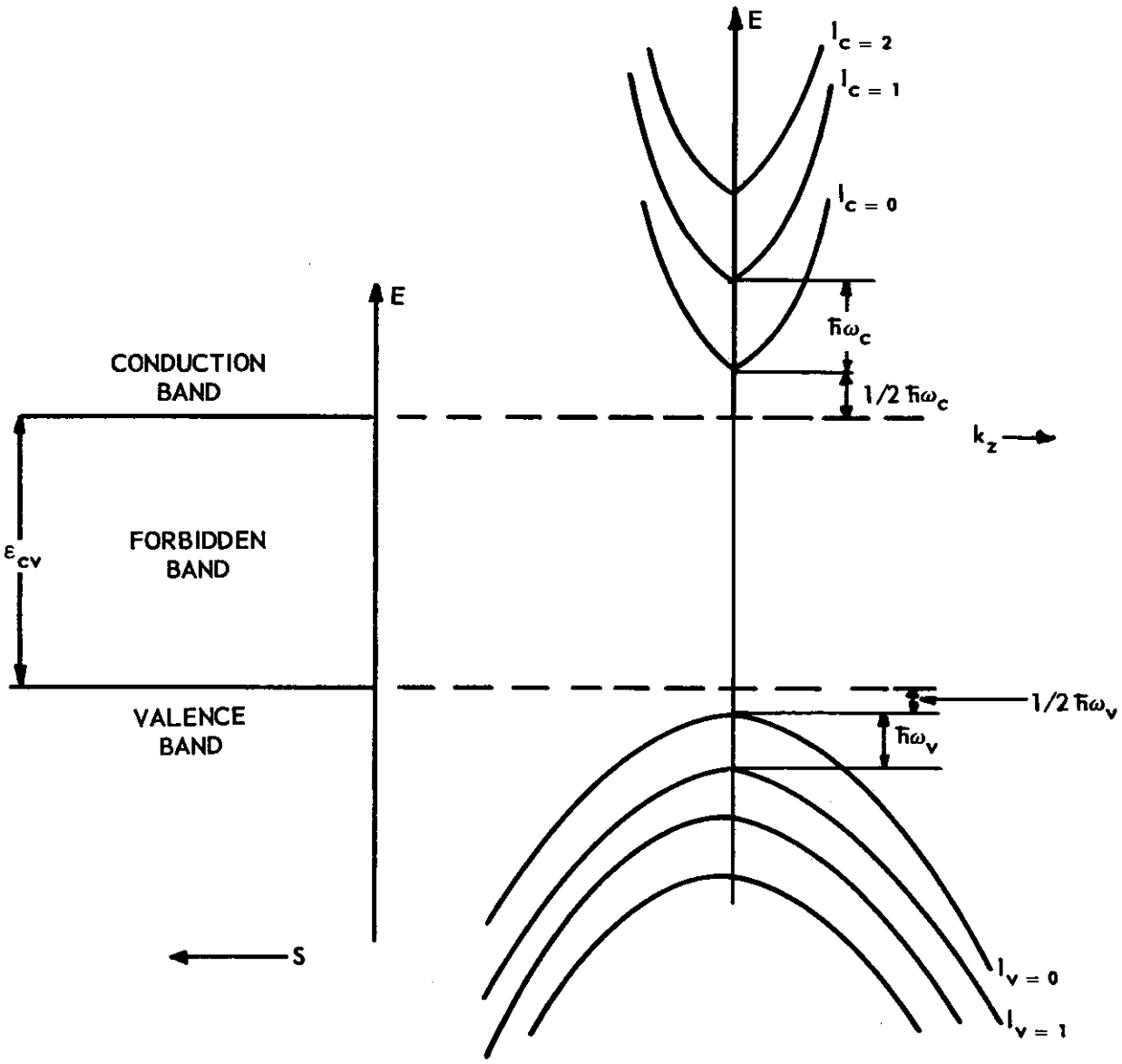

Figure 4. The Effect of a Magnetic Field in the z-Direction on the Spherical Conduction and Valence Bands of a Semiconductor.

depend on the orientation of the electric vector of the incident radiation. $\Delta M_J = 0$ is the rule for the electric vector parallel to the applied magnetic field. For a more detailed analysis of the selection rules and for departures from spherical bands, the reader is referred to the literature.[5,6]

B. Impurity Photoionization Magneto-Optic (IPMO) Effect

The analysis of the IPMO[5] effect follows closely the analysis given above for the IMO effect except that transitions between an impurity level and either the valence band or the conduction band are considered. The quantization of the valence band and conduction band occurring when a magnetic field is applied gives rise to a structure in the absorption due to the presence of the impurity level.

J. R. Stevenson

REFERENCES

1. D. Shoenberg, "The de Haas-van Alphen Effect," Progress in Low Temperature Physics 2, (New York: Interscience Publishers, 1957).

2. F. Seitz, Modern Theory of Solids, (New York: McGraw-Hill, 1940), p. 580.

3. R. E. Peierls, Quantum Theory of Solids, (London: Oxford University Press, 1955).

4. E. Burstein, G. S. Picus and H. A. Gebbie, "Report of NRL Progress," (Washington: Department of the Navy, August 1956).

5. E. Burstein, G. S. Picus, R. F. Wallis, F. Blatt, "Magneto-Optic Studies of Energy Band Structure in Semiconductors," in A Decade of Basic and Applied Science in the Navy, (Washington: Department of the Navy, March 1957).

6. E. Burstein, G. S. Picus, R. F. Wallis, F. Blatt, "Zeeman Magneto-Optic Studies of Interband Transitions in Semiconductors," Physical Review 113, 15 (1959).

3. THE MAGNETIC BARRIER LAYER EFFECT

The magnetic barrier layer effect is the rectification phenomena which occurs in a slab of intrinsic semiconductor when it is placed in crossed electric and magnetic fields and when opposite sides are treated to give widely different surface recombination velocities.

A qualitative explanation of the principle was made by Moss.[1] In an intrinsic specimen with no magnetic field, the charge carrier flow is dependent upon the applied electric field, as shown in Figure 5(a). In this case there is no rectification, the carrier distribution is uniform in the specimen, and the a-c response curve is constant with zero slope. See Figures 5(d) and (g) respectively. With a magnetic field in quadrature with the electric field, both types of charge carriers are deflected to one side of the specimen, as in the Hall effect, so that the carrier concentration is nonuniform. If the two sides of the specimen have markedly different surface recombination velocities, the carrier distributions will change considerably as the electric field is reversed, as suggested by comparing Figures 5(b) and (e) with Figures 5(c) and (f). Rectification effects are then evident as in Figure 5(h).

A quantitative theoretical treatment of the effect is formidable, and simplifying conditions are usually imposed. For example, Moss treats the steady state case of an intrinsic specimen where $n = p = n_i + \Delta p$. He makes the assumptions that (1) there is no net flow of current in the direction of the Hall field and (2) there is negligible space charge. Thus, the current density in the y-direction due to holes is

$$J_y^+ = -eD \frac{d}{dy} \Delta p - eE_x \theta_p \mu_n (P_i + \Delta p) \qquad (3.1)$$

Substituting Equation (3.1) into the continuity equation:

$$-\frac{d}{dy} J_y^+ = e \frac{\Delta p}{T} , \qquad (3.2)$$

renders:

$$\frac{d^2}{dy^2} \Delta p + \frac{\theta_p E_x \mu_n}{D} \frac{d}{dy} \Delta p - \frac{\Delta p}{L^2} = 0 \qquad (3.3)$$

where D is the ambipolar diffusion constant, and $L = (Dt)^{1/2}$ is ambipolar diffusion length. Moss defines the boundary conditions to be:

$$y = a/2, \qquad J_y^+ = -eS_1 \Delta p$$
$$y = -a/2, \qquad J_y^+ = eS_2 \Delta p \qquad (3.4)$$

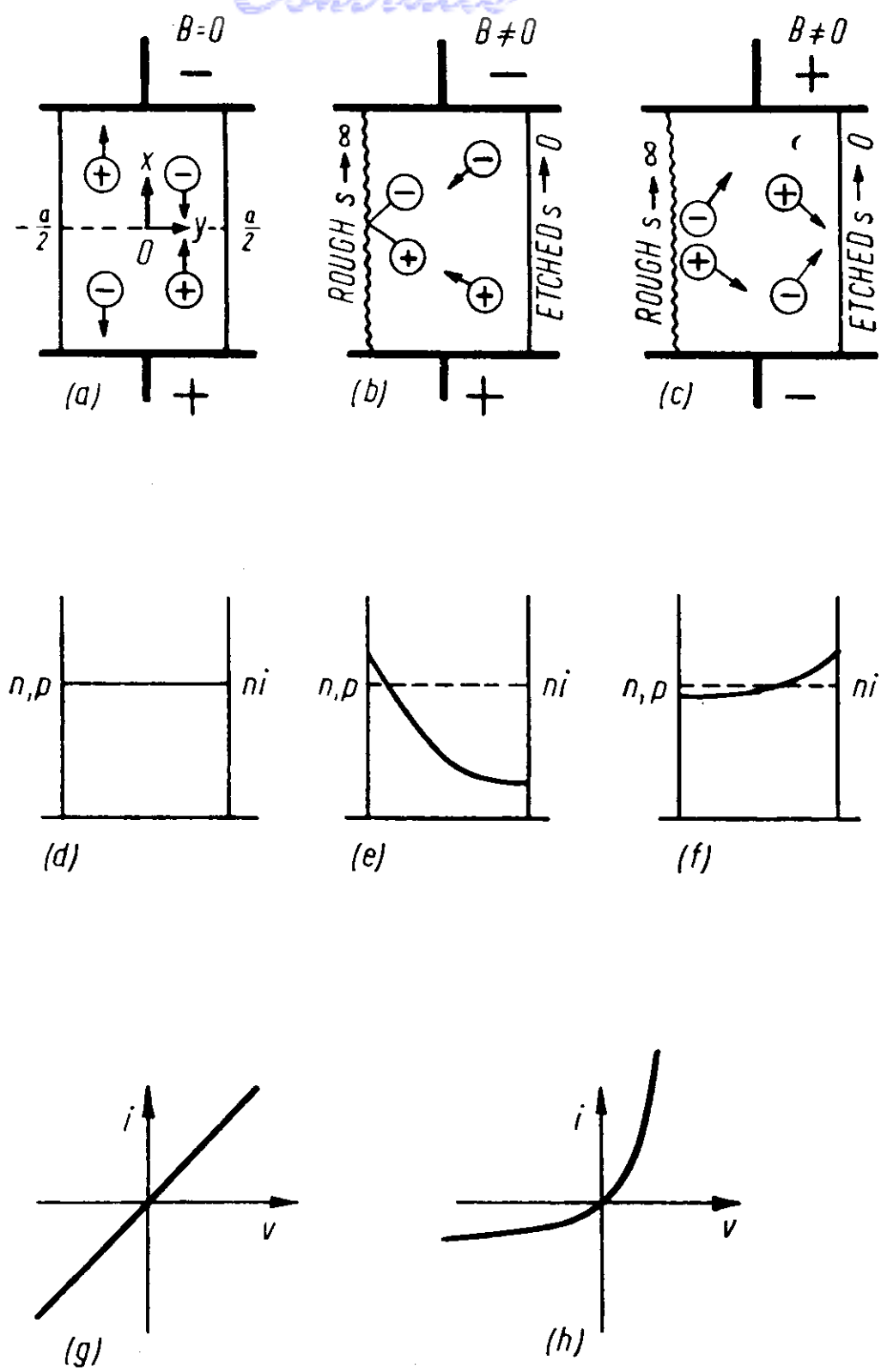

Figure 5. Magnetic Barrier Layer Effect (after Moss[1]). By permission of Interscience Publishers, Inc. and Friedr. Vieweg and Sohn.

where a is the half-width of the specimen, and where S_1 and S_2 are surface recombination velocities. As a result, Equation (3.3) can be solved for the increase in carrier concentration, Δp.

$$\Delta p = e^{-yZ/L} \left\{ A \exp \frac{y}{L} \sqrt{1 + Z^2} + C \exp \frac{-y}{L} \sqrt{1 + Z^2} \right\} \qquad (3.5)$$

where $Z = \frac{\Theta_p E_x \mu_n L}{ZD} = \frac{B E_x \mu_p \mu_n L}{ZD}$ (3.6)

A and C are constants of integration, and B is the magnetic induction.

Moss also gives an expression for the relative conductivity of the specimen, which is defined as

$$\lambda = \frac{1}{a n_i} \int_{-a/2}^{a/2} p\,dy. \qquad (3.7)$$

The expression is

$$\lambda = 1 - \frac{2Z}{g} \left\{ \frac{(1 + Z^2)^{1/2} [\cosh g (1 + Z^2)^{1/2} - e^{gZ}] + Z \sinh g (1 + Z^2)^{1/2}}{(1 + Z^2)^{1/2} \cosh g (1 + Z^2)^{1/2} + Z \sinh g (1 + Z^2)^{1/2}} \right\} \qquad (3.8)$$

where $g = a/L$.
This expression may be evaluated for various assumptions about the sizes of Z, S_1, and S_2.[1]

The magnetic barrier layer effect was discovered by the semiconductor group at Siemens, and papers have been published by several members of that group.[2] Madelung, et al.,[3] have presented a detailed analysis for both the steady-state and time-dependent behavior of the effect, as well as calculating theoretical rectification curves for various parameter values.

A bibliography on this effect is included in the paper by Moss.[1]

F. B. Dyer

REFERENCES

1. T. S. Moss, Semiconductors and Phosphors, Edited by M. Schön and H. Welker, (New York: Interscience Publishers, 1958), p. 108-9.
Review article.

2. O. Madelung, L. Tewordt, and H. Welker, "Zur Theorie der Magnetischen Sperrschicht in Halbleitern," Zeitschrift für Naturforschung 10, Series A, 476 (1955).

Theoretical article in German.

3. E. Weisshaar, "Magnetische Sperrschichten in Germanium. II." Zeitschrift für Naturforschung 10, Series A, 488 (1955).

Experimental article in German.

4. ZENER EFFECT†

Zener[1] proposed field-induced band-to-band transitions of electrons as a possible cause of dielectric breakdown and derived the probability of an electron tunneling through the barrier presented by the forbidden energy region.

In analyzing interband transitions it is usually supposed that a uniform field, $\mathcal{E}$, acts over a region x units long, such as a p-n junction, of a crystal. The case usually examined is the one-dimensional one. Now all the valence electrons within this region are subjected to the field simultaneously and all are given the same chance to tunnel through the barrier of height E_g and width x_3, where $x_3 \sim E_g/e\mathcal{E}$. Thus, if the number of unit cells subjected to the field is n, the current is

$$I = n \sigma e \nu P \tag{4.1}$$

where σ is the number of electrons per unit cell, ν is the number of times per second an electron strikes the barrier, and P is the barrier transparency (P is proportional to the probability of direct tunneling).

The time rate of change of momentum is equal to the applied force; therefore

$$\dot{k} = \frac{e\mathcal{E}}{\hbar}, \tag{4.2}$$

where k is the wave number associated with an electron of momentum $p = \hbar k$. In the crystal lattice a k interval of $2\pi/a$ where a is the unit cell dimension must be traversed for a full cycle from the upper band edge to the lower band edge and back to the upper band edge. Therefore the time between collisions with the barrier is

$$\frac{\Delta k}{\Delta t} = \frac{e\mathcal{E}}{\hbar}$$

using

$$\Delta k = 2\pi/a$$

$$\Delta t = \frac{\hbar \Delta k}{e\mathcal{E}} = \frac{h}{ae\mathcal{E}} -$$

or

$$\nu = \frac{ae\mathcal{E}}{h} \tag{4.3}$$

Thus, the emitted current density is given approximately by[2]

†The article supplements the article of the same name in our WADC Technical Report 59-737 and covers mainly the tunnel effect observed in narrow p-n junctions.

$$J = (z\, e^2/a^2 h)V\, P, \tag{4.4}$$

where V is the voltage drop in the distance x.

As a first approximation, an expression for P may be written as

$$P = \exp\left\{-\frac{4}{3}\sqrt{\frac{2m_{eff}}{\hbar}}\;\frac{E_g^{3/2}}{e\mathcal{E}}\right\} \tag{4.5}$$

Where m_{eff} is the effective mass of the electron. This expression is analogous to the one for external field emission and follows directly from the WKB approximation.[3] Zener, however, improved somewhat on this by adding to the expression for the potential a periodic term, $\epsilon(x)$, representing the effect of the crystal lattice. By solving the steady-state Schrodinger equation with the condition that $e\mathcal{E}a \ll E_g$, Zener arrived at the barrier transparency as

$$P = \exp\left\{-\frac{\pi^2 ma}{eh^2}\cdot\frac{E_g^2}{\mathcal{E}}\right\} \tag{4.6}$$

where m is the free mass of the electron.

While Zener provided a good foundation for the understanding of this effect, his derivation of equation (4.6) does not take into account the effect of the lattice on the motion of the electron within the forbidden band, and, furthermore, it is based on a free-electron model which is more appropriate to wide energy bands and narrow forbidden energy gaps. These points have been considered by Franz,[4] who obtained

$$P = \exp\left\{-\pi^2\sqrt{\frac{2m'}{2eh}}\cdot\frac{E_g^{3/2}}{\mathcal{E}}\right\}, \tag{4.7}$$

where

$$m' = 2\,\frac{m^2a^2Eg}{\hbar^2} \tag{4.8}$$

would make equation (4.7) essentially the same as equation (4.6).

While numerous studies[5,6,7] have been made in attempts to obtain better values for the barrier transparency, one fairly recent study by Keldysh[8] has taken into account the electron-phonon interaction which exists in the crystal. Keldysh obtained three expressions for the barrier transparency, one of which is P_D, which represents the direct transition tunneling probability and is

$$P_D = \exp\left\{-\frac{\pi\sqrt{m^*}}{2e\hbar\mathcal{E}}\;E_g^{3/2}\right\} \tag{4.9}$$

where m* is the reduced effective mass. For indirect transitions, the effect of phonon cooperation has to be included and P for phonon absorption, is

$$P_A = \exp\left\{-\frac{4\sqrt{2m^*}}{3e\hbar}\left(\frac{E_g - \hbar\omega}{\mathcal{E}}\right)^{3/2}\right\} \qquad (4.10)$$

where $\hbar\omega$ is the phonon energy. For phonon emission, P becomes

$$P_E = \exp\left\{\frac{-4\sqrt{2m^*}}{3e\hbar}\left(\frac{E_g + \hbar\omega}{\mathcal{E}}\right)^{3/2}\right\} \qquad (4.11)$$

Keldysh defines m* as

$$m^* = \frac{m_c^* m_v^*}{(m_c^* + m_v^*)} \quad , \qquad (4.12)$$

where m_c^* and m_v^* refer to electrons and holes, respectively. Note that, for the case of indirect transitions, equation (4.4) becomes

$$J = A\mathcal{E}^r[NP_A + (N + 1)P_E], \qquad (4.13)$$

where A is a constant which includes Z, e, a, h; and $\mathcal{E}^r$ is used rather than V because of the effect of some of the corrections[4,9] which are applied; and r is some power between one and three. The N is the phonon density. It must also be said that these expressions are for one phonon energy only. Further terms[8] would also be needed if multiphonon processes are important.

Considerable experimental interest has been directed toward the study of the tunneling process in p-n junctions in silicon and germanium in recent years. McAfee, et al.[2] first interpreted the breakdown in germanium p-n junctions as due to the Zener effect. Other experiments[10] were able to show that the avalanche effect was predominant in the wider p-n junctions (greater than 1000 Å wide). More recently Chynoweth and McKay[11] were able to study the breakdown behaviour of junctions as narrow as about 400 Å in silicon. Such narrow junctions require very steep impurity-concentration gradients which, in turn, necessitate the use of materials so heavily doped that they are degenerate (the Fermi level at zero applied voltage lies within the valence band on the p-side and the conduction band on the n-side). Such junctions exhibit fields of between 10^5 and 10^6 volts/cm. Since the various theories require fields of the order of 10^6 volts/cm for the Zener effect to be important in determining the current, only small applied voltages were necessary for the studies of these junctions.

Esaki[12] studied very narrow junctions in germanium and discovered that certain types possessed regions of negative resistance in the forward direction. These are the so-called Tunnel Diodes. These diodes require a very

high doping level (for instance, phosphorus-doped silicon requires an impurity concentration of greater than 6×10^{19} donors/cc) and junctions which are 100-200 Å wide.

Tunnel diodes have been formed from p-n junctions in silicon, germanium, and in group III-V semiconductors. These three basic types provide the experimenter with the means to study many of the details of semiconductor physics in general and the tunneling phenomenon in particular. The silicon types allow the study of indirect transitions[13,14] with germanium types showing either direct, or direct and indirect, depending upon the impurity types.[13,14] The group III-V types exhibit polarons, phonons, and direct tunneling.[15,16]

Tunnel diodes are also useful as devices for electronic functions as they do exhibit a region of negative resistance. They retain this region over a wide range of temperatures although very high temperatures cause a permanent change. Their high frequency response will probably be limited by external elements, such as stray inductance and capacitance, since the tunneling is a majority carrier effect and as such is limited ultimately only by the bulk relaxation time. Voltage of operation is low--0.05 to 0.5 volt--but current levels can be chosen, almost at will, from 100 microamperes to 10 amperes.

The tunnel diodes in general possess very limited sensitivity to gamma and light radiations, and operate in ambients of high nuclear radiation intensity. Fast neutron bombardment produces permanent changes in the negative resistance and reduces the voltage swing; however, gallium arsenide units have operated under fast neutron doses of 10^{17} nvt.

F. B. Dyer

REFERENCES

General:

(A) A. G. Chynoweth, "Internal Field Emission," Progress in Semiconductors Vol. 4, Editor Gibson, John Wiley & Sons, Inc., New York, (1960).

(B) E. Spenke, Electronic Semiconductors, McGraw-Hill Book Company, Inc., New York, (1960).

Cited:

1. C. Zener, "A Theory of the Electrical Breakdown of Solid Dielectrics," Proceedings of the Royal Society, series A, 145, 523, (1934).

2. K. B. McAfee, E. J. Ryder, W. Shockley, and M. Sparks, "Observations of Zener Current in Germanium P-N Junctions," Physical Review, (L), 83, 650, (1951).

3. D. Bohm, Quantum Theory, Prentice-Hall, Inc., Englewood Cliffs, N. J., (1951).

4. W. Franz, "Dielectric Breakdown," Handbuch der Physick, Vol. 17, (1956).

5. W. V. Houston, "Acceleration of Electrons in a Crystal Lattice," Physical Review, 57, 184 (1940).

6. G. H. Wannier, "Possibility of a Zener Effect," Physical Review, (L), 100, 1227, (1955). Also, Errata to above reference. Physical Review, 101, 1835, (1956).

7. J. Homilius, and W. Franz, "Raumliche Verallgemeiuerung der Zenerschen Formel Fur die innere Feldmission," Zeitschrift fur Naturforschung 9A, 5, (1954), Also: "Theorie der inneren Feldermission in Kubischen Kristallen," Zeitschrift fur Naturforschung 9A, 205, (1954).

8. L. V. Keldysh, "Behavior of Non-Metallic Crystals in Strong Electric Fields," Soviet Physics JETP 6, 763, (1958), Also: "Influence of the Electron-Hole Pairs in a Strong Electrical Field," Soviet Physics JETP 7, 665, (1958).

9. E. O. Kane, "Zener Tunneling in Semiconductors," Physics and Chemistry of Solids, 12, 181, (1960).

10. K. B. McAfee, and G. L. Pearson, "The Electrical Properties of Silicon P-N Junctions Grown," Physical Review 87, 190, (1952).

11. A. G. Chynoweth and K. G. McKay, "Internal Field Emission in Silicon P-N Junctions," Physical Review, 106, 603, (1958).

12. L. Esaki, "New Phenomenon in Narrow Germanium P-N Junctions," Physical Review (L), 109, 603, (1958).

13. N. Holonyak, Jr., I. A. Lesk, R. N. Hall, J. J. Tiemann, and H. Ehrenreich, "Direct Observations of Phonons During Tunneling in Narrow Junction Diodes," Physical Review Letters, 3, 167, (1959).

14. A. G. Chynoweth, W. L. Feldmann, C. A. Lee, R. A. Logan, G. L. Pearson, and P. Aigrain, "Internal Field Emission at Narrow Silicon and Germanium P-N Junctions," Physical Review, 118, 425, (1960).

15. R. N. Hall, J. H. Racette, and H. Ehrenreich, "Direct Observation of Polarons and Phonons During Tunneling in Group 3-5 Semiconductor Junctions," Physical Review Letters, 4, 456, (1960).

16. A. G. Chynoweth and R. A. Logan, "Internal Field Emission at Narrow P-N Junctions in Indium Antimonide," Physical Review, 118, 1470, (1960).

5. HIGH-VOLTAGE PHOTOVOLTAIC EFFECT

Larger-than-band-gap photovoltages have recently been observed on films of CdTe by Pensak[1] and Goldstein[2] and on single crystals of ZnS by Ellis[3] and Lempicki.[4] These voltages have been 100 volts or more for crystals a few millimeters long. Cheroff and Keller[5] found that both the magnitude and the sign of photovoltage depend upon the wavelength of the exciting light.

It has been suggested that the magnitude of the photovoltage can be explained by postulating p-n junctions connected like batteries in series[2,6] or other types of barriers associated with crystallographic disorder.[3,4,7,8] Direct experimental evidence for either has been lacking, however.[4] Moreover, these hypotheses offer no explanation of the reversal of sign.

Since the theory of the ordinary photovoltaic effect[7,9] does not account for the anomalous effects noted in ZnS and CdTe and the various theories[2,3,6,8] proposed for explaining the high-voltage photovoltaic effect appear to be insufficient, this article can only review the literature on the subject and cannot present a complete picture of the high-voltage photovoltaic effect.

B. Goldstein and L. Pensak[6] made an extensive study of the high-voltage photovoltaic effect in thin films of cadmium telluride. They noted photovoltages as high as 100 volts/mm at room temperature. They found that an oblique angle of deposition of the vapor onto the substrate was required. They also found that the temperature, type of substrate, and residual gases (principally oxygen) affected the magnitude and sign of the photovoltage. The films were believed to be very close to stoichiometric composition, since the bulk resistivity of the films was much higher than that of the original material (film dark resistivity $\sim 10^8$ ohm-cm and original material $\sim 10^6$ to 0.3 ohm-cm). They also found that the photovoltage is given by the empirical relation

$$V = \lambda \ln (K L + 1) \tag{5.1}$$

where

$$\lambda = \frac{k T}{e}$$

V = open circuit photovoltage

K = ratio of short-circuit current to thermal reverse-saturation current

L = light intensity

and the resistance is given by

$$R(L) = \frac{1}{L} \ln (K L + 1). \tag{5.2}$$

However, the fact that the resistance of the nonphotovoltaic film varies in exactly the same way as it does for the strongly photovoltaic films indicates

that the dependence of the resistance on light intensity is due to some property of the film itself and not merely to the presence of a photovoltage. They also made a study of the physical properties of the films by means of x-rays and polarized light. Anisotropic scattering of light and polarization were noted and were interpreted as being due to small angled facets on the surface. X-ray measurements showed that the films consisted of CdTe crystallites whose size was comparable with the film thickness. They proposed a model consisting of an aligned array of many photovoltaic elements. It was proposed that the alignment was due to the angle of deposition of material, and that the photovoltaic elements arose from the warping of the energy bands at the interfacial surfaces of the crystallites. Such warping has been treated theoretically by E. O. Johnson.[10]

Ellis[3] grew ZnS crystals from the vapor in the form of clear fibers or platelets that contained random stacking faults and in some places had ordered arrangements of stacking faults with periodicities of as many as 40 double layers. X-ray diffraction studies showed that the growth direction was also that of the sulfur-zinc vector in the bonds perpendicular to the stacking faults. Under ultraviolet light, many of the crystals produced greater-than-band-gap photovoltages. Microscope and x-ray studies indicated that the higher photovoltages were produced in the crystals with the larger number of stacking faults. Fields as high as 100 volts/cm at room temperature were observed and the direction of the electric field was the same as the growth direction. Ellis felt[3] that the evidence did not support the conclusion that the photovoltage in the CdTe films was caused by the same mechanism (stacking faults) as that in ZnS crystals.

Lempicki[4] has also studied the high-voltage photovoltaic effect (anomalous photovoltaic effect) in ZnS single crystals. The crystals were grown by a vapor phase method and ranged in structure from hexagonal to cubic with varying amounts of stacking faults. Some crystals showed bands of different birefringence sharply separated by planes perpendicular to the c-axis. The larger-than-band-gap photovoltage was observed in those crystals with stacking faults. Under monochromatic excitation, the photovoltage measured parallel to the c-axis showed two sign reversals at about 3300 Å and 3500 Å and peaks at approximately 3250 Å and 3400 Å. The position of the 3400 Å peak varied about 70 Å, depending upon the crystal structure. In the direction perpendicular to the c-axis, the photovoltage did not change sign and remained smaller than the band gap. Hexagonal crystals free of stacking faults did not show anomalous photovoltages, but heat treatment caused the appearance of both. A pyroelectric polarization was found to be correlated with the sign of photovoltage.

Lempicki reached three conclusions from the results of his experiments:

(1) The anomalous photovoltaic effect in ZnS crystals is connected with crystalline disorder and most probably with stacking faults.

(2) The position of the positive peak depends upon the predominant structure present.

(3) Crystals which show disorder give rise to a pyroelectric current on heating and a correlation exists between the direction of this current and the photovoltage.

T. Figielski[8] has analyzed the work of J. Starkiewicz[11] and R. J. Berlaga[12] on microcrystalline layers of PbS and the work of A. Wolska[13] on layers of Tl_2S. In each case, these workers found a higher-than-band-gap photovoltaic effect. The work of R. J. Berlaga,[12,14] in particular, appears very similar to that of Goldstein and Pensak[6] using PbS instead of CdTe. Figielski arrived at the conclusion that the high-voltage photovoltaic effect consists of "a typical photovoltaic effect on the inter-crystalline boundaries, such as should occur when the latter are nonsymmetrically illuminated." A photovoltaic effect of this latter type was previously investigated by Figielski.[15]

F. B. Dyer
V. Crawford

REFERENCES

1. L. Pensak, "High-Voltage Photovoltaic Effect," Phys. Rev. 109, 601 (1958).

2. B. Goldstein, "Properties of Photovoltaic Films of CdTe," Phys. Rev. 109, 601 (1958).

3. S. G. Ellis, et al., "Photovoltages Larger Than the Band Gap in Zinc Sulfide Crystals," Phys. Rev. 109, 1860 (1958).

4. A. Lempicki, "Anomalous Photovoltaic Effect in ZnS Single Crystals," Phys. Rev. 113, 1204 (1959).

5. G. Cheroff and P. Keller, "Optical Transmission and Photoconductive and Photovoltaic Effects in Activated and Unactivated Single Crystals of ZnS," Phys. Rev. 111, 98 (1958).

6. B. Goldstein and L. Pensak, "High-Voltage Photovoltaic Effect," J. Appl. Phys. 30, 155 (1959).

7. N. J. Merz, Helv. Phys. Acta 31, 625 (1958).

8. T. Figielski, "On a Possible Explanation of Strong Photovoltaic Effects in PbS Layers," Bulletin de L'Academic Polonaise des Sciences, Serie des Sci., Math., Astr., et Phys., Vol. VII, No. 3 (1959).

9. Wright Air Development Division, Research on Various Phenomena for the Performance of Circuit Functions. WADC Technical Report 59-737 (October 1959).

10. E. O. Johnson, "Comparison of the Semiconductor Surface and Junction Photovoltages," RCA Rev. 18, 556 (1957).

11. J. Starkiewicz, et al., "Photovoltaic Effects in Microcrystalline Layers," Nature 158, 28 (1946).

12. R. J. Berlaga, et al., Zh techn. fiz 25, 1378 (1955).

13. A. Wolska, unpublished work, quoted from No. 8.

14. R. J. Berlaga, et al., "Photovoltaic Effects in PbS Layers," Zh techn. fiz 26, 3 (1956).

15. T. Figielski, L. Sosnowski, Congress International sur la Physique de l'Etat Solide et ses Applications á l'Electronique et aux Télè-communications, (Bruxelles: 1958).

6. THERMOELECTRIC EFFECTS

Three thermoelectric effects have been experimentally established. The Seebeck effect is the appearance of a voltage ΔV in an open circuit consisting of two different conductors when there is a temperature difference ΔT between their junctions.

$$\Delta V = S_{12}\Delta T$$

S_{12} is the thermoelectric power between the conductors 1 and 2. The Peltier effect is the reversible rate of accumulation of heat, ΔQ watts, at the boundary between two conductors when a current, ΔI amperes, flows.

$$\Delta Q = \pi_{12}\Delta I,$$

where π_{12} is the Peltier coefficient between the conductors 1 and 2.

The Thomson effect is the reversible rate of accumulation of heat, Δq watts, by a current, ΔI amperes, in the portion of a conductor in the presence of a temperature gradient $\partial T/\partial x$.

$$\Delta q = \sigma_T \Delta I \frac{\partial T}{\partial x},$$

where σ_T is the Thomson coefficient of the given conductor.

It can be shown thermodynamically that the thermoelectric coefficients defined above are related, at any absolute temperature T, by the following relations:

$$\pi_{12} = TS_{12} \tag{6.1}$$

$$\sigma_{T_1} - \sigma_{T_2} = T\,(\partial S_{12}/\partial T). \tag{6.2}$$

Equation (6.1) was first obtained by Lord Kelvin[1] and is commonly known as the Kelvin relation.

The left side of equation (6.2) is the difference between two terms, each of which depends on the properties of a single conductor. Hence the absolute thermoelectric power of a substance is defined so that S_{12} is equal to the difference between the absolute thermoelectric powers of conductors (1) and (2), i.e., $S_{12} = S_2 - S_1$.

The relations, corresponding to (6.1) and (6.2), between the absolute thermoelectric coefficients will be deduced below without resort to thermodynamics.

To discuss these thermoelectric effects, other than thermodynamically, it is necessary to present some of the basic theory concerning the motion of electrons in a solid in the presence of an electric field and a thermal gradient. The subsequent discussion follows closely the treatments given by F. J. Blatt[2] and F. Seitz.[3] It is assumed that the one electron approximation is valid and that a single energy band is present in the solid. Some results will be obtained with the further assumption that the energy of an electron is independent of the direction of its wave vector $\vec{k}$, i.e., the energy surfaces in k-space are spherical.

The distribution of the electrons in a solid can be described in terms of a distribution function $f(\vec{k},\vec{r})$ so that the average number of electrons in the volume element $d\vec{r}$ with wave vectors in the element $d\vec{k}$ is equal to

$$\frac{1}{4\pi^3} f(\vec{k},\vec{r})\, d\vec{r}\, d\vec{k}. \tag{6.3}$$

The various electronic transport properties of a solid are known if the behavior of $f(\vec{k},\vec{r})$ under the influence of electric and magnetic fields and thermal gradients can be determined. In the absence of externally applied fields or thermal gradients, $f(\vec{k},\vec{r})$ is just the Fermi-Dirac distribution f_o where

$$f_o(\vec{k}) = f_o(\epsilon) = \frac{1}{e^{\frac{\epsilon-\eta}{kT}} + 1} \tag{6.4}$$

Here η is the Fermie energy and ϵ is the kinetic energy of an electron.

A condition on $f(\vec{k},\vec{r})$ can be obtained, whenever the system is in the steady state, by requiring the $f(\vec{k},\vec{r})$ be independent of time. $f(\vec{k},\vec{r})$ may vary with time due to two independent causes:

1. A continuous variation due to the motion of the electrons from one region of space to another as a result of the acceleration of charge carriers by electric and magnetic fields and thermal gradients;

2. A discontinuous variation because of the relatively discontinuous changes in velocity which accompany collisions with lattice vibrations, lattice imperfections, and boundaries.

We therefore write

$$\frac{\partial f}{\partial t} = \left(\frac{\partial f}{\partial t}\right)_d + \left(\frac{\partial f}{\partial t}\right)_c = 0, \tag{6.5}$$

where $\left(\frac{\partial f}{\partial t}\right)_d$ represents the drift term resulting from applied fields and thermal

gradients and $(\frac{\partial f}{\partial t})_c$ represents the collision term.

The expression for $(\frac{\partial f}{\partial t})_d$ can be shown to be

$$(\frac{\partial f}{\partial t})_d = -\frac{e}{\hbar}[\vec{E} + \frac{\vec{v}}{c} \times \vec{H}] \cdot \vec{\nabla}_k f - \frac{\partial f}{\partial T} \vec{v} \cdot \vec{\nabla}_r T, \qquad (6.6)$$

where $\vec{\nabla}_k f$ and $\vec{\nabla}_r T$ represent the derivatives of $f(\vec{k},\vec{r})$ and T with respect to the components of $\vec{k}$ and $\vec{r}$, and $\vec{v}$ is the electron velocity. Putting (6.6) into (6.5) results in the Boltzmann equation,

$$\frac{e}{\hbar}[\vec{E} + \frac{\vec{v}}{c} \times \vec{H}] \cdot \nabla_k f + \frac{\partial f}{\partial t} \vec{v} \cdot \vec{\nabla}_r T = (\frac{\partial f}{\partial t})_c \qquad (6.7)$$

Provided a suitable expression can be obtained for the collision term, the Boltzmann equation can be used to discuss a variety of effects produced in a solid by the application of electric and magnetic fields and/or thermal gradients, e.g., the Peltier, Seebeck, Thomson, Hall, Nernst and Ettinghausen effects.

The collision term may be described in terms of some function $S(\vec{k},\vec{k}')$ which is the probability per unit time interval that an electron in a state corresponding to a wave vector $\vec{k}$ makes a transition to a state corresponding to a wave vector $\vec{k}'$ due to collisions. However, the problem is usually simplified by assuming that the deviation of $f(\vec{k},\vec{r})$ from equilibrium can be described in terms of a single relaxation time $\tau(\vec{k})$. The approach to equilibrium of $f(\vec{k},\vec{r},t)$, the distribution function at a certain instant in time, as the result of collisions is then given by

$$(\frac{\partial f}{\partial t})_c = -\frac{f - f_o}{\tau} \qquad (6.8)$$

The procedure for the determination of $f - f_o$ is to expand $f(\vec{k},\vec{r})$ in a series about $f_o(\vec{k})$ and retain only the first two terms as follows:

$$f(\vec{k},\vec{r}) = f_o(\vec{k}) - \vec{v} \cdot \vec{\Psi}(\vec{k},\vec{r}) \frac{\partial f_o}{\partial \epsilon} \qquad (6.9)$$

When (6.9) is substituted into the Boltzmann equation, $\vec{\Psi}(\vec{k},\vec{v})$ can be evaluated in terms of the applied fields and thermal gradients. When this is done for $\vec{H} = 0$, the following is obtained for $f(\vec{k},\vec{v})$,

$$f(\vec{k},\vec{v}) = f_o - \tau \vec{v} \cdot \left\{ e\vec{E} - T\vec{\nabla}_r (\frac{\eta}{T}) - \frac{\epsilon}{T} \vec{\nabla}_r T \right\} \frac{\partial f_o}{\partial \epsilon} \qquad (6.10)$$

where second order terms in $\vec{E}$ and T have been neglected.

The electric current density, $\vec{J}$, and the electronic contribution to the thermal current, $\vec{Q}$, can be evaluated. $\vec{J}$ and $\vec{Q}$ are defined by the following:

$$\vec{J} = \frac{e}{4\pi^3} \int \vec{v}\, f(\vec{r},\vec{k})\, d\vec{k} \tag{6.11}$$

$$\vec{Q} = \frac{1}{4\pi^3} \int \epsilon \vec{v}\, f(\vec{r},\vec{k})\, d\vec{k}. \tag{6.12}$$

Substitution of (6.10) into (6.11) and (6.12) results in

$$\vec{J} = K_1[e^2 \vec{E} - eT \vec{\nabla}(\tfrac{\eta}{T})] - K_2(\tfrac{e}{T}) \vec{\nabla} T \tag{6.13}$$

$$\vec{Q} = K_2[e \vec{E} - T\vec{\nabla}(\tfrac{\eta}{T})] - K_3 (\tfrac{1}{T}) \vec{\nabla} T \tag{6.14}$$

where for spherical energy surfaces,

$$K_n = \frac{4}{3m^*} \int_0^\infty N(\epsilon)\, \tau\, \epsilon^n \frac{\partial f_0}{\partial \epsilon}\, d\epsilon. \tag{6.15}$$

$N(\epsilon)$ is the density of states in energy space and m* is the electron effective mass.

A. Seebeck Effect

The Seebeck effect results from the fact that when a thermal gradient exists in a solid an electric field is produced. This can readily be seen from equation (6.13) for $\vec{J}$ is equal to zero. Solving for $\vec{E}$ and substituting

$$T \vec{\nabla}(\tfrac{\eta}{T}) = T [-\frac{\eta}{T^2} \vec{\nabla} T + \frac{1}{T} \vec{\nabla} \eta] \tag{6.16}$$

then

$$\vec{E} = \frac{1}{e} [\vec{\nabla} \eta + S \vec{\nabla} T]. \tag{6.17}$$

S is the absolute thermoelectric power of a material and is given by

$$S = \frac{1}{eT} (\frac{K_2 - \eta K_1}{K_1}) \tag{6.18}$$

The integrals K_η can be approximated by using either the Fermi-Dirac distribution function or the Maxwell-Boltzmann distribution function, depending on whether the current carriers are degenerate or nondegenerate. When the carriers are degenerate

$$S = \frac{\pi^2 k^2 T}{3e} \left[\frac{\partial \log \sigma(\epsilon)}{\partial \epsilon}\right]_{\epsilon = \eta} \tag{6.19}$$

and when they are nondegenerate

$$S = \frac{k}{e}\left[r + \frac{5}{2} - \frac{\eta}{kT}\right] \tag{6.20}$$

In (6.20) η is measured from the conduction band edge and r arises from the assumption that the relaxation time τ is given by

$$\tau = \tau_o \epsilon^r$$

For the nondegenerate case the magnitude of S is as much as 10^3 times that for the degenerate case.

The origin of the Seebeck potential can now be explained by using equation (6.17). Consider a circuit constructed of two different conductors, 1 and 2, and suppose their junctions are at temperature T_0 and T_1 as shown.

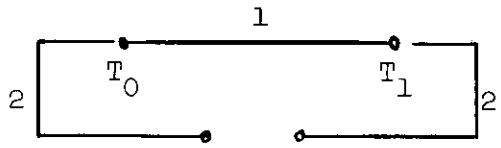

The electromotive force generated is given by

$$V_{12}(T_0, T_1) = -\oint \vec{E} \cdot d\vec{r} = \int_{T_0}^{T_1} (S_2 - S_1)\, dT, \tag{6.21}$$

since the line integral of $\vec{\nabla}\eta$ about a closed path is zero. Therefore, if two conductors having different absolute thermoelectric powers are joined together such that their junctions are kept at different temperatures, an electromotive force of thermal origin will result.

Note that since S is related linearly to e, the sign of $v_{12}(T_0, T_1)$ depends on the sign of the current carriers in the two materials. Hence, in equation (6.21), $v_{12}(T_0, T_1)$ would be largest if the current carriers were holes in material 2 and electrons in material 1.

B. Thomson Effect

The rate at which heat accumulates in a unit volume of a conductor that is carrying both electrical and thermal currents is given by

$$\frac{dH}{dt} = \vec{J} \cdot \vec{E} - \vec{\nabla} \cdot \vec{Q}. \tag{6.22}$$

Solving equation (6.13) for $\vec{E}$ and using equation (6.5) one obtains,

$$\frac{dH}{dt} = \frac{J^2}{\sigma} - T \vec{J} \cdot \vec{\nabla} S - \vec{\nabla} \cdot \vec{Q}, \tag{6.23}$$

where $\sigma = J/E = e^2 K_1$. The first term will be recognized as the Joule heat; the second term represents a reversible accumulation of heat which may be written

$$\left(\frac{dH}{dt}\right)_T = - T \frac{\partial S}{\partial T} \vec{J} \cdot \vec{\nabla} T = - \sigma_T \vec{J} \cdot \vec{\nabla} T. \tag{6.24}$$

This equation defines the Thomson coefficient σ_T. It follows that

$$\sigma_T = T\left(\frac{\partial S}{\partial T}\right) \qquad \text{and} \quad S = \int_0^T (\sigma_T/T)\, dT. \tag{6.25}$$

The Thomson effect is the only one of the thermoelectric effects that can be observed in a single homogeneous substance.

C. Peltier Effect

The Peltier effect is the reversible accumulation of heat at the boundary between two conductors when a current flows from one to the other. This effect can be explained in terms of the absolute Peltier coefficient, π, of a substance. It is defined as the energy flux per unit current when the substance is isothermal and when the zero of energy is taken at the Fermi level.

The energy flux, when zero energy is taken at the Fermi level, is just

$$\vec{Q'} = \left(\frac{1}{4\pi^3}\right) \int (\epsilon - \eta)\, \vec{v}\, f\, (\vec{r},\vec{k})\, d\vec{k} \tag{6.26}$$

or

$$\vec{Q'} = \vec{Q} - \eta\left(\frac{\vec{J}}{e}\right), \tag{6.27}$$

where $\vec{J}$ and $\vec{Q}$ are given by equations (6.13) and (6.14). Setting $\vec{\nabla}T$ equal to zero in (6.13) and (6.14) one obtains for π,

$$\pi = \frac{Q - \eta \left(\frac{J}{e}\right)}{J} = \frac{K_2 - \eta K_1}{eK_1} \tag{6.28}$$

or

$$\pi = TS, \tag{6.29}$$

which is just the Kelvin relation.

To explain the Peltier effect consider the junction between two dissimilar conductors through which a current is flowing as shown below.

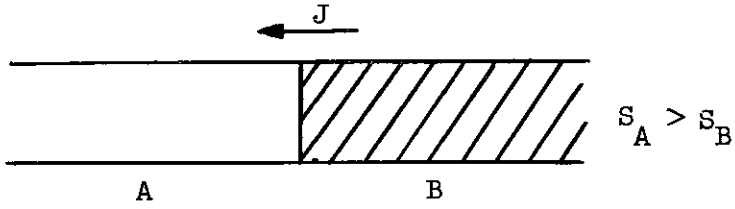

According to equation (6.23), the reversible accumulation of heat per unit volume is given by

$$\left(\frac{dH}{dt}\right)_R = - T \vec{J} \cdot \vec{\nabla} S \tag{6.30}$$

Since $\vec{\nabla} S$ is nonzero only at the junction, then

$$\left(\frac{dH}{dt}\right)_{AB} = T J (S_B - S_A) = \pi_{AB} J, \tag{6.31}$$

where $\pi_{AB} = \pi_B - \pi_A$.

In the previous discussion, it was implicitly assumed that the only influence of lattice vibrations (phonons) is to provide a mechanism by which the distribution function can approach equilibrium in a manner described by a relaxation time τ. In an actual case, however, the phonon distribution is disturbed by the presence of a thermal gradient and/or an electric current. It is therefore necessary to include a phonon contribution to both π and S. See the following article on Phonon Drag for a calculation of this contribution.

Interest in the thermoelectric effects stems from several different viewpoints. The thermocouple application of the Seebeck effect is well known. However, since the conductivity of a solid depends on the scattering mechanism, the density of charge carriers, and the energy band structure, equation (6.31) indicates that it is possible to obtain information about these properties of

a solid from measurements of the thermoelectric power. Considerable interest also stems from the reversible conversion of thermal energy to electrical energy which is possible in a thermoelectric circuit. A discussion of some experimental arrangements for measuring the thermoelectric effects, including a considerable number of references to the theory, measurement, and the application of the thermoelectric effects can be found in the book "Methods of Experimental Physics."[5]

R. M. Nicklow

REFERENCES

1. W. Thomson, "Mathematical and Physical Papers," Cambridge University Press, London, 1882, Vol. I, p. 232.

2. F. J. Blatt, "Theory of Mobility of Electrons in Solids," Solid State Physics, 4, 199-366 (1957).

3. F. Seitz, The Modern Theory of Solids, McGraw-Hill Co., 1940.

4. Conyers Herring, "Theory of the Thermoelectric Power of Semiconductors," Physical Review 96, 1163-1187 (1954).

5. H. P. R. Frederikse, V. A. Johnson, and W. W. Scanlon, "Thermoelectric Effects," Methods of Experimental Physics 6B, 114-128 (1959).

7. PHONON DRAG

The phonon drag effect was discovered as a result of experiments made almost simultaneously by Frederikse[1] and Beballe.[2] They found that the thermoelectric power of germanium rises at low temperature to many times the value predicted by previous theories. The interpretation given independently by Frederikse[1,3] and Herring[4] was that the additional thermoelectric power resulted from the drag exerted on charge carriers by the phonons which travel preferentially from hot to cold in a thermal gradient. Phonons are quantized normal mode lattice vibrations and in problems concerning thermal properties of a solid, they are frequently considered as particles with energy $\hbar\omega$, quasi-momentum $\hbar\vec{k}$, velocity $\partial\omega/\partial k$, and obeying Bose-Einstein statistics.

The drag of charge carriers and phonons on each other is assumed to be mutual so that the theoretical problem can be approached by consideration of the phonon effect on the Peltier heat π or on the thermoelectric power S. In an isothermal sample, π is enhanced by the dragging of phonons by electrons and in a thermal gradient, S is enhanced by the dragging of electrons by phonons. The solution of the problem for either π or S will be equivalent because of the Kelvin relation, $\pi = TS$.

The major part of the following discussion was obtained from that of C. Herring.[5] His article contains many references to the theory and measurements of the phonon drag effect.

From the definition of the absolute Peltier heat (see the description of the Peltier effect in the preceding article on Thermoelectric Effects), the phonon contribution to the Peltier heat, π_p, is given by the ratio of the energy flux of the phonon system to the electron current density. The energy flux of the phonon system is

$$\vec{F}_p = \sum_{\vec{q},\alpha} N(\vec{q},\alpha)\,\hbar\omega(\vec{q},\alpha)\,\vec{v}(\vec{q},\alpha) \qquad (7.1)$$

where

$\vec{q}$ = phonon wave vector

α = polarization index

$N(\vec{q},\alpha)$ = number of phonons with wave vector $\vec{q}$ and polarization α.

Now the phonons which contribute to the energy flux are those which the electrons can exert a drag on, i.e., those which can receive crystal momentum due to interaction with electrons. The phonons which will receive appreciable momentum from the electron current are the low energy, long wavelength phonons. It is therefore a fair approximation to set

$$\vec{v}(\vec{q},\alpha) = C_\alpha \vec{q}_\alpha / q_\alpha$$

and

$$\omega(\vec{q},\alpha) = C_\alpha q_\alpha$$

where C_α = the velocity of the phonons with polarization α.

Equation (7.1) then becomes

$$\vec{F}_p = \sum_{\vec{q},\alpha} N(\vec{q},\alpha)\, \hbar\, q_\alpha\, C_\alpha^2 \,. \tag{7.2}$$

Now

$$\sum_{q} N(\vec{q},\alpha)\, \hbar\, \vec{q}_\alpha = \vec{P}_\alpha \tag{7.3}$$

is just the crystal momentum of all the modes of polarization α, so

$$\vec{F}_p = \vec{P}_\ell\, C_\ell^2 + \vec{P}_t\, C_t^2 = (\vec{P}_\ell + \vec{P}_t)\, \bar{C}^2 \tag{7.4}$$

where l and t refer to longitudinal and transverse modes respectively and $\bar{C}$ is a suitable average of the two velocities. We now have a relation between the phonon energy flux and the phonon momentum, which is a quantity conserved in collisions of phonons with electrons.

To calculate $(\vec{P}_\ell + \vec{P}_t)$ we assume that there is a single effective relaxation time $\bar{\tau}$ which describes the collision processes that are trying to restore the phonons to equilibrium. Then

$$\left[\frac{\partial}{\partial t}\ (\vec{P}_\ell + \vec{P}_t)\right]_{\text{coll.}} = -\frac{\vec{P}_\ell + \vec{P}_t}{\bar{\tau}} \tag{7.5}$$

The rate at which $(\vec{P}_\ell + \vec{P}_t)$ changes due to collisions with electrons is equal to the fraction f of crystal momentum lost by the electrons to the phonons times the rate at which the electrons are receiving crystal momentum from the electric field, i.e.,

$$\left[\frac{\partial}{\partial t}\ (\vec{P}_\ell + \vec{P}_t)\right]_{\text{elec.}} = + f\, ne\, \vec{E} \tag{7.6}$$

where n is the concentration of electrons.

The total rate of change of $\vec{P}_\ell + \vec{P}_t$ is then

$$\frac{d}{dt}\ (\vec{P}_\ell + \vec{P}_t) = + f\, ne\, \vec{E} - \frac{(\vec{P}_\ell + \vec{P}_t)}{\bar{\tau}} \tag{7.7}$$

In the steady state $\frac{d}{dt}\ (\vec{P}_\ell + \vec{P}_t) = 0$, so that

$$f\, ne\, \vec{E} = + (\vec{P}_\ell + \vec{P}_t)/\, \bar{\tau} \tag{7.8}$$

Now the current density of the electrons is related to the electric field by the following relation:

$$\vec{J} = ne\vec{v} = ne\mu\vec{E} \tag{7.9}$$

where μ is the mobility. Thus

$$(\vec{P}_{\ell} + \vec{P}_{t}) = + \vec{\tau} f \vec{J}/\mu \tag{7.10}$$

Combining equations (7.4) and (7.10) we have for the phonon contribution to the Peltier heat, π_p,

$$\pi_p = \frac{F_p}{J} = + \frac{\bar{c}^2 f \bar{\tau}}{\mu} \tag{7.11}$$

and then from equation (7.1)

$$S_p = + \bar{c}^2 f \bar{\tau}/\mu T. \tag{7.12}$$

A refinement of (7.12) can be obtained by letting c, f, and τ be functions of $\vec{q}$, so that

$$S_p = + \sum_{q} [c(\vec{q})]^2 f(\vec{q}) \tau(\vec{q})/\mu T. \tag{7.13}$$

W. Shockley[6] obtains a result for S_p which is similar to (7.12) except that he introduces a relaxation constant ν, instead of $\bar{\tau}$, and a phonon mass.

It is now desirable to discuss what is known about how $\tau(\vec{q})$ depends on the temperature T and on the wave number $\vec{q}$. The most important contributions to $\tau(\vec{q})$ arises from phonon-phonon and phonon-boundary collisions. Phonon-boundary scattering can normally be described by a relaxation time τ_b which is independent of q and T. Phonon-phonon scattering and μ account for the temperature dependence of S_p.

For samples large enough for boundary scattering to be negligible and at temperatures well below the Debye temperature, phonon-phonon collision theory predicts that as $q \to 0$

$$[\tau_{\ell}(q)]^{-1} = A_{\ell} T^3 q^2 \tag{7.14}$$

and

$$[\tau_t(\vec{q})]^{-1} = A_t T^4 q \tag{7.15}$$

where l and t refer to the longitudinal and transverse modes respectively. Thus it is expected that the longitudinal modes will contribute more than the transverse modes to the thermoelectric power. One usually sets

$$[\tau_\alpha(\vec{q})]^{-1} = A_\alpha T^{3-s-\gamma} q^{2+s} \tag{7.16}$$

where for longitudinal modes as $q \to 0$, $s \to 0$ and γ goes from 0 at low T to 2 at high T; for transverse modes $s \to -1$ and γ goes from 0 to 3.

In the case where q is small enough to neglect transverse modes and for $\mu \sim T^{-3/2}$ in (7.12), the temperature variation of S_p is approximately given by:

$$S_p \sim T^{-7/2 + 1/2\, s + \gamma}. \tag{7.17}$$

If the τ for the transverse phonon modes are not negligible compared to those of the longitudinal modes, the observed S_p will be a sum of two expressions of the form (7.17), with different values of s. And if τ is not $\ll \tau_b$, the two relaxation times must be combined as will be done later.

As the temperature decreases $\tau_\alpha(\vec{q})$ increases to the point where it is highly probable that a phonon will travel through the entire specimen without colliding with any other phonons. At very low temperatures only scattering from the boundary remains. In this temperature range it is a good approximation to let

$$c_\alpha(\vec{q})\, \tau_\alpha(\vec{q}) = L(\vec{q}) \tag{7.18}$$

It is assumed that L(q) is independent of the phonon wavelength and of temperature but depends on the orientation of $\vec{q}$ with respect to the axis of the specimen. By weighting the different directions in proportion to $c(\vec{q})\, f(\vec{q})$ one can obtain a mean value for (7.18) for each polarization mode. Equation (7.13) then becomes

$$S_p = (\bar{L}_\ell \bar{c}_\ell f_\ell + \bar{L}_t \bar{c}_t f_t)/\mu T. \tag{7.19}$$

For a specimen of square cross section and for $\bar{L}_t = \bar{L}_\ell$, $\bar{L}_\alpha$ is 1.1 times the length of a side of the square. For the case of purely lattice scattering of electrons (7.19) is proportional to $T^{1/2}$.

When phonon-phonon scattering and boundary scattering are of comparable importance it is necessary to solve an equation relating the rate at which the phonons receive crystal momentum and the rate at which it is lost due to collisions with other phonons and with the boundary in the steady state. Herring[4] has done this for the simple case of a plane parallel slab with a current parallel to the surface. He found that the ratio ρ of the S_p of a finite specimen to that of an infinite specimen is a function of a variable ξ_α where

$$\xi_l \propto 1/(T^4 \bar{L}_l)$$

$$\xi_t \propto 1/(T^{9/2} \bar{L}_t) \qquad (7.20)$$

ρ is nearly unity for $\xi_\alpha \sim 3 \times 10^{-3}$ and nearly zero for $\xi_\alpha \sim 50$. These values were taken from a plot of ρ vs ξ_α in Herring's paper.[4]

The above discussion is valid only for the case of low carrier densities. This made it possible to treat the perturbation of the phonon system by the carriers as small enough so that its reaction back on the carriers could be neglected. This meant that in the calculation of π_p, the rate of loss of crystal momentum from the electric current to the phonons could be assumed the same as if the phonons were in thermal equilibrium. It is easy to see that an increase in carrier density will cause a decrease in π_p and hence S_p. At high carrier densities phonon-electron collisions, which cause the phonons to lose crystal momentum, become important so that energy flux of the phonon system is reduced. It can be shown[5] that the carrier density reduces S_p according to

$$S_p = S_{po} \left[1 + \frac{3S_{po}}{(k/e)} \frac{n}{n_m}\right]^{-1} \qquad (7.21)$$

where S_{po} is the limit of S_p for very small carrier density and n_m is the number of phonons responsible for the energy flux in the definition of π_p.

R. M. Nicklow

REFERENCES

1. H. P. R. Frederikse, "Thermoelectric Power in Germanium Single Crystals," Physical Review 91, 491 (1953).

2. T. H. Geballe, "The Seebeck Effect in Germanium," Physical Review 92, 857 (1953).

3. H. P. R. Frederikse, "Thermoelectric Power of Germanium Below Room Temperature," Physical Review 92, 248 (1953).

4. C. Herring, "Theory of the Thermoelectric Power of Semiconductors," Physical Review 96, 1163 (1954).

5. C. Herring, "The Role of Low Frequency Phonons in Thermoelectricity and Thermal Conduction," Semiconductors and Phosphors, Interscience Publishers, New York 184-235 (1958).

6. W. Shockley, "Transmitted Phonon Drag," Structure and Properties of Thin Films, John Wiley and Sons, Inc. Publishers, New York.

8. CYCLOTRON RESONANCE IN METALS

Cyclotron resonance in metals is the resonance absorption of electromagnetic energy of frequency, ω, which is a multiple of the cyclotron frequency $\Omega = \frac{eH}{mc}$, when a stationary magnetic field is applied parallel to the metal surface.

Cyclotron resonance in metals, which is also called the Azbel'-Kaner effect after the investigators who first predicted and discussed the effect theoretically,[1,2,3] has now been observed in a number of metals. The effect is related to but differs significantly from that discussed in our WADC Technical Report No. 59-737 of October, 1959. The cyclotron resonance effect discussed previously refers to the resonance absorption of electromagnetic energy by electrons or holes in a semiconductor or semimetal.

Classically, one can picture an electron which has a component of velocity in the direction of a uniform stationary magnetic field parallel to the metal surface as following a helical path, the axis of the helix being along the field direction as shown schematically in Figure 6.

Because of the high concentration of electrons in a metal the skin depth, δ, corresponding to the penetration of electromagnetic energy into the metal, is a small fraction of the radius, r, of the orbit. This is in contrast to the semiconductor case where the opposite is true. If the mean free path of

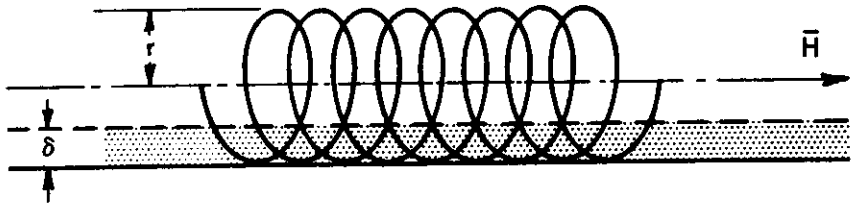

Figure 6. The Trajectory of an Electron in a Magnetic Field.

the electron in the metal is long compared to the radius of the orbit then the electron will make a large number of revolutions before being scattered by lattice vibrations, imperfections, or the surface. In practice, this condition is satisfied by using high purity samples maintained at liquid helium temperatures. Each time the electron enters the region of penetration of the electromagnetic field it will absorb energy if the frequency, ω, of the radiation is a multiple of the cyclotron frequency, $\Omega = \frac{eH}{mc}$. Because of the closer analogy of this effect with the cyclotron, Azbel' and Kaner have suggested[2] that the term cyclotron resonance be restricted to the metal case and that the effect in the semiconductor case where absorption

can take place over the entire orbit and only for a single frequency be called diamagnetic resonance.

The cyclotron resonance effect is related to the electronic structure of the metal and, therefore, a study of this effect should provide some information about the detailed characteristics of the Fermi surface.[4] We shall briefly indicate the nature of this relationship by examining the motion of an electron in wave number or k-space under the influence of an applied uniform magnetic field, $\vec{H}$. Since the electron does not gain any energy from the magnetic field it moves in an orbit on a constant energy surface. The orbit is defined by the intersection of a plane perpendicular to the magnetic field, $\vec{H}$, and the constant energy surface. The time integral around the orbit then leads to an orbit frequency, ω, from which one can define an effective mass, m*, different from the free electron mass. Experimentally determined effective masses enable one, in principle, to verify theoretically predicted orbits and thus establish details of the Fermi surface.

The force, $\vec{F}$, on an electron due to the magnetic field $\vec{H}$ is given by the relation

$$\vec{F} = \dot{\vec{P}} = -(e/c)\,\vec{v} \times \vec{H} \tag{8.1}$$

where P is the time derivative of the crystal momentum, $\vec{P}$, and $\vec{v}$ is the velocity of the wave packet representing the electron. In wave number space $\vec{P}$ is replaced by $\hbar\vec{k}$ and $\vec{v}$ is expressed as $\hbar^{-1}\, dE/d\vec{k}$. Since the force due to $\vec{H}$ is perpendicular to $\vec{v}$, no work is done on the electron and therefore the electron's energy is unchanged. Also, the component of $\vec{k}$ in the direction of the field, k_H remains constant. As a result, the orbit of the electron in k-space is given by the intersection of the plane, k_H = constant, and a constant energy surface. An equation for the orbit frequency, given by Harrison,[4] can be obtained. If $\vec{k}$ is further resolved in the plane into components tangential and normal to the orbit k_t and k_n respectively, then the equation of motion can be written:

$$\hbar\dot{k}_t = -(e/c)H\hbar^{-1}\,\partial E/\partial k_n \tag{8.2}$$

so that

$$dt = -(\hbar^2\, c/eH)\,(\partial k_n/\partial E)\,dk_t. \tag{8.3}$$

Taking the time integral around a closed orbit gives the period, τ_c, where

$$\tau_c = (\hbar^2 c/eH)\oint (\partial k_n/\partial E)\,dk_t$$

$$= (\hbar^2 c/eH)\quad (\partial A/\partial E)_{k_H} \tag{8.4}$$

where $(\partial A/\partial E)_{k_H}$ is the change of the orbit area in wave-number space in the

plane, k_H = constant, with respect to energy. The orbit or cyclotron frequency is

$$\omega_c = \frac{2\pi}{\tau_c} = (2\pi eH/\hbar^2 c)/(\partial A/\partial E)_{k_H}. \qquad (8.5)$$

If one defines a cyclotron effective mass, m*, in terms of this frequency by $\omega_c = eH/m^*c$ then the oscillations in 1/H have a period $\Delta(1/H) = e/c\omega_c m^*$.

As an example of the types of electron orbits that may occur in k-space we have reproduced in Figure 7 energy bands for aluminum in the reduced zone scheme showing the Fermi surfaces obtained by Harrison[4,5] and have indicated typical orbits lead to three effective masses, two of which have been observed experimentally.[6,7]

Besides aluminum cyclotron resonance has been observed in copper,[8,11] zinc,[9] and tin.[10] Experiments are usually performed at microwave frequencies, e.g., 24,000 mc/sec, and at about 4.2° K. The sample is carefully oriented and placed in the end wall of a cavity with the stationary magnetic field parallel to the sample surface. The resonances are detected by standard microwave techniques for measuring changes in power absorption and the effect of different orientations of the magnetic field in the plane of the surface is investigated. Galt, Merritt, Yager, and Dail,[9] in their experiments with zinc single crystals, also examined the result of placing the magnetic field normal to the sample surface and propose this method for distinguishing between effects due to electrons and those due to holes. An explanation of the masses obtained for the magnetic field normal to the surface has recently been given.[12]

The difficulty of obtaining a surface smooth and parallel to a magnetic field has been recognized. In fact, Phillips has proposed[13] that the condition for resonance be that the drift velocity in the direction of the magnetic field is zero. Then, even though the magnetic field is tilted slightly to the surface and the surface is not atomically smooth, a resonance would still occur for electrons in those regions of the surface which are nearly parallel to the field. Harrison[4] has also considered this problem and concludes that there is still an uncertainty as to whether such a condition is necessary. An interesting idea, the existence of open magnetic orbits due to the complicated nature of the Fermi surface in some polyvalent metals, has been pointed out by Blount.[14] According to Blount these open orbits which extend indefinitely in k-space can lead to resonances as well as the closed orbits.

The cyclotron resonance in metals gives information on the rate of change of orbit area with energy; from this information one would hope to obtain $\partial E/\partial \vec{K}$ but a knowledge of the geometry of the Fermi surface is required also. Other solid state effects which give information on the Fermi surface in metals are the de Haas van Alphen effect, the acoustomagnetic effect (oscillations in the ultrasonic attenuation as a function of magnetic field), and the anomalous skin effect.

E. J. Scheibner

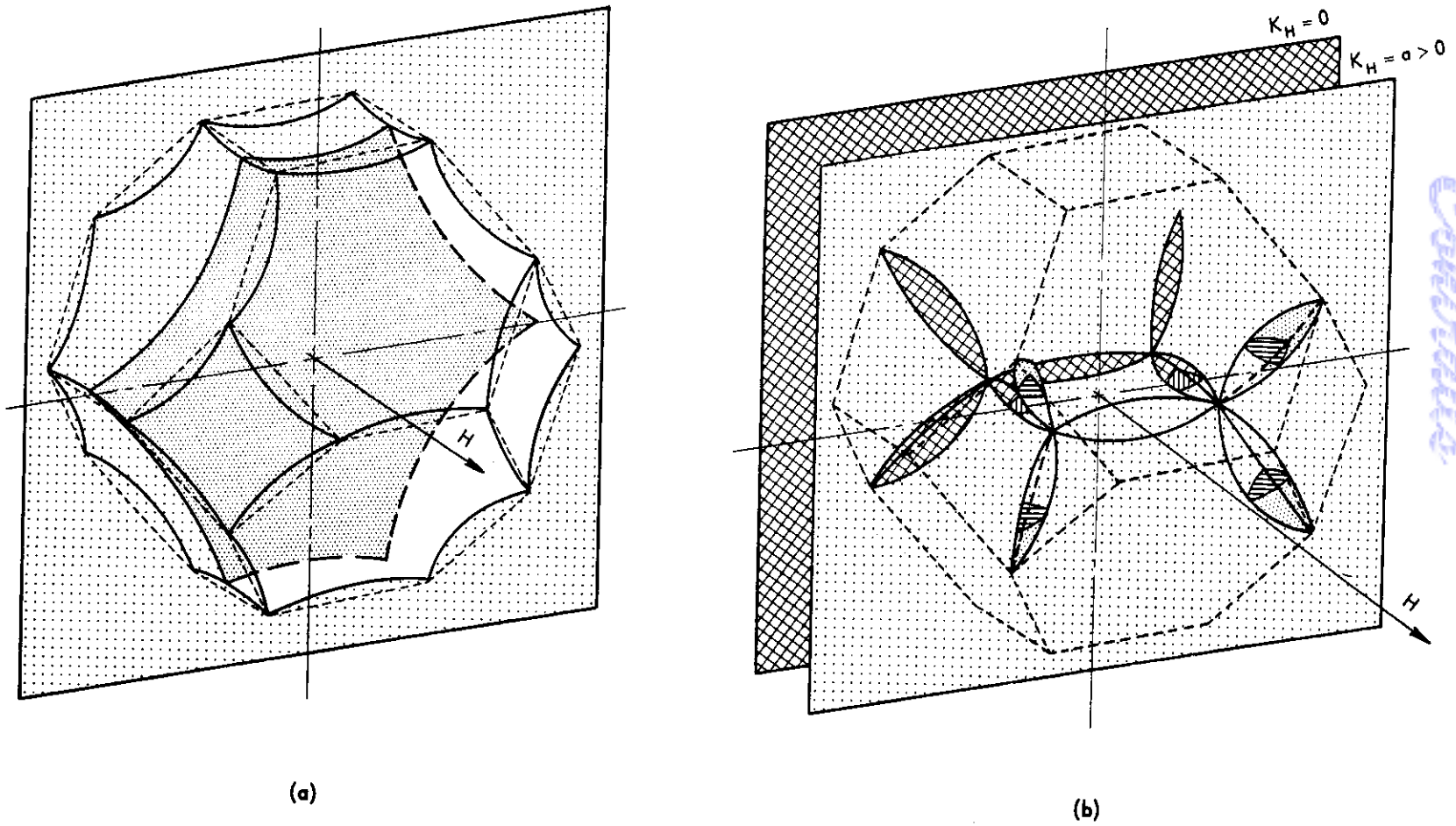

Figure 7. Fermi Surfaces in (a) the 2nd and (b) 3rd Reduced Zones of Aluminum Showing Orbit Areas Corresponding to Different Cyclotron Masses.

REFERENCES

1. M. Ia. Azbel' and E. A. Kaner, "Cyclotron Resonance in Metals," Soviet Physics JETP 3, 772, (1956).

2. M. Ia. Azbel' and E. A. Kaner, "Theory of Cyclotron Resonance in Metals," Soviet Physics JETP 5, 730 (1957).

3. M. Ia. Azbel' and E. A. Kaner, "Cyclotron Resonance in Metals," Physics and Chemistry of Solids 6, 113, (1958).

4. W. A. Harrison, "Electronic Structure of Polyvalent Metals," Physical Review 118, (1960).

5. W. A. Harrison, "Band Structure of Aluminum," Physical Review, 118, 1182, (1960).

6. D. N. Langenberg, and T. W. Moore, "Cyclotron Resonance in Aluminum," Physical Review Letters 3, 137, (1959).

7. E. Fawcett, "Cyclotron Resonance in Aluminum," Physical Review Letters 3, 139, (1959).

8. D. N. Langenberg and T. W. Moore, "Cyclotron Resonance in Copper," Physical Review Letters, 3, 328, (1959).

9. J. K. Galt, F. R. Merritt, W. A. Yager, and H. W. Dail, Jr., "Cyclotron Resonance Effects in Zinc," Physical Review Letters, 2, 292, (1959).

10. A. F. Kip, D. N. Langenberg, B. Rosenblum, and G. Wagoner, "Cyclotron Resonance in Tin," Physical Review 108, 494, (1957).

11. E. Fawcett, "Cyclotron Resonance in Tin and Copper," Physical Review 103, 1582, (1956).

12. P. A. Bezuglyi and A. A. Galkin, "Cyclotron Resonance in Tin at 9300 Mc/s," Soviet Physics JETP 6, 831, (1958).

13. J. C. Phillips, "Cyclotron Resonance in Metals," Physical Review Letters, 3, 327, (1959).

14. E. I. Blount, "Direct Observation of Open Magnetic Orbits," Physical Review Letters 4, 114 (1960).

9. ACOUSTOMAGNETIC EFFECT

Acoustomagnetic resonance is that phenomena which is characterized by minima in the attenuation of applied sound in a pure metal crystal at low temperatures and in an applied magnetic field.

The first experimental evidence that electrons in metals could contribute significantly to the attenuation of megacycle sound waves was obtained by Bömmel.[1] The importance of the electronic system was indicated by the observed change in attenuation upon crossing the superconducting transition. Pippard's[2] free electron gas theory successfully accounted for the major experimental features of this attenuation.

Bömmel[3] later found a nonmonotonic dependence of the attenuation upon magnetic field in tin at liquid helium temperatures. The attenuation was found to be periodic in the reciprocal of the applied magnetic field. Pippard[4] proposed that such oscillations could arise from a matching of the diameters of electron orbits in a magnetic field and the wavelength of the incident sound wave. Later theoretical work[5,6,7,8,9] has verified that this explanation is qualitatively correct. Since Bömmel's original experiments, work has been done on copper[10,11] and tin,[12] bismuth,[13] gold and silver[14] and aluminum.[12,15]

The detailed theory developed by Cohen, Harrison, and Harrison,[9] which is a self-consistent, semiclassical treatment of a free electron gas in a positive background supporting a sound wave, gives the resonance condition as

$$d = \frac{2p_F c}{eH_o} \approx n\lambda, \qquad (9.1)$$

where d is the orbital diameter of an electron at the Fermi surface and p_F is the Fermi momentum. H_o is the applied magnetic field and c and e are physical constants. λ is the wavelength of the sound and n is an integer. One notes that the periods in $1/H_o$ scale with λ rather than with $1/w$ as in cyclotron resonance.

The quantity of interest experimentally is the attenuation coefficient, α, which gives the exponential decay of sound intensity with distance. The physical origin of the attenuation lies in the dissipation, through collisions, of the kinetic energy associated with displacement and distortion of the electron orbit by the sound wave. It is the amplitude of this displacement which becomes a maximum at geometric, or magneto-acoustic, resonance. When the displacement amplitude is a maximum, the electrons follow the motion of the lattice most effectively and the attenuation is a minimum.[13] Equation (9.1) gives the values of H_o for minimum attenuation. Another way of saying this is that the geometric resonances have to do with the strength of the interaction between the particular orbits and the electric field and are not due to resonant absorption of energy.

The attenuation coefficient, α, is the power density dissipated per unit energy flux, or[9]

$$\alpha = \frac{Q}{1/2\ M\ |\vec{\mu}|^2\ \nu_s}, \tag{9.2}$$

where M is the mass of the metal under investigation, ν_s is the velocity of sound, $\vec{\mu}$ is the velocity field ($\vec{\mu}(\vec{r},t) \alpha \exp[i(\vec{q}\cdot\vec{r}-\omega t)]$ where $\vec{q}$ is the sound wave propagation vector, ω is the sound frequency), and Q is the net power dissipated per unit volume and is given by

$$Q_i = \frac{N_o m\ |\vec{\mu}|^2}{2\tau}\ S_{ii}, \tag{9.3}$$

where N_o = electrons/ per unit volume, m is the mass of the electron, τ is the relaxation time and S_{ii} represents the tensor which relates Q to the electric field and conductivity -- S_{ii} is of the order of unity.[9]

From equations (9.2) and (9.3) α becomes

$$\alpha_i = \frac{m \nu_F S_{ii}}{M\ \nu_s \ell} \tag{9.4}$$

where $\ell = \nu_F t$ is the mean free path of an electron and ν_F is the Fermi velocity. Since α, by its nature, is the reciprocal of the mean free path, L, of the sound wave, the relation between L and ℓ implied by (9.4) is

$$L_i = \frac{M \nu_s}{m \nu_F}\ \frac{\ell}{S_{ii}}\ . \tag{9.5}$$

For copper, for example,[9] M ν_s/M ν_F is about 100 so that

$$L_i \simeq \frac{100\ \ell}{S_{ii}}\ . \tag{9.6}$$

Ease of measurement and the general order of magnitude of background attenuation require[9] that L be of the order of 1 cm, thus ℓ must be of the order 0.1 mm or longer for readily observable attenuation by electrons. This then requires pure material and low temperatures. The evaluation of $\| \sigma \|$ the conductivity tensor, in the presence of a magnetic field leads[9] to terms which have a Bessel function dependence. Since the tensor $\| S \|$ involves the conductivity tensor these oscillatory terms give α an oscillatory behavior.

Morse, Myers and Walker,[14] using acoustomagnetic resonance, were able to show that the Fermi surfaces in gold and silver contact the Brillouin zone boundary in the <111> directions. This shape is similar to that of copper, which was studied by the anomalous skin effect (See the next article in this report).

F. B. Dyer

REFERENCES

1. H. E. Bömmel, "Ultrasonic Attenuation in Superconducting Lead," Physical Review (L), 96, 220, (1954).

2. A. B. Pippard, "Ultrasonic Attenuation in Metals," Philosophical Magazine, 46, 1104, (1955).

3. H. E. Bömmel, "Ultrasonic Attenuation in Superconducting and Normal-Conducting Tin at Low Temperatures," Physical Review (L), 100, 758 (1955).

4. A. B. Pippard, "A Proposal for Determining the Fermi Surface by Magneto-Acoustic Resonance," Philosophical Magazine, 2, 1147, (1957).

5. M. S. Steinberg, "Viscosity of the Electron Gas in Metals," Physical Review, 109, 1486, (1958), also "Magnetic Effects in the Attenuation of Transverse Acoustic Waves by Conduction Electron Transport," Physical Review (L), 110, 772, (1958).

6. M. J. Harrison, "Magnetic Field Dependence of Ultrasonic Attenuation," Physical Review Letters, 1, 441, (1958).

7. T. Kjeldaas, "Theory of Ultrasonic Cyclotron Resonance in Metals at Low Temperatures," Physical Review, 113, 1473, (1959).

8. T. Kjeldaas and T. Holstein, "Oscillatory Magneto-Acoustic Effect in Metals," Physical Review Letters, 2, 340, (1959).

9. M. H. Cohen, M. J. Harrison, and W. A. Harrison, "Magnetic-Field Dependence of the Ultrasonic Attenuation in Metals," Physical Review, 117, 937, (1960).

10. R. W. Morse, H. V. Bohm, and J. D. Gavenda, "Electron Resonances with Ultrasonic Waves in Copper," Physical Review (L), 109, 1394, (1958).

11. R. W. Morse, J. D. Gavenda, "Magnetic Oscillations of Ultrasonic Attenuation in a Copper Crystal at Low Temperatures," Physical Review Letters, 2, 250, (1959).

12. D. H. Filson, "Low-Temperature Ultrasonic Attenuation in Tin and Aluminum," Physical Review, 115, 1516, (1959).

13. D. H. Reneker, "Ultrasonic Attenuation in Bismuth at Low Temperatures," Physical Review, 115, 303, (1959).

14. R. W. Morse, A. Myers, C. T. Walker, "Fermi Surfaces of Gold and Silver from Ultrasonic Attenuation," Physical Review Letters, 4, 605, (1960).

15. B. W. Roberts, "Magneto-Acoustic Oscillations and the Fermi Surface in Aluminum," Physical Review, 119, 1889, (1960).

10. ANOMALOUS SKIN EFFECT

The normal skin effect refers to the damping of an electromagnetic wave in a conductor such that the skin depth, $\delta_o = (2\pi\omega\sigma)^{-1/2}$, gives the penetration distance to a point where the amplitude of the electric vector is equal to 1/e its value at the surface; when conditions exist which make ℓ, the mean free path of electrons, much greater than skin depth, δ_o, the effect is called the anomalous skin effect.

Observations of the anomalous skin effect are usually made by measuring the surface resistance of high purity metals at high frequencies and low temperatures. The surface resistance cannot easily be measured directly but it is deduced from the amount of high frequency power absorbed by the sample. This effect has been studied in a number of metals including Au[1,3], Al[1,3], Ag[1,3], Su[1,2,3,4], Cd[3], Pb[3], Cu[1,3,5], and Bi[6]. The most recent detailed studies are those by Pippard on copper[5] and Smith on bismuth[6] single crystals.

It has been shown theoretically[7,8] that information about the Fermi surface can be obtained from studies of the anomalous skin effect in pure metals. The method is not straightforward since the surface resistance is related to the curvature of the Fermi surface perpendicular to a particular line on the surface.[9] The interpretation of the measurements requires some previous knowledge or assumption about the shape of the Fermi surface. The method has advantages, however, since there is no need to know electron velocities or relaxation times. As stated by Pippard[5] the anomalous skin effect may be useful for supplementing information obtained by the de Haas-van Alphen effect on the more complex metals and it may provide details, which might not be known otherwise, on the Fermi surfaces of the simpler metals such as gold, copper, and silver.

The theory of the effect is best compared to that of the classical or normal skin effect. Consider first the classical skin effect for a semi-infinite metallic specimen with cartesian axes x and y in the plane of the surface and z directed along the normal into the specimen. The surface impedance, z, is defined as the ratio of the rf electric field E(o) at the surface to the total current flowing, $\int_o^\infty J(z)dz$. The surface resistance, R, is the real part of the surface impedance. Using Maxwell's equations, neglecting the displacement current, and making use of the relation, $J = \sigma E$, the following classical skin effect equations are obtained for the electric field, E(z), the skin depth, δ_o, and the surface impedance, z.

$$E(z) = E(o) \exp\left[-(1 + i)\, z/\delta_o\right] \qquad (10.1)$$

$$\delta_o = (2\pi\omega\sigma)^{-1/2} \qquad (10.2)$$

$$Z = (4\pi i\omega/\sigma)^{1/2} \qquad (10.3)$$

where σ is the d.c. conductivity of the specimen and ω is the angular frequency

of the incident rf wave. According to these equations, the surface conductivity, $\sum \equiv 1/R$, should increase uniformly with $\sigma^{1/2}$. London[2] observed, in measurements of the high frequency resistance of tin, that $\sum$ was not given by the above relations and was the first to suggest that the discrepancy was due to the fact that the mean free path of electrons happened to be greater than the skin depth, δ_o. Pippard[1] and Reuter and Sondheimer[11] examined this problem further and, pointing out that Ohm's law no longer holds because the electron doesn't move in a constant field between collisions, obtained an integradifferential equation for $E(z)$. Reuter and Sondheimer solved the equation for the free electron model and for the limiting cases of diffuse reflection of electrons (in which drift momentum is reduced to zero) and specular reflection (in which drift momentum is maintained). For both cases, in the limit, $\delta_o \ll \ell$, $\sum$ approaches a constant value $\sum_\infty$ which is independent of σ. Figure 8 compares the form of variation of $\sum$ with σ for the normal skin effect and the anomalous skin effect. It is the

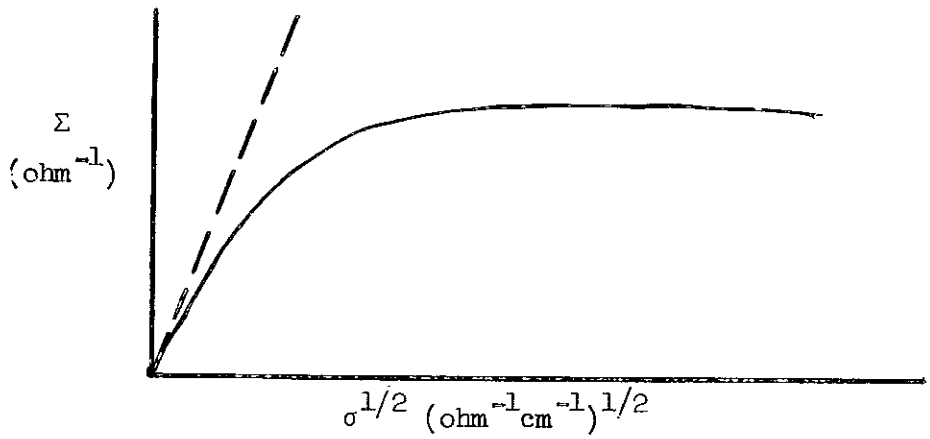

Figure 8. Surface Conductivity Curves Showing the Normal Skin Effect (Dashed Line) and the Anomalous Skin Effect (Solid Line).

extreme anomalous range where $\sum$ is independent of σ that useful information related to the Fermi surface can be obtained.

In general, the surface resistance is a tensor varying according to the angle between the current direction and a principal axis. For a plane surface ($z = o$) with the x- and y-axis along the principal axes of the tensor, the surface resistance can be written

$$R = R_x \cos^2\theta + R_y \sin^2\theta \qquad (10.4)$$

where θ is the angle between the current direction and the x-axis. In his discussions, Pippard[5] uses an "ineffectiveness concept" in which he assumes

that only those electrons which have velocities parallel to the specimen surface are effective in determining the surface resistance. On this basis he derives the following expression for R_x (and a similar one for R_y) in the limit of infinite mean free path:

$$R_x = \frac{\sqrt{3}}{2}\left\{\frac{\pi\omega^2\hbar^3}{e^2\int|\rho_y|dy}\right\}^{1/3} \qquad (10.5)$$

where ρ_y is the radius of curvature of the Fermi surface in a plane normal to the y-axis at a point on an "effective zone" of the Fermi surface and the integral is taken over the entire effective zone. The effective zone is defined by the locus of all points on the Fermi surface at which the normal to the Fermi surface is perpendicular to the z-axis. Electrons near this zone are those whose velocities are essentially parallel to the specimen surface.

Note that the curvature of the Fermi surface appears in an integral which is to be integrated over a path on the Fermi surface. Hence, unless some knowledge exists about the Fermi surface, the determination of its shape from anomalous skin effect measurements must be a time-consuming, trial-and-error method. By just such a method Pippard[5] arrived at a detailed shape of the Fermi surface of copper and the conclusion that the surface touches the Brillouin zone boundaries in the vicinity of the <111> directions. Smith,[6] using a model of the energy bands in bismuth due to Shoenberg,[12] found that his results for the surface resistance of the semi-metal could be explained by a Fermi surface consisting of six electron ellipsoids and two hole ellipsoids as shown in Figure 9. His data are in essential agreement with de Haas-van Alphen and cyclotron resonance experiments.

E. J. Scheibner

REFERENCES

1. A. B. Pippard, "The Anomalous Skin Effect in Normal Metals," Proc. Roy. Soc. A191, 385 (1947).

2. H. London, "The High Frequency Resistance of Superconducting Tin," Proc. Roy. Soc. A176, 522 (1940).

3. R. G. Chambers, "The Anomalous Skin Effect," Proc. Roy. Soc. A215, 481 (1952).

4. E. Fawcet, "The Surface Resistance of Normal and Superconducting Tin at 36 kMc/s," Proc. Roy. Soc. A232, 519 (1955).

5. A. B. Pippard, "An Experimental Determination of the Fermi Surface in Copper," Phil. Trans. Roy. Soc. A250, 325 (1957).

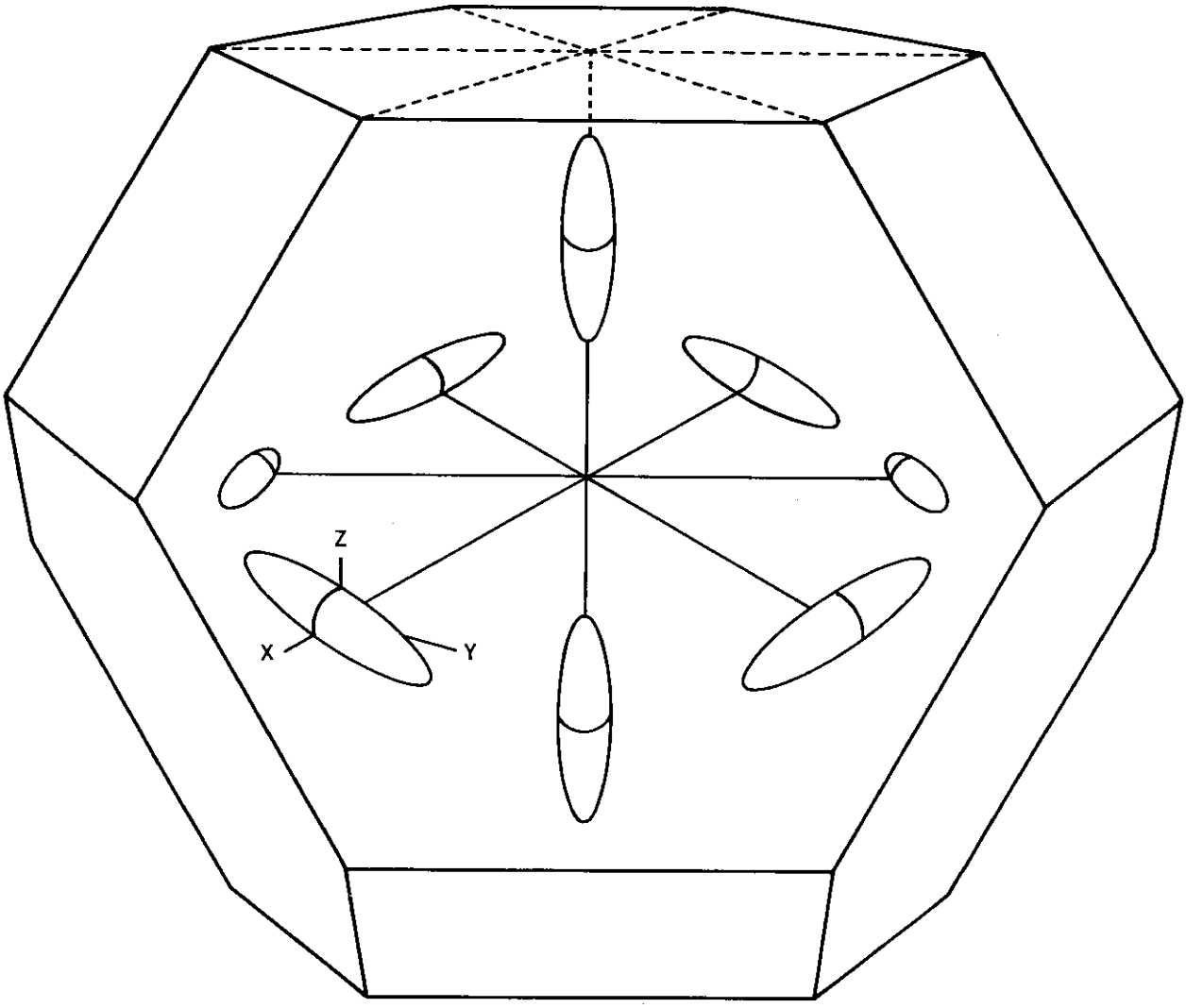

Figure 9. Fermi Surface of Bismuth Showing Six Electron Ellipsoids which Tilt Alternately in Opposite Directions and Two Hole Ellipsoids. (after Smith[6]).

6. G. E. Smith, "Anomalous Skin Effect in Bismuth," Phys. Rev. 115, 1561 (1959).

7. A. B. Pippard, "The Anomalous Skin Effect in Anisotropic Metals," Proc. Roy. Soc. A224, 273 (1954).

8. E. H. Sondheimer, "The Theory of the Anomalous Skin Effect in Anisotropic Metals" Proc. Roy. Soc. A224, 260 (1954).

9. W. A. Harrison, "Electronic Structure of Polyvalent Metals," Phys. Rev. 118, 1190 (1960).

10. R. G. Chambers, "Our Knowledge of the Fermi Surface," Can. J. Phys. 34, 1395 (1956).

11. G. E. H. Reuter and E. H. Sondheimer, "The Theory of the Anomalous Skin Effect in Metals," Proc. Roy. Soc. A195, 336 (1948).

12. J. S. Dhillon and D. Shoenberg, "The De Haas van Alphen Effect," Phil. Trans. Roy. Soc. A248, 1 (1955).

11. THE MOSSBAUER EFFECT

The Mossbauer effect is the resonance absorption of gamma rays in the case where both emitting and absorbing nuclei are prevented from recoiling.

Consider a free nucleus of mass M in an excited state which is E units of energy above the ground state. The nucleus decays to the ground state by emitting a photon of energy $h\nu$ (h is Planck's constant, ν the frequency of the photon). The law of conservation of momentum requires that the nucleus must recoil with a momentum equal and opposite to that of the photon. Energy conservation then demands that the photon energy, $h\nu$, must be less than E by an amount equal to the kinetic energy, R, of the recoiling nucleus. The calculation of R follows in Figure 10. The conservation laws when applied to the

momentum = 0
kinetic energy = 0
internal energy = E

(a) Nucleus before emission of photon.

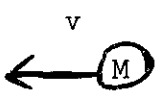

momentum = $-Mv$
kinetic energy = $1/2\ Mv^2$
internal energy = 0

momentum = $h\nu/c$
energy = $h\nu$

(b) Nucleus and photon after emission.

Figure 10. Energy and Momentum Relations in the Emission of a Photon from a Nucleus.

system depicted in Figure 10 yield

$$h\nu = E - 1/2v^2 = E - R, \tag{11.1}$$

$$h\nu/c = Mv, \tag{11.2}$$

where v is the recoil velocity of the nucleus and c is the velocity of light. Eliminating v and solving the resulting equation for $h\nu$, one obtains

$$h\nu = Mc^2 \left\{-1 + \sqrt{1 + 2E/(Mc^2)}\right\}, \tag{11.3}$$

where the extraneous root (with a minus sign in front of the radical) has been dropped. Since in any case of interest Mc^2 is much larger than E, the higher order terms in $E/(Mc^2)$ may be dropped in the binomial-theorem expansion of

(11.3). Then

$$h\nu = E - E^2/(2Mc^2). \tag{11.4}$$

Comparision of (11.1) and (11.4) shows that

$$R = E^2/(2Mc^2). \tag{11.5}$$

The absorption of a photon by a free nucleus at rest is the inverse of the emission process just described, and will take place only if the energy of the photon is E + R. Of course, the gamma rays have a natural line width. What is really necessary for appreciable absorption to take place is that the photon energy be within this natural width of being equal to E + R. The energy difference of 2R between emission and absorption must be made up before a gamma ray can be absorbed by a nucleus of the same species as that which emitted it.

Some possible methods of making up the 2R difference are (1) Doppler shifting the emitted photons by rapidly moving the source; (2) heating both the source and absorber so that the spectral lines are sufficiently temperature broadened to have an appreciable overlap region; (3) using a source which is recoiling with an appropriate velocity as the result of a previous decay. Each of these methods is difficult experimentally.

Mossbauer's contribution[1,2,3] to the resonance absorption of gamma rays was to eliminate the recoil. He accomplished this feat by using nuclei which were tightly bound to their crystal lattice. Under proper conditions the recoil momentum is taken up by the whole crystal and no energy is transferred to the internal vibrations of the lattice. Equation (11.5) shows that the recoil energy varies inversely with the mass of the recoiling particle. The recoil energy of a crystal containing, say, 10^{20} nuclei is quite negligible.

Mossbauer demonstrated the effect by showing[1] that an increase in the temperature of his absorber was accompanied by a decrease in the absorption. This result is quite the opposite from that which is observed with free absorbers in a gas, and is interpreted as arising from the decreased probability for a no-recoil absorption when the thermal vibrations of the lattice are intense.

Possibly more dramatic was Mossbauer's demonstration[2] with the Doppler effect. When the source and absorber were in relative motion with a velocity on the order of 1 cm/sec the absorption decreased by a factor of 2. In this experiment, as well as in the temperature shift experiment, Mossbauer used the 129-kev gamma rays from Ir^{191}. The half-width of the gamma ray is thus shown to be approximately 10^{-5} ev.

The detailed theory for the no-recoil emission of a gamma ray has been adapted from a theory due to Lamb[4] on resonance absorption of neutrons by nuclei in crystals. Visscher[5] discusses this theory rather completely.

In essence, the Mossbauer effect will be observed if the emitting nucleus is in a host crystal which has a low Debye-Waller temperature factor, i.e., has large elastic constants, and if the energy of the emitted photon is sufficiently small, usually in the 10 - 150 kev range. Since the emitting nucleus must be in an excited state before emission, it must be an intermediate step in the decay of some other radioactive nucleus. For example, the Ir^{191} used by Mossbauer resulted from the beta-decay of Os^{191} according to the decay scheme of Figure 11.

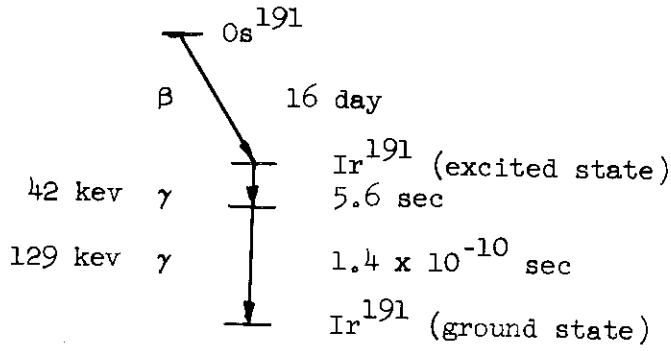

Figure 11. Decay Scheme of Os^{191} to Ir^{191}.

Not all of the γ-emissions are of the no-recoil type, even though the conditions mentioned above are satisfied. For example, both theory and experiment[6] show that the fraction of the photons emitted without recoil from Sn^{119} is 0.285 at 77°K and 0.045 at 300°K.

The Mossbauer effect permits direct measurements to be made of the natural width of γ-ray spectral lines. As pointed out by Visscher[5] it permits determinations of the frequency distribution of lattice vibrations in a different and possibly easier manner than the previously used methods. Also, the effect has been used as a tool with which to check the prediction of the theory of general relativity concerning the frequency shift of a photon in a gravitational field.[7] For this experiment Pound and Rebka used the 14.4 kev, 0.1 microsecond level in Fe^{57}, the parent nucleus of which was Co^{57}. The fractional frequency-shift for photons rising in a gravitational field was found to be different from that for photons falling, and the observed difference was in excellent agreement with the prediction of general relativity. The frequency shifts were measured in each case by noting the relative velocity of source and observer required to peak the absorption. Temperature control is extremely important in an experiment of this kind. The second order Doppler shifts caused by lattice vibrations would have been as large as the effect sought by Pound and Rebka if the temperatures of source and absorber had varied by as little as 1°C.

Vernon Crawford

REFERENCES

1. R. L. Mossbauer, "Kernresonanzfluoreszenz von Gammastrahlung in Ir^{191}," Zeitschrift fur Physik 151, 124 (1958).

2. R. L. Mossbauer, "Kernresonanzabsorption von Gammastrahlung in Ir^{191}," Naturwissenschaften 45, 538 (1958).

These two papers present the experimental arrangements and results which demonstrate the existence of the Mossbauer effect.

3. R. L. Mossbauer, "Kernresonanzabsorption von γ-Strahlung in Ir^{191}," Zeitschrift fur Naturforschung 14a, 211 (1959).

This paper is essentially a review of the first two. All three are in German, of course.

4. W. E. Lamb, Jr., "Capture of Neutrons by Atoms in a Crystal," Physical Review 55, 190 (1939).

The original statement of the basic theory, but as applied to the capture of neutrons rather than of gammas.

5. W. M. Visscher, "Study of Lattice Vibrations by Resonance Absorption of Nuclear Gamma Rays," Annals of Physics 9, 194 (1960).

A review of experiments and theory. Special attention is paid to the light which the Mossbauer effect sheds on the spectrum of lattice vibrations.

6. R. Barloutaud, E. Cotton, J. Picou, and J. Quidort, "Absorption resonnante sans recul du rayonnement γ de 23.8 keV de ^{119}Sn," Comptes Rendus des Seances de l'academie des Sciences, Paris 250, 319 (1960).

7. R. V. Pound and G. A. Rebka, Jr., "Apparent Weight of Photons," Physical Review Letters 4, 337 (1960).

TECHNIQUES: AN ULTRA-HIGH VACUUM SYSTEM

A. Introduction

This section describes a vacuum system designed for producing various types of thin films of high purity at ultra-high vacua by vapor deposition on a variety of substrates. The material was presented in more detail in a paper given by Mr. C. R. Meissner at the Sixth National Vacuum Symposium of the American Vacuum Society in Cleveland, Ohio, on October 12-14, 1960. The paper will be published in the transactions of the Symposium.

B. Pumping Station

The main vacuum system consists of a simple series connection of forepump, foreline valve, oil diffusion pump, chevron baffle, and a liquid nitrogen cooled copper coil within a bell jar. (Figure 12).

The 1300 liters/minute forepump is located in a structure outside the laboratory. Two 3-inch forelines extend into adjacent laboratories for deposition work with two pumping stations on a planned time-sharing basis. The forepump line is provided with thermocouple gauge tubes, a shut-off valve, and also a test nipple for supplementary vacuum work.

The four-jet oil diffusion pump of new design has a pumping speed of approximately 1300 liters per second down to 3×10^{-6} Torr. Cooled alcohol is circulated by a positive displacement pump through the associated chevron baffle. An adaptor ring joins the baffle to the bell-jar plate. This combination of pump and baffle blanks off at a pressure of approximately 10^{-9} Torr.

The use of a high vacuum valve has been purposely omitted in this equipment so that the lowest possible pressure and a high pumping speed can be obtained and also maintained under operating conditions. Back streaming of forepump oil is prevented by pumping through the diffusion pump and by locating the forepump some distance away. Cooling of the diffusion pump oil is done by circulating water through a copper coil located in the boiler of the pump.

The bell jar plate is so designed that jars of either 8-, 12-, 14- or 32-inch diameters and of various configurations can be accommodated. Figure 12 shows a 14- x 18-inch bell jar with cage and counter weight.

Various mechanical feed-throughs permit up to six independent mechanical motions and at least sixteen leads have been provided for electrical measurements and test functions.

The equipment above the bell jar plate is shown in Figure 13. It reflects our special requirements of low pressures being maintained during high filament temperatures and periods of gas evolution during the deposition. A cold trap of the liquid nitrogen circulating type has been found to be very satisfactory.[1]

[1] A High Vacuum Laboratory for the Vapor Deposition of Conductors and Dielectrics by C. Robert Meissner, Third National Vacuum Symposium Transactions, page 15, 1956.

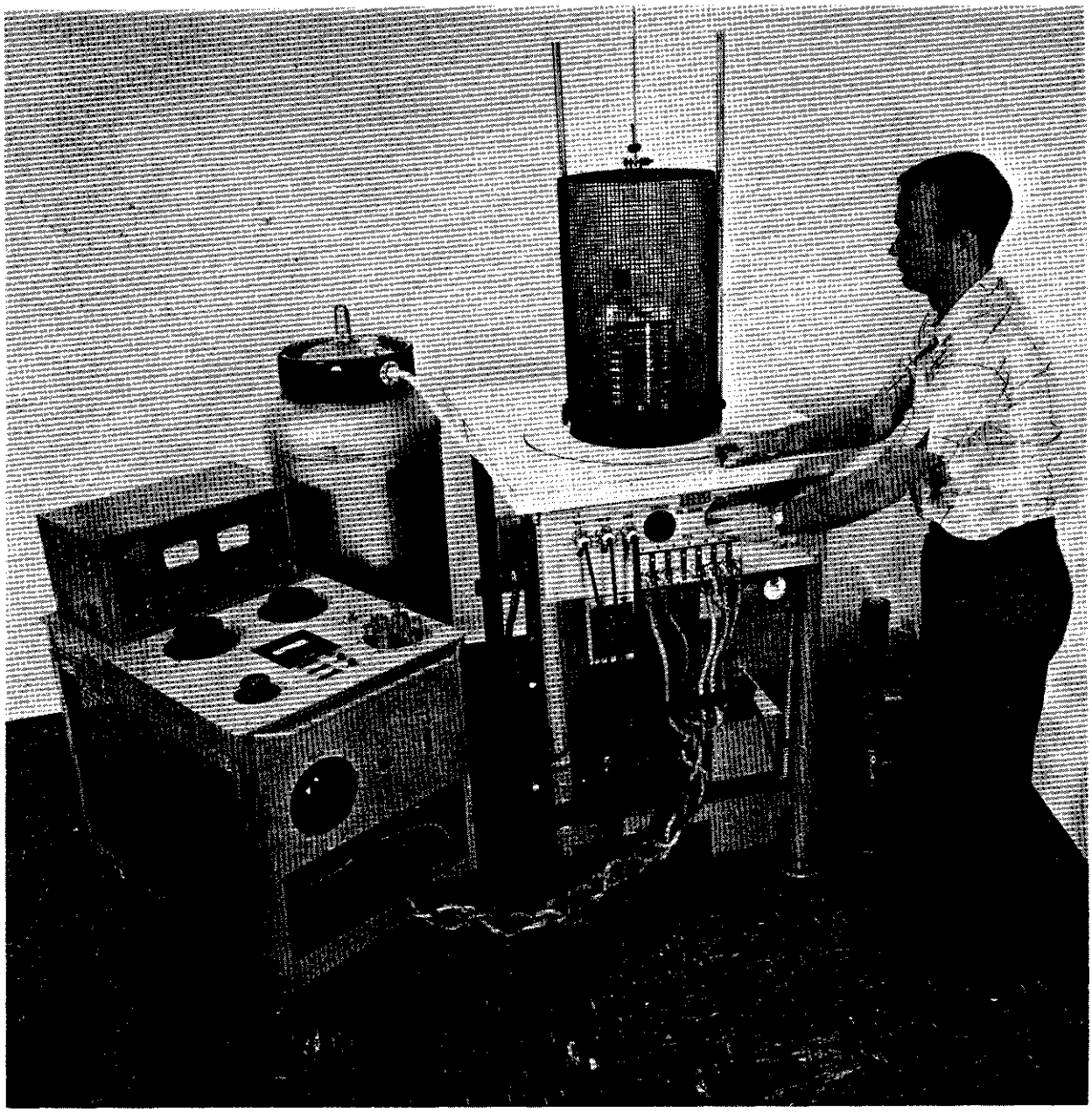

Figure 12. The Ultra-High Vacuum System.

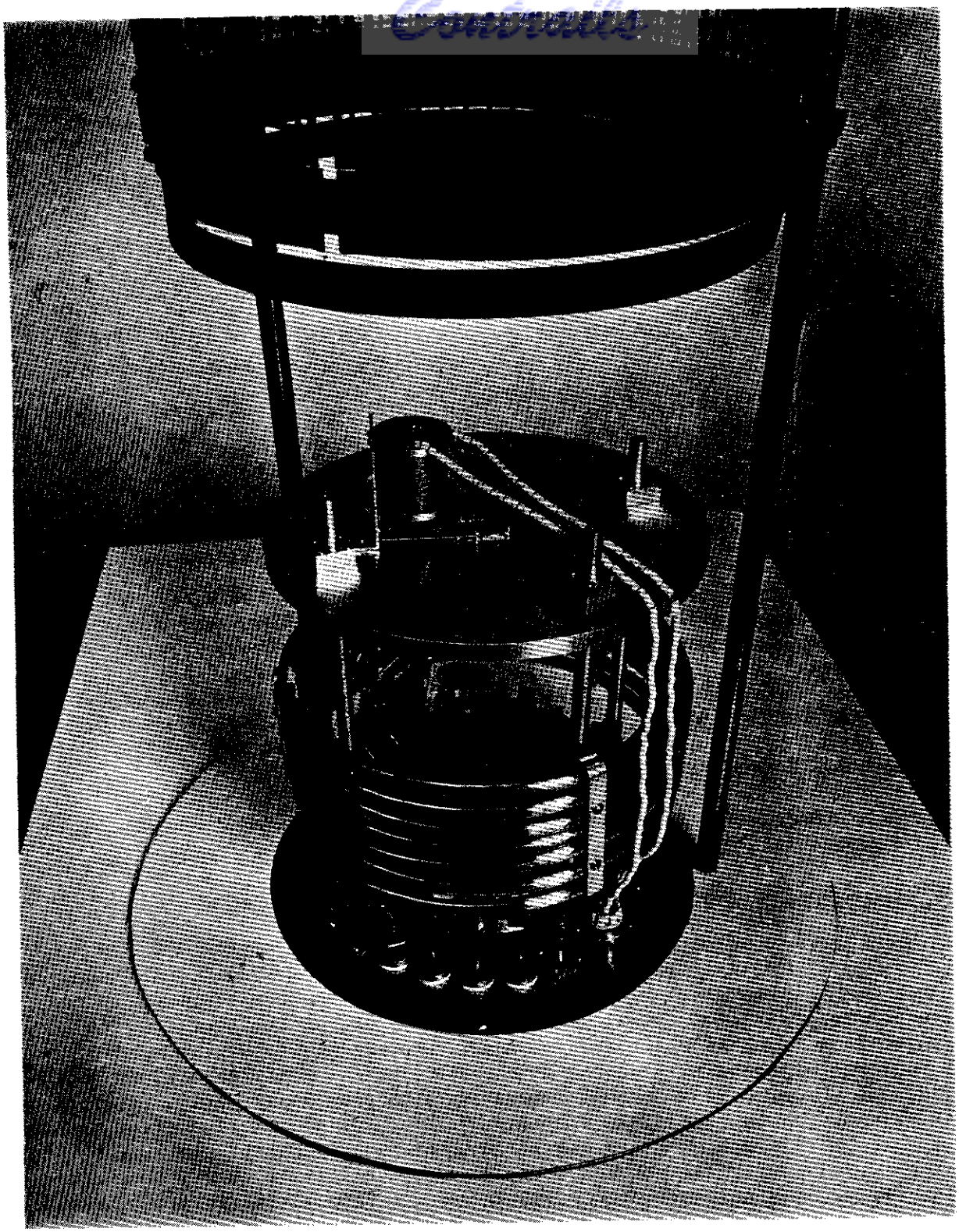

Figure 13. The Bell Jar Equipment with Substrate Carrier Liquid Nitrogen Cooled Trap and Filament Turret Switch.

The trap consists of special feed-through fittings with a length of one-half-inch copper tubing to give a cooling surface twelve times the throat area of the pump. The tubing is shaped into a coil to completely surround the work area which is also the principal source of gas evolution. In Table I is shown the liquid nitrogen consumption of this trap under some conditions of operation.

Table I

Liquid Nitrogen Requirements

Test Condition	Length of Test	Total Consumption	
	Minutes	Lbs.	Liters
Initial cooling from 23° C[2]	10	1.5	0.80
To balance minimum heat loss (ionization gauge operating)	60	10.0	5.60
Dissipating 300 watts of power in one filament	15	3.4	1.92
Dissipating 300 watts in each of three filaments	15	9.0	5.00

The total pressure of the system is measured with a Bayard-Alpert type ionization gauge located in the bell jar. The location of this gauge has been chosen so that it will be shielded from large temperature excursions.

All materials used within the high vacuum portions of the system have been carefully selected for low vapor pressure, and pump-out channels have been provided for all gasket grooves, screw-threads, and other isolated cavities to prevent virtual leaks from those sources.

A schematic diagram of the vacuum system and associated electrical circuits is shown in Figure 14.

C. Vapor Deposition Equipment

A filament turret, as shown in Figure 15 was designed to enable the preparation of a variety of multi-element alloys and multi-layers of films. Eight filament carriers can be seen displayed in fixed stations on an open ring-type turntable which can be positioned by external controls. Through the center of the open ring extends a track on which the filament carriers may travel when moved by two steel tapes actuated by a second external control. Positioned along the center track are three pairs of contact shoes connected by heavy cables to three independently variable sources of AC filament power. Any combination of up to three of the eight filament carriers may be arrayed on the center track and brought into registry with the contact shoes so that the filaments may be heated and the charges on them be evaporated. The filaments themselves are continuously

[2] This test was conducted as follows: With the pressure at approximately 10^{-7} Torr and the trap still at room temperature, the flow of liquid nitrogen was adjusted so that the discharge was on the verge of being liquid. This rate was maintained until discharge did become liquid and the elapsed time noted.

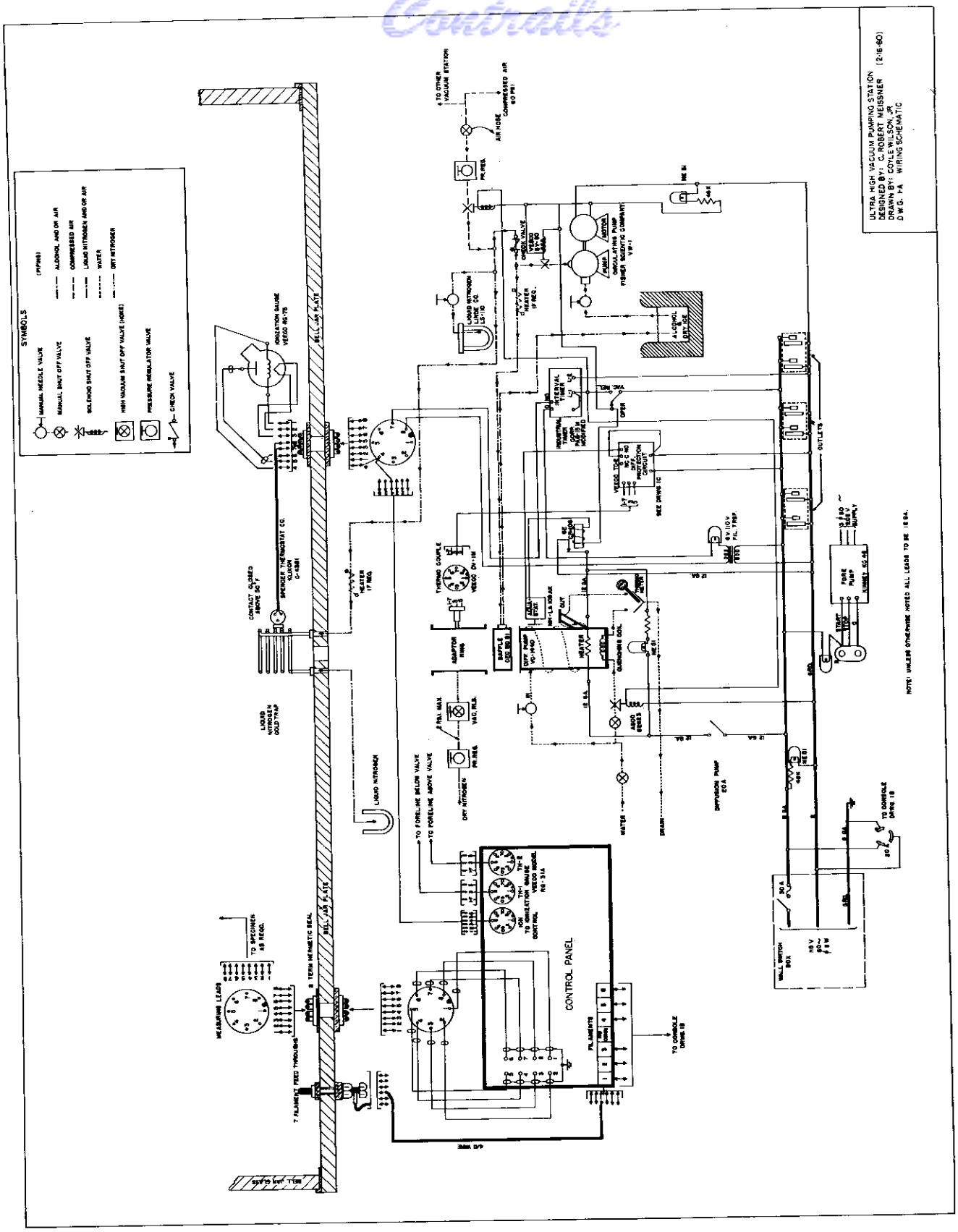

Figure 14. System Wiring Schematic.

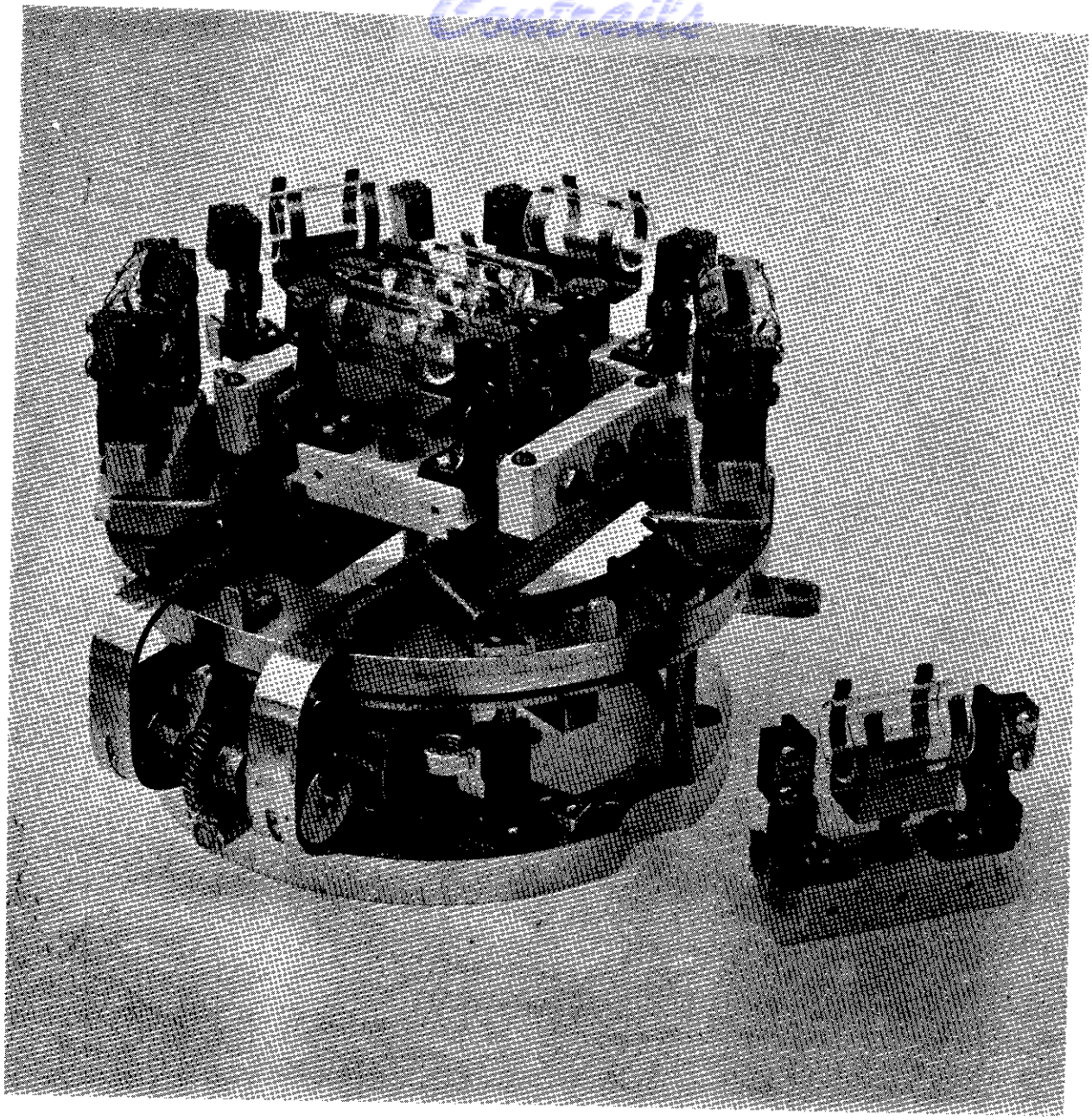

Figure 15. Filament Turret Switch and Filament Carriers.

under tension even when at white heat and may be of any configuration. Either boat or wire shaped structures may be used. Each filament is surrounded by a slotted glass tube capped by tungsten end shields so that the evaporants will emerge only in a wedge shaped pattern which may be aimed at the substrate as required.

D. Substrate Carrier

Upward vapor deposition is used in nearly all our work and the substrate usually consists of flat surfaces such as microscope slides. In Figure 16 is shown one version of a substrate carrier with cutouts for the slides. The filament-to-substrate distance may be varied between a minimum of approximately 4 inches and a maximum of approximately 9 inches. The carrier is also equipped with a masking disk for the desired film geometry and a drive for rotating the disk. The masking ribbon shown is used in connection with the well-known method of measuring film thicknesses with an optical interferometer. A system of springs holds the ribbon tightly against the substrate to obtain a sharp image (Figure 17). The ribbon tension may be released prior to rotating the masking disk to a new position by energizing the electromagnet.

E. Substrate Temperature Control

A pair of special fittings, similar to those used for the liquid nitrogen cold trap, permit the introduction of a liquid coolant into the vacuum chamber. Soft annealed copper tubing and guarded flexible bellows are brazed to a copper heat exchanger and to the fittings forming a closed cooling system within the bell jar. Interchangeable copper shoes, shaped to fit specific experiments, are provided with thermocouples for monitoring the temperature. These are placed upon the reverse side of the substrate and the heat exchanger unit placed in turn upon it with good thermal contact. A cartridge-type heater inserted into the well of the heat exchanger is connected to an external temperature controller. Temperatures in the range from -150°C to approximately +450°C can be obtained.

F. Accessory Equipment

An accessory piece of equipment used with the high vacuum system is a separate console to furnish up to 300 Amperes at low voltage for each of the three filaments as shown at the left in Figure 1. Its schematic wiring diagram is given in Figure 18. A voltage adjusting transformer is connected in series with each of the three heavy duty step-down transformers. The current drawn by the individual filaments can be selectively monitored by a meter. Provision is also made for flash-evaporation techniques. The low and the high currents desired for a filament can be preset and changed abruptly by operating the Preheat-Flash switch. At the same time a second filament can be heated independently to any temperature.

After the films have been made, the console may be rolled away to make room for other test equipment which needs to be close to the specimen still under vacuum. This mobility makes the power unit available for use on some of our other systems.

C. R. Meissner

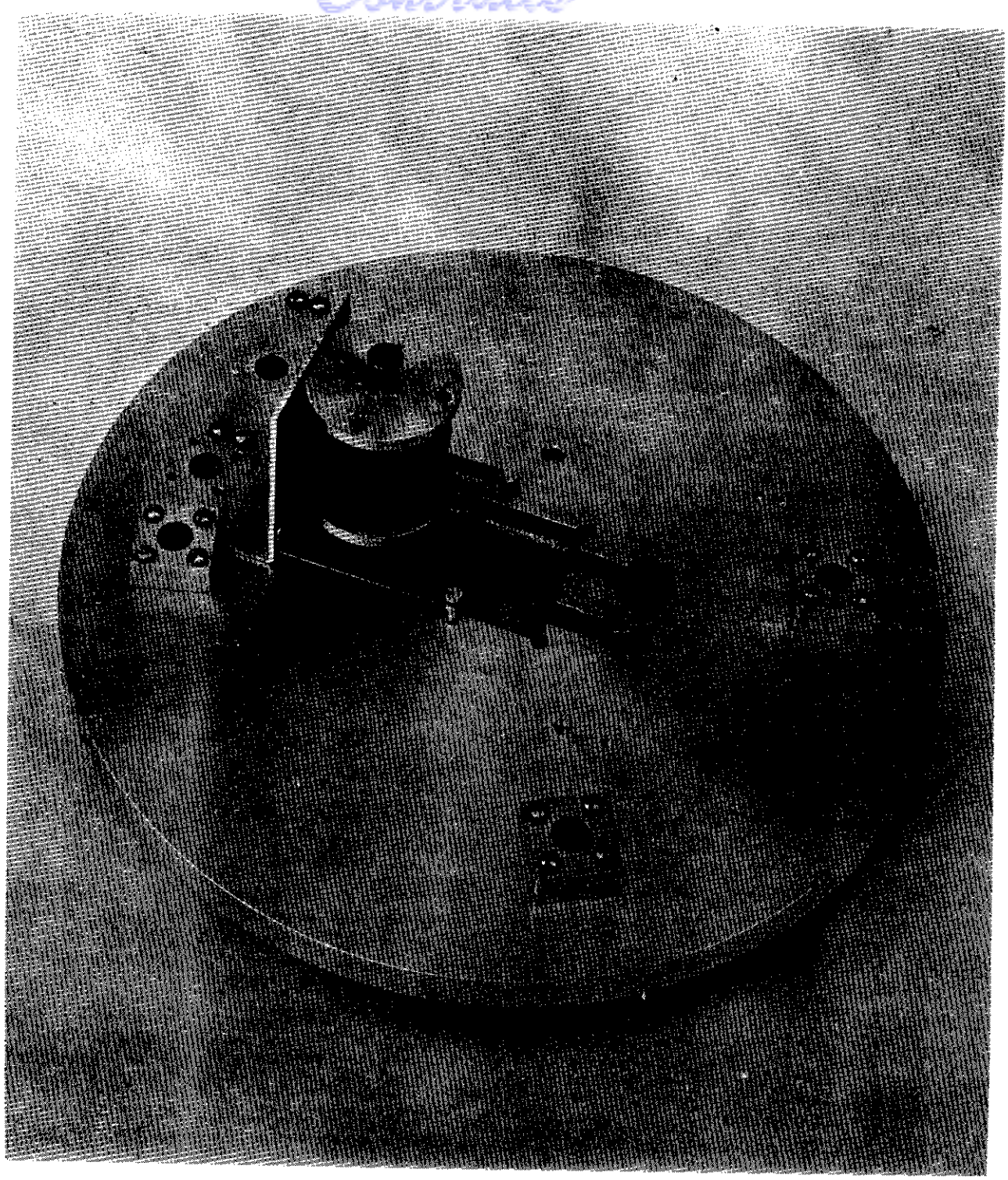

Figure 16. Substrate Carrier - Top View.

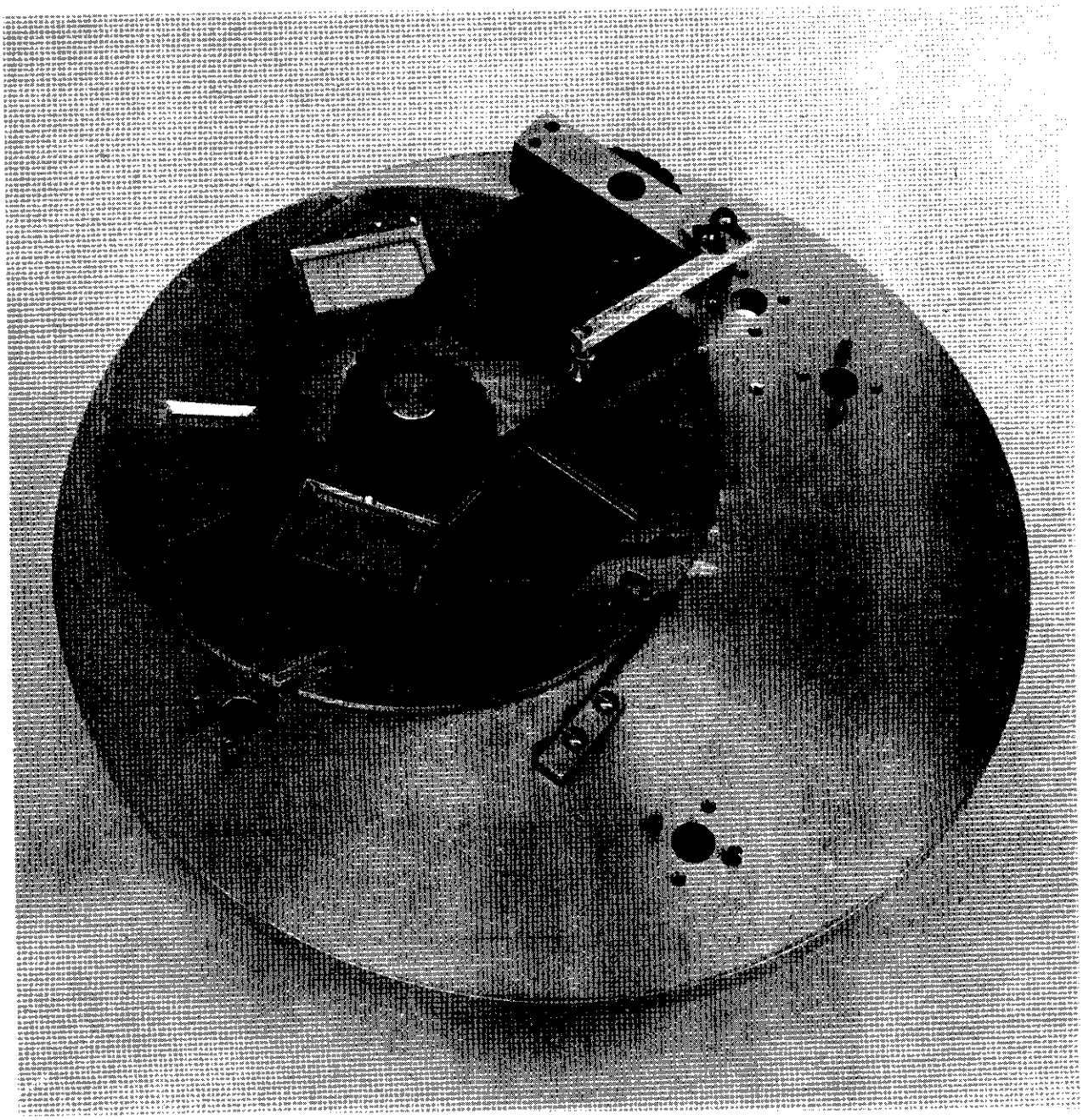

Figure 17. Substrate Carrier - Bottom View.

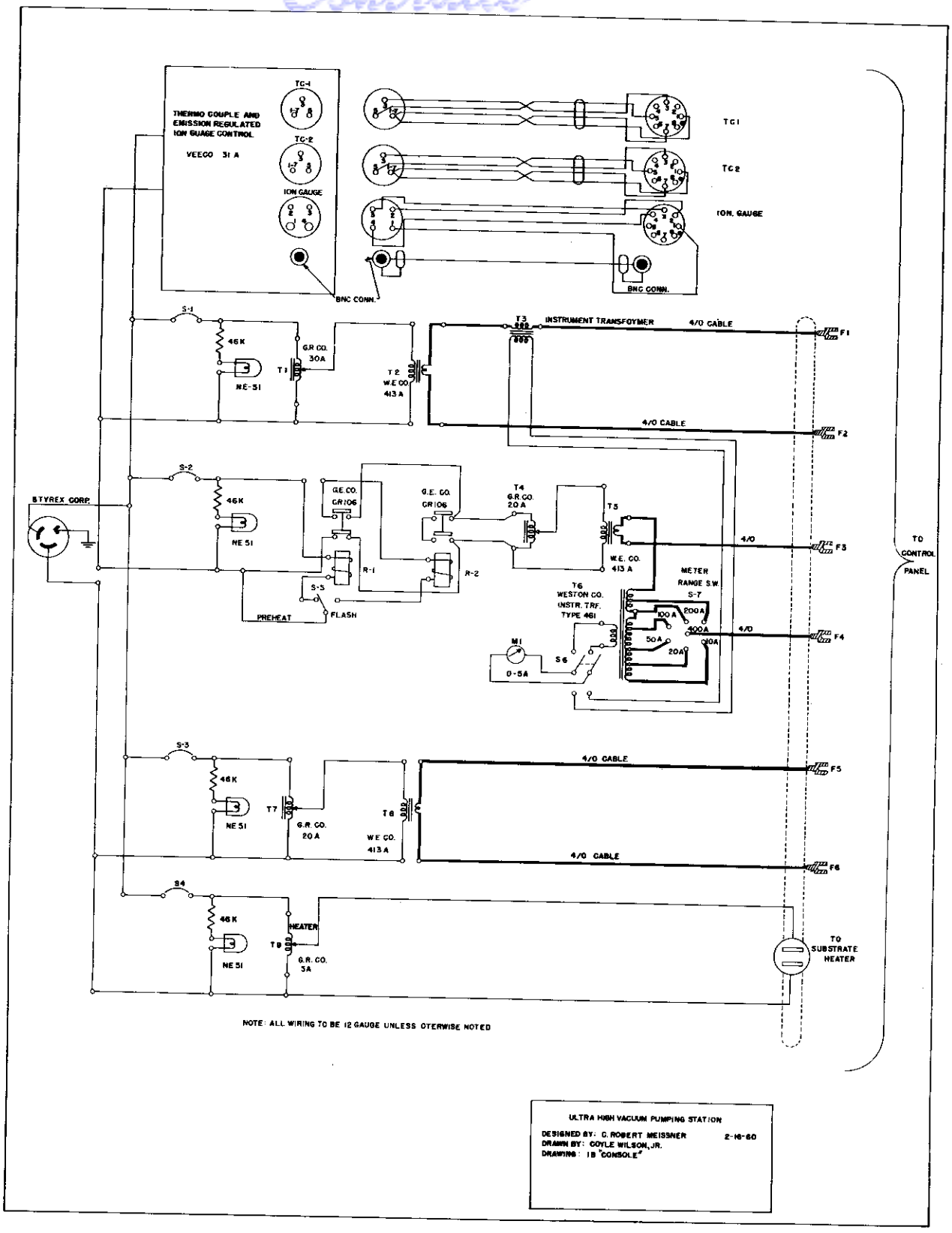

Figure 18. Console Wiring Schematic.

SECTION IV

LITERATURE SURVEY

Sub-Group 1 -- Galvanomagnetic and Thermomagnetic Effects

1.1 R. S. Allgaier, "Magnetoresistance in PbS, PbSe, and PbTe at 295°, 77.4°, and 4.2° K," Phys. Rev. 112, No. 3, 828-36 (November 1, 1958).

Experimental results on the magnetoresistance of single crystals of PbS, PbSe, and PbTe are reported at temperatures of 4.2° K, 77.4° K, and 295° K. The samples had mobilities which change from 500-1700 cm^2/v-sec at room temperature to as high as 800,000 cm^2/v-sec at 4.2° K. The effective mass was found to be very anisotropic. In PbTe, the ratio of the effective mass in a longitudinal direction to the effective mass in a transverse direction was estimated to be between 4 and 6.

1.2 G. S. Anderson, S. Legvold and F. H. Spedding, "Hall Effect in Lu, Yb, Tm and Sm," Phys. Rev. 111, No. 5, 1257-8 (September 1, 1958).

The Hall effect in Lutetium is relatively independent of temperature between 40° K and 320° K. The value of the Hall coefficient for Lu at room temperature is -0.535×10^{-12} volt-cm/amp-oe. The Hall coefficient for Ytterbium has a value of 3.77×10^{-12} volt-cm/amp-oe and is independent of temperature between 80° K and 300° K. The Hall coefficient for Thulium has a value of -1.8×10^{-12} volt-cm/amp-oe between 300° K and 360° K but increases to -5.0×10^{-12} volt-cm/amp-oe at 40° K. The increase is attributed to the extraordinary Hall effect. The Hall coefficient for Saynarium is negative at room temperature but is positive and has a pronounced field dependence at 100° K.

1.3 S. Asanabe and A. Okazaki, "Anomalous Behavior in the Hall Coefficients on the Semiconducting Compounds SnSe and GeSe," Phys. Soc. Lond. Proc. 73, 824-7 (May 1, 1959).

An unusual behavior of the resistivity and Hall Coefficients of SnSe single crystals is reported. After quenching a sample from about 500° C to room temperature there is observed a maximum in R vs 1/T at about 200° C which disappears after long annealing below 200° C.

1.4 J. Babiskin, P. G. Siebenmann, "New Type of Oscillatory Magnetoresistance in Metals," Phys. Rev. 107, 1249-54 (September 1957).

In carefully performed experiments on the magnetoresistance of thin sodium wires at 1° K no characteristic H^{-1} oscillations of the de Haas-van Alphen type were found but a magneto-oscillatory behavior arising from "size effects," as predicted by theory, was observed.

1.5 M. Bailyn, "Transport in Metals: Effect of the Non-Equilibrium Phonons," Phys. Rev. 112, No. 5, 1587-98 (December 1, 1958).

The Boltzmann transport equation is solved by the variational method when three types of interaction are considered: (1) electron-electron, (2) electron-phonon, (3) phonon-phonon. Results are in general agreement with experiment except for the observed positive thermo-electric power of lithium metal.

1.6 I. W. Band, "New Look at the Theory of Electron-Phonon Resonance I," Amer. J. Phys. 27, No. 6, 397-403 (September 1959).

In this paper the quantum mechanics of an electron in a vibrating linear lattice is developed. Special attention is then given to electron-phonon resonance resulting from degenerate energy states.

1.7 A. C. Beer, "Fine Structure in the Hall Coefficient," J. Phys. Chem. Solids 8, 507-11, 530 (January 1959).

Fine structure in the Hall coefficient for non-degenerate semiconductors was found; a warping of the heavy mass band is proposed to explain the structure.

1.8 C. J. Bergeron, C. G. Grenier, and J. M. Reynolds, "Oscillatory Ettinghausen-Nernst Effect," Phys. Rev. Letters 2, No. 2, 40-1 (January 15, 1959).

Oscillations are reported in the Ettinghausen-Nernst potential. The potential is periodic in H^{-1} at liquid helium temperatures. The results for a single crystal of zinc give a period of 6.3×10^{-4} gauss $^{-1}$.

1.9 J. W. Buttrey, "Small Magnetic Field Mapping Probes in Thin Semiconducting Films," Rev. Sci. Instrum. 30, No. 9, 815-17 (September 1959).

Germanium probes having active areas of approximately 10 square microns were found to have a sensitivity of 100 oe. Results obtained on thin InSb films indicate small area probes of this material should be sensitive to fields smaller than five oersteds.

1.10 R. O. Carlson, "Electrical Properties of Mercury Telluride," Phys. Rev. 111, No. 2, 476-8 (July 15, 1958).

Contains experimental measurements of resistivity, Hall effect, thermal conductivity and thermoelectric power of polycrystalline HgTe down to liquid hydrogen temperatures. A complicated conduction band is suggested by an observed magneto-Hall effect in which the Hall coefficient depends on the magnetic field and changes sign at temperatures as low as 20° K.

1.11 R. A. Coldwell-Horsfall and D.ter Haar, "On the Hall Effect in Bismuth," Physica 24, No. 10, 848-54 (October 1958).

A theoretical calculation of the Hall coefficient in bismuth yields the correct oscillatory behavior at low temperatures but predicts a field dependence of the steady state part of the Hall coefficient proportional to H or $H^{1.3}$ whereas experiment shows an H^2 dependence.

1.12 F. Garcia-Moliner, "Magnetoresistance and Fermi Surface of Alkali Metals," Proc. Phys. Soc. 72, Pt. 6, 996-1000 (December 1958).

Theoretical results are compared with magnetoresistance measurements to determine the degree of anisotropy in the Fermi surface of the alkali metals. The elements in order of increasing anisotropy are sodium, rubidium, potassium, caesium and lithium.

1.13 J. F. Gibbons, "Hall Effect in High Electric Fields," Proc. Inst. Radio Engrs. 47, No. 1, 102 (January 1959).

Calculations are made to determine the optimum Hall voltages which can be obtained from several known semiconductors. At high electric fields a Hall voltage can be obtained which is relatively independent of temperature and gives maximum response for a given semiconductor.

1.14 K. G. Günther, "Evaporated Layers of Semiconducting III-V Compounds InAs and InSb," Z. Naturforsh. 13a, No. 12, 1081-9 (December 1958).

An evaporation method in which an exact relationship between the temperatures of the components and the substrate is given. Measurements of the Hall effect in n-type InAs films (thickness 0.5-35μ) show a dependence on crystallite size. Reasons for this dependence are discussed.

1.15 L. P. Kao and E. Katz, "Phenomenological Theory of Anisotropic Isothermal Galvanomagnetic Effects," J. Phys. Chem. Solids 6, No. 2-3, 223-35 (August 1958).

The relative orientation between the magnetic field and the crystal axes along with the effect of crystal symmetry are investigated with respect to the Hall effect and magnetoresistance. The analysis results in a tabulation of use to the experimenter in planning and interpreting galvanomagnetic measurements and in estimating errors due to misalignment.

1.16 D. K. C. MacDonald, "Magneto-Resistance in Metals," Philosophical Magazine 2, 97-104 (1957).

An anomalous behavior was noted in the magneto-resistance of sodium and rubidium. This behavior appeared to depend on the attainment of large values of the ratio ℓ/r where ℓ is the mean free path of the electrons and r is the orbital radius.

1.17 B. J. O'Brien and C. S. Wallace, "Ettinghausen Effect and Thermomagnetic Cooling," J. Appl. Phys. 29, No. 7, 1010-12 (July 1958).

The Ettinghausen effect was used to obtain a measurable cooling effect. A current was passed through a 99% Bi and 1% Pb alloy in the presence of a magnetic field of 1000 gauss. A current of 5 amperes gave a maximum cooling of 0.25° C of one end of the slab with respect to the other end in a room temperature resevoir. The cooling effect had a parabolic dependence on the current.

1.18 P. J. Price, "Theory of Transport Effects in Semiconductors: Thermoelectric," Phys. Rev. 104, 1223 (1956).

A phenomenological theory of the thermoelectric effects is developed. The formulas are applied to a two band semiconductor and the effect of a strong magnetic field and the effect of strain on the thermoelectric power are treated.

1.19 L. Reimer, "Electrical Conductivity of Evaporated Layers of Amorphous Germanium," Z. Naturforsh. 13a, No. 7, 536-41 (July 1958).

Measurements of the temperature dependence of the resistivity of amorphous Germanium films in vacuum between 20 to 400° C are made and compared with the single crystal values.

1.20 L. Reimer, "Electron Optical Investigation of the Structure of Evaporated Films of InSb," Z. Naturforsh. 13a, No. 2, 148-52 (February 1958).

Electron diffraction and macroscopy studies of 400 Å InSb films on SiO were made to determine the dependence of their structure on the temperature of the SiO during deposition. Hall effect and magnetoresistance studies were also made on films thicker than 1 micron.

1.21 J. Smit, "Hall Effect in Ferromagnetics," Nuovo Cimento Suppl. 6, No. 3, 1177-82 (1957).

Theoretical arguments showing that the extraordinary Hall coefficient is proportional to ρ^2 and thus for a perfectly periodic lattice it should equal zero. The consequences of an imperfect periodic lattice are considered. (This supplement contains many papers on magnetism.)

1.22 M. S. Steinberg, "Viscosity of the Electron Gas in Metals," Phys. Rev. 109, No. 5, 1486-1492 (March 1958).

A theoretical article in which the coefficient of shear viscosity of a free electron gas interacting with thermal phonons and local crystal inhomogeneities is computed. The effect of a transverse magnetic field is determined for the case when a time of relaxation exists.

1.23 I. M Tsidil'kovskii, "Adiabatic Galvano- and Thermo-Magnetic Phenomena in Semiconductors. I. Impurity Semiconductors," Zh. Tekh. Fiz. 28, No. 7, 1371-81 (1958)

All transverse effects vary in inverse proportion to the effective magnetic fields in strong fields while in weak fields they vary linearly with the effective magnetic fields. The Hall effect is an exception. All transverse effects with the exception of the Hall effect must show a maximum at intermediate fields. All longitudinal galvanomagnetic and thermomagnetic effects are independent of the field in the strong field case whereas they are proportioned to the square of the effective magnetic field in the weak field case. Consequently the longitudinal effects would exhibit a saturation in the intermediate field.

1.24 I. M. Tsidil'kovskii, "The Nernst-Ettinghausen Effect in Mercury Telluride," Zh. Tekh. Fiz. 27, No. 8, 1744-52 (1957).

The Nernst-Ettinghausen effect was used to determine the magnetude and temperature dependence of the ratio between the electron and hole mobilities. If a measurement of one of the mobilities is made by use of the Hall effect, the Nernst-Ettinghausen effect can be used to determine the temperature dependence of the other.

See also: I - 2.1, 3.5, 3.6, 4.11, 5.2, 5.5, 5.13, 7.3, 7.12.

Sub-Group 2 -- Photo Effects

2.1 J. Aron and G. Groetzinger, "Longitudinal Photomagnetoelectric Effect in Germanium," Phys. Rev. 100, 1128-1129 (1955).

The emf developed parallel to the gradient of light absorption (Dember emf) in a germanium crystal is reduced by the application of a transverse magnetic field. It is reduced about 10% with 5000 gauss applied. The effect is quadratic up to 2000 gauss and linear then to 4000 gauss.

2.2 M. Balkanski and R. D. Waldron, "Internal Photoeffect and Exciton Diffusion in Cadmium and Zinc Sulphides," Phys. Rev. 112, No. 1, 123-35 (October 1, 1958).

The diffusion of excitons and the accompanying energy transport was found to account for a large part of the photoconductivity of cadmium and zinc sulfide at frequencies below the absorption edge. This indirect photocurrent showed a nearly linear dependence on the incident light intensity.

2.3 R. J. Berlaga, "Photovoltaic Effects in PbS Layers," Z. Tech. Physik. 25, 1378 (1955).

E.M.F.'s of 3 volts were noted in PbS layers without previous electrical formation of the layers. The samples were made by evaporation of PbS onto glass and heating to 500-600° C in the presence of various gases.

2.4 F. C. Brown, "Transient Photoconductivity in AgCl at Room Temperature," J.Phys. Chem. Solids 4, No. 3, 206-16 (1958).

Experimental results from pulsed measurements of photoconductivity in AgCl are presented. Small photoconductivity with an electron lifetime of 10^{-8} sec or less is associated with crystals at room temperature when the crystals have been prepared so as to remove moisture and products of hydrolysis. Large photoconductivity with an electron lifetime in the order of 10^{-6} sec is associated with crystals grown in air. The presence of Ag_2O decreasing the number of electron traps is suggested as a mechanism for increasing the lifetime. No noticeable contribution to the photoconductivity by holes was observed.

2.5 G. Cheroff and S. P. Keller, "Optical Transmission and Photoconductive and Photovoltaic Effects in Activated and Unactivated Single Crystals of ZnS," Phys. Rev. 111, 98 (1958).

Experiments were performed on single crystals of ZnS and of ZnS activated with Mn, Cu, and Al. Reversals in the sign of the photovoltage were measured as a function of the wavelength of incident light.

2.6 T. Figielski, "On a Possible Explanation of Strong Photovoltaic Effects in PbS Layers," Bull. Acad. Polon. Sci. Ser. Sci. Math. Astron. Phys. 7, No. 3, 179-81 (1959).

"It is the author's opinion that the phenomenon consists in a typical photovoltaic effect on the intercrystalline boundaries, such as should occur when the latter are non-symmetrically illuminated."

2.7 W. W. Gärtner, "Depletion-Layer Photoeffects in Semiconductors," Phys. Rev. 116, No. 1, 84-86 (October 1, 1959).

The theory of photoconduction through the reverse-biased p-n junction in semiconductors is developed without the customary assumption that carrier generation in the junction depletion layer is negligible. This treatment leads to a voltage dependence of the photocurrent and its spectral distribution.

2.8 B. Goldstein and L. Pensak, "High-Voltage Photovoltaic Effect," J. Appl. Phys. 30, No. 2, 155-61 (February 1959).

A photo voltage as high as 200 volts was noted in thin films of CdTe. The film was deposited at 250° C and at an oblique angle (to the vertical). The model proposed is one of assuming the warping of the surface forms a series of photovoltaic junctions, giving a series addition of voltage. Experimental data are included. The model is not completely satisfactory.

2.9 P. Gosar, "On the Lateral Photovoltaic Effect in P-N Junctions," Compt. Rend. Acad. Sci. 247, 1975 (December 1958).

The effect is produced between two different points of the p-type part of a p-n photo-junction, or between two different points of the n-type part, simple one-dimensional considerations are given to study the effect theoretically.

2.10 E. F. Gross, "Optical Spectrum and Magneto-Optical Properties of Excitons," J. Phys. Chem. Solids 8, 172-6 (January 1959).

Measurements of the Stark effect and Zeeman effect on excitons in Cu_2O show that these excitons have extremely large diameters of the order of 1000 A. The existence of ortho and para excitons is proposed. The large diamagnetism of the excitons might result in a measurable change of the magnetic susceptibility when the crystal is irradiated in the exciton region of the spectrum.

2.11 M. Kikuchi, "Observation of the Lateral Photovoltage by Surface Field Effect," J. Phys. Soc. Japan 13, 1061 (September 1958).

With an electrode at high potential close to one side of a Ge rod and a light beam focused on the other side, a voltage is developed across the ends of the rod. The magnitude and sign of the voltage depend on the position of the light spot and on whether the Ge is n- or p-type.

2.12 B. T. Kolomiets and V. N. Larichev, "(A Contribution to) the Question of the Mechanism of Conduction and Photo-Conduction in Polycrystalline Layers of Semiconductors of the PbS Group," Zh. Tekh. Fiz. 28, No. 6, 1358-62 (1958).

The non-linearity of volt-ampere characteristics of vacuum deposited and oxygen activated layers of the PbS group were found to be temperature dependent. The existence of a quantitative relationship between the magnitude of photosensitivity and the degree of non-linearity of the volt-ampere characteristics is postulated.

2.13 M. V. Kot and G. P. Sorokin, "The Electrical Conductivity and Photoconductivity of Films of the Aluminum--Antimony System Prepared by Vekshinskii's Method," Zh. Tekh. Fiz. 28, No. 8, 1657-61 (1958).

The electrical conductivity and photoconductivity of Al-Sb films indicate the existence of a mixture of AlSb and Al_3Sb compounds. The maximum of spectral sensitivity for Al_3Sb is at 1.6 ev while the value for AlSb is 1.3 ev. The photoconductivity of Al_3Sb has a very marked increase at low temperatures.

2.14 A. Lempicki, "Anomalous Photovoltaic Effect in ZnS Single Crystals," Phys. Rev. 113, No. 5, 1204-9 (March 1, 1959).

A study was made of sixteen ZnS crystals which exhibited larger-than-usual photovoltages and several other unusual photoproperties. He felt that the information obtained helped to establish a connection between crystal disorder and the photovoltage.

2.15 A. H. Sommer, "N-Type and P-Type Conduction in Alkali-Antimonide Photoemitters," J. Appl. Phys. 29, No. 11, 1568-9 (November 1958).

A possible connection between the polarity of the charge carriers and the electron affinity is suggested. High quantum efficiency of photoemission is associated with p-type conduction. The compounds K_3Sb and Na_3Sb are n-type while Cs_3Sb and the multiple alkali antimonides are p-type.

2.16 J. Starkiewicz, L. Sosnowski, and O. Simpson, "Photovoltaic Effects in Microcrystalline Layers," Nature (letter) 158, 28 (1946).

E.M.F.'s of several volts were noted samples of PbS which had been "formed" electrically. The samples consisted of several microcrystalline layers of PbS.

2.17 S. V. Vonsovskii and A. V. Sokolov, "Photoelectric Surface Effect in Ferromagnetic Materials," Doklady Akad. Nauk SSSR 76, No. 2, 197-200 (1951). (Translation)

A theoretical paper in which it is shown that the photoelectric current and the effective work function of ferromagnetic materials depend on the magnitude of the spontaneous magnetization (see also A. B. Cardwell, Phys. Rev. 76, 125 (1949)).

See also: I - 7.26; II - 3.1.

Sub-Group 3 -- Thermal Effects

3.1 B. Abeles, "Thermal Conductivity of Germanium in the Temperature Range 300° - 1080° K," J. Phys. Chem. Solids 8, 340-3, 361-2 (January 1959).

Measurements show a pronounced contribution to the thermal conductivity of germanium at high temperatures by electrons and a consequent departure from the $1/T$ law.

3.2 S. V. Airapetyants and others, "The Mobility of Electrons and Holes in Solid Solutions Based on Lead and Bismuth Tellurides," Zh. Tekh. Fiz. 27, No. 9, 2167-9 (1957).

The thermal conductivity of a compound (used as a positive branch of a thermoelement) may be reduced without reducing the mobility of the holes by partially replacing the cations in the lattice. To obtain the same result for the negative branch of a thermoelement, the anions must be partially replaced. The effects are postulated to be more apparent in compounds which are more polar than the tellurides of bismuth and lead.

3.3 A. E. Bowley, R. Delves and H. J. Goldsmid, "Magnetothermal Resistance and Magneto-Thermoelectric Effects in Bismuth Telluride," Proc. Phys. Soc. 72, Pt. 3, 401-10 (September 1958).

Magnetoresistance was found to be proportional to H^2 except for pure n-type material at field above 7000 oersteds. The ratio of thermal resistivity to electrical resistivity remained independent of magnetic field even for the pure n-type material. A large contribution due to phonon scattering was postulated.

3.4 J. Callaway, "Model for Lattice Thermal Conductivity at Low Temperatures," Phys. Rev. 113, No. 4, 1046-51 (February 15, 1959).

A phenomenological model allows calculation of the thermal conductivity for isotropic solids at low temperatures. The thermal conductivity of natural germanium is predicted to be proportional to $T^{-3/2}$ but proportional to T^{-2} in the single isotope material. Theoretical results are found to be in reasonable good agreement for germanium in the temperature range of 2° - 100° K. Boundary scattering predominates to 5° or 6° K at which temperature the isotope scattering becomes predominant. In the region of 40° K, three phonon scattering and umklapp scattering becomes dominant.

3.5 T. H. Geballe, "Radiation Effects in Semiconductors: Thermal Conductivity and Thermoelectric Power," J. Appl. Phys. 30, No. 8, 1153-7 (August 1959).

The use of thermal conduction and thermoelectric measurements to detect lattice imperfections is discussed. Representative examples of experimental work which has been done are discussed.

3.6 T. C. Harman, J. H. Cahn and M. J. Logan, "Measurement of Thermal Conductivity by Utilization of the Peltier Effect," J. Appl. Phys. 30, 1351-9 (September 1959).

An experimental technique for the accurate measurement of thermal conductivity is described in detail. The measurements allow calculation of the absolute value of the thermoelectric power, thermal conductivity electrical resistivity, and thermoelectric figure of merit. Theory is presented for the case in which radiative heat transfer is important, but only for cylindrical samples.

3.7 J. Hori and T. Asahi, "On the Vibration of Disordered Linear Lattice," Progr. Theoret. Phys. 17, No. 4, 523-42 (April 1957).

A method for obtaining the vibrational modes of a linear lattice with several impurities located at given positions or at random is developed. Several examples of varying complexity are treated in detail.

See also: I - 6.1, 6.13, 7.6, 7.14.

Sub-Group 4 -- Acoustic Phenomena

4.1 H. E. Bömmel, "Ultrasonic Attenuation in Superconducting and Normal-Conducting Tin at Low Temperatures," Phys. Rev. (L) 100, 758 (October 1955).

Careful experiments with 99.998% pure tin single crystals showed an oscillatory behavior in the attenuation of sound with an applied magnetic field. Measurements were made at 10.3, 20, and 28 Mc/sec. The field was varied from 0 to ~ 1000 gauss.

4.2 H. E. Bömmel, "Ultrasonic Attenuation in Superconducting Lead," Phys. Rev. (L), 96, No. 1, 220-221 (October 1954).

Experimental evidence was obtained which demonstrated that electrons could contribute to the attenuation of megacycle sound waves. The importance of the electronic system was indicated by the observed change in attenuation upon crossing the superconducting transition.

4.3 Daniel H. Filson, "Low-Temperature Ultrasonic Attenuation in Tin and Aluminum," Phys. Rev. 115, 1516-19 (September 1959).

Two samples were investigated in the range of 100 Kc/s to one Mc/s, at liquid helium temperatures. High-purity tin yielded experimental

results in excellent agreement with theory. The attenuation in high-purity aluminum was proportional to the electrical conductivity but averaged 45% higher than theoretically predicted. The theory used was based on an ideal metal and predicts the attenuation is proportional to the square of the frequency and to the electrical conductivity.

4.4 T. Kjeldaas, Jr., and T. Holstein, "Oscillatory Magneto-Acoustic Effect in Metals," Phys. Rev. Letters 2, No. 8, 340-41 (April 1959).

A theoretical discussion of the magneto-acoustic oscillation which were predicted by Pippard. The oscillatory part of the attenuation arose in a Bessel type term.

4.5 Edward Lax, "Acoustic Attenuation in Aluminum Due to Electron-Lattice Interaction," Phys. Rev. 115, 1591-94 (September 1959).

The attenuation of sound due to the interaction of electrons with the lattice was measured in pure polycrystalline aluminum at low temperatures. Measurements were made from 26 to 130 Kc/s. The temperature was varied from 3° to 70° K. A detailed agreement between the shape of the attenuation and conductivity curves was obtained, but the experimental attenuation was 50% greater than could be explained by the present theory.

4.6 R. W. Morse, H. V. Bohm, and J. D. Gavenda, "Electron Resonances with Ultrasonic Waves in Copper," Phys. Rev. (L) 109, No. 4, 1394-96 (February 1958).

Measurements made on very pure polycrystalline copper at liquid helium temperatures indicated resonances with sound waves of 51.6 Mc/sec, 30.5 Mc/s and 26 Mc/s. The magnetic field was varied up to 11,000 gauss.

4.7 R. W. Morse and J. D. Gavenda, "Magnetic Oscillations of Ultrasonic Attenuation in a Copper Crystal at Low Temperatures," Phys.Rev. Letters 2, No. 6, 250-52 (March 1959).

Attenuation measurements were made of both longitudinal and shear waves at frequencies between 15 Mc/s and in magnetic fields at strengths up to 6500 gauss. Temperature was varied between 1° K and 4.2° K. Oscillatory behavior was noted in the attenuation and was in essential agreement with the model proposed by Pippard.

4.8 A. B. Pippard, "Ultrasonic Attenuation in Metals," Philosophical Magazine 46, 1104-14 (1955).

The attenuation of ultrasonic waves by conduction electrons is analyzed in terms of the free-electron model of a metal. Tentative suggestions are made as to possible explanations of the effects observed when the metal becomes superconducting.

4.9 Darrell H. Reneker, "Ultrasonic Attenuation in Bismuth at Low Temperatures," Phys. Rev. 115, 303-313 (July, 1959).

The attenuation of ultrasonic waves in bismuth was measured at frequencies between 12 and 84 Mc/s for various orientations. The magnetic field dependence of the attenuation at low temperatures exhibited three distinct oscillatory components and a saturation region at fields between 5 and 1600 oersteds.

4.10 M. S. Steinberg, "Magnetic Effects in the Attenuation of Transverse Acoustic Waves by Conduction Electron Transport," Phys. Rev. (L) 110, 772-773 (May 1958).

A theoretical discussion which predicts an attenuation which is dependent upon the square of the frequency - in the strong field limit.

4.11 G. D. Whitfield, "Theory of Electron-Phonon Interactions," Phys. Rev. (L) 2, No. 5, 204-5 (March 1959).

The theory of the interaction of electrons and acoustic phonons in nonpolar crystals is formulated in terms of a set of basis states, whose wave functions are essentially Bloch functions that deform with the lattice. The interaction may then be calculated in terms of the strain tensor. A result of the theory is a generalization of the deformation potential theorem.

See also: I - 1.6, 7.10, 7.19, 7.20.

Sub-Group 5 -- Magnetization Effects

5.1 G. A. Alers, J. R. Neighbours and H. Sato, "Dependence of Sound Velocity and Attenuation on Magnetization Direction in Nickel at High Fields," J. Phys. Chem. Solids 9, 21-7 (1959).

Changes in the velocity of transverse waves of the order of 0.1 percent were observed. A phenomenological theory based on magnetoelastic coupling is used.

5.2 J. A. Allen, "Evaporated Metal Films," Rev. Pure Appl. Chem. 4, No. 2, 133-170 (1954).

This is a general review of evaporated metal thin films, summarizing the state of the art. A total of 381 references is listed.

5.3 R. E. Behringer, "Comments on a Theory of Double Bloch Walls in Thin Films," J. Appl. Phys. 29, No. 9, 1380-1 (September 1958).

This letter comments on a theory proposed by Jan Kaczer, J. Appl. Phys. 29, 569 (1958) to explain the existence of double Bloch walls in thin (<30A) with the assumption that dipole-dipole interaction energy can be neglected.

5.4 L. C. F. Blackman, "Cooperative Magnetism in Oxide Structures. I. Antiferromagnetism and Ferromagnetism," Research 12, No. 5, 164-71 (May 1959).

This article is a review of the antiferromagnetic and ferromagnetic properties of certain oxide systems and includes a discussion of the current theories of indirect magnetic exchange interaction. It is not highly mathematical. Part II deals with ferromagnetism -- see Research, June 1959.

5.5 R. Brout and H. Suhl, "Effects of Spin-Orbit Coupling in Rare Earth Metals and in Solutions of Rare Earth," Phys. Rev. 2, No. 8, 387 (April 1959).

This letter attempts to point out the effect of spin-orbit coupling in three phenomena which occur in rare earth metals or solutions:

1) The reduction of superconducting transition temperature in dilute solutions of the rare earths in lanthanum or of rare earth compounds in $CeRu_2$ or $OsRu_2$.

2) An extra resistance of the pure metals due to spin disorder scattering.

3) An indirect exchange coupling among the ion spins in analogy with the Ruderman-Kittel mechanism of nuclear spin-spin interaction in metals.

5.6 G. A. Busch and R. Kern, "Magnetic Properties of $A^{III}B^{V}$ Compounds," Helv. Phys. Acta 32, 24-57 (March 10, 1959).

The magnetic susceptibilities of Si, GaP, GaAs, GaSb, InP, $InP_{0.2}As_{0.8}$, InAs and InSb were measured from 60° K to just below the respective melting points. The computed values differ in some cases from the experimental values.

5.7 K. Chu and J. R. Singer, "Thin Film Magnetization Analysis," Proc. Inst. Radio Engrs. 47, 1237-44 (July 1959).

A graphical method is described for analysis of the magnetization conditions of thin ferromagnetic films and for predicting the hysteresis loop shapes.

5.8 A. G. Chynoweth, "Pyromagnetic Effect: A Method for Determining Curie Points," J. Appl. Phys. 29, 563-5 (March 1958).

A dynamic technique for studying pyromagnetic effect has been developed. The change in the intensity of magnetization with temperature shows a sharp peak at Curie point.

5.9 K. Dwight, N. Menyuk and D. Smith, "Further Development of the Vibrating-Coil Magnetometer," J. Appl. Phys. 29, No. 3, 491-2 (March 1958).

This article refers to improvements which were made on the original instrument (Revs. Sci. Instr. 27, 261, 1956). The present model is shown to be within an order of magnitude of the ultimate theoretical limit.

5.10 E. E. Huber, Jr., D. O. Smith and J. B. Goodenough, "Domain-Wall Structure in Permalloy Films," J. Appl. Phys. 29, No. 3, 294-5 (March 1958).

Domain wall structure in Permalloy films in the thickness range 25 to 2000° A was studied by the Bitter technique. A new type of 180° wall was observed: the main wall was cut at regular intervals by short, right-angle "cross-ties" which terminate in free, single ends. A new model is proposed in which the axis of rotation is itself thought to rotate about the axis of the wall to give a "cork screw" configuration of spins and a large decrease in associated magnetostatic energy.

5.11 M. J. Klein and R. S. Smith, "Thin Ferromagnetic Films," Phys. Rev. 81, 378 (1951).

In this oft-cited paper the authors advance their theoretical treatment of the question of temperature dependence of spontaneous magnetization in very thin ferromagnetic films, based on the Bloch spin-wave theory. They show that the temperature dependence varies from a $T^{3/2}$ law for thick films to a linear function for two-dimensional lattices.

5.12 Y. Le Corre, "The Magnetic Crystallographic Groups and Their Properties," J. Phys. Radium 19, No. 10, 750-64 (October 1958).

Taking into account the reversal of magnetic moment, the number of crystalline classes are 122 and the number of space groups are 1,651. Some tables are given indicating which of the 122 classes can be diamagnetic or paramagnetic ferromagnetic, antiferromagnetic or piezomagnetic. It is suggested that it might be possible to influence the class of domains formed on cooling a crystal through its Curie or Néel point by suitable physical conditions, such as, for MmF_2, by cooling through the Néel point in the presence of a magnetic field and mechanical strain properly oriented.

5.13 H. Levenstein, "The Growth and Structure of Thin Metallic Films," J. Appl. Phys. 20, 306 (1949).

The author, basing his discussion on electron microscope and electron diffraction studies, reviews the influence of several factors -- melting point, rate of impingement, rate of evaporation, degree of vacuum -- on the structure of thin films of 35 metals.

5.14 Jaroslav Pačes, "Determination of Spontaneous Magnetization in the Curie Point Region," Československ. časopis pro fysiku 8, 566-574 (1958). (Translation)

An evaluation of methods for determining the spontaneous magnetization in the vicinity of the Curie point. The methods considered are: (1) that of even phenomena, i.e., square dependence of certain phenomena upon magnetization; (2) that of lines of equal magnetization; (3) that of anomalies of nonmagnetic properties; and (4) that of thermodynamic coefficients.

5.15 E. W. Pugh, "Completely Nonmagnetic Alloy for Instrumentation in Magnetic Fields," Rev. Sci. Instrum. 29, No. 12, 1118-19 (December 1958).

This article describes the techniques used in fabricating a nonmagnetic alloy from ultra-pure copper and nickel (Cu-96.3%; Ni-3.7%) which is almost field independent down to 2° K.

5.16 S. Yamaguchi, "Magnetic Perturbation of Cathode Rays," Nuovo Cimento 10, No. 4, 714-17 (November 16, 1958).

Reports on observations of the splitting of an electron beam upon penetration of a magnetic sample due to polarization and the effect of the exchange force between spins of the incident electrons and the oriented spins of the magnet.

See also: I - 1.21, 2.17; III - 1.4.

Sub-Group 6 -- Semiconductor Effects

6.1 B. N. Brockhouse, "Lattice Vibrations in Silicon and Germanium," Phys. Rev. Letters 2, No. 6, 256-57 (March 1959).

Measurements were made with neutrons of 1.900, 1.350, and 1.693 Å wavelengths. Values of important frequencies (units 10^{12} cps) are: Raman (q = o) 15.3 ± .3, TO [001] 14.2 ± .3, L [001] 11.9 ± .5, TA [001] 4.35 ± .15.

6.2 A. R. Calawa, R. H. Rediker, B. Lax and A. L. McWhorter, "Magneto-Tunneling in InSb," Phys. Rev. Letters 5, No. 2, 55 (July 1960).

Studies were made on InSb junction diodes which exhibit Esaki characteristics. Current vs voltage plots were made at 77° K with applied magnetic fields ranging up to 88,000 gauss. A marked decrease in the tunneling current was noted with increasing field. An expression for the rate of Zener tunneling per cc, in the presence of a magnetic field, was given.

6.3 A. G. Chynoweth, W. L. Feldmann, C. A. Lee, R. A. Logan, G.L. Pearson and P. Aigrain, "Internal Field Emission at Narrow Silicon and Germanium P-N Junctions," Phys. Rev. 118, No. 2, 425-434 (April 1960).

Experiments were performed on narrow junctions of Si and of Ge. The results tend to verify the expressions for the Zener current which were given by Keldysh (JETP 6, 763, and 7, 665 (1958)).

6.4 A. G. Chynoweth and K. G. McKay, "Internal Field Emission in Silicon P-N Junctions," Phys. Rev. 106, 418-426 (May 1957).

This article provides positive experimental proof of the existence of internal field emission in narrow silicon p-n junctions.

6.5 A. G. Chynoweth, G. H. Wannier, R. A. Logan and D. E. Thomas, "Observation of Stark Splitting of Energy Bands by Means of Tunneling Transitions," Phys. Rev. Letters 5, No. 2, 57 (July 1960).

Experiments on InSb p-n junctions, which exhibit tunneling, seem to verify G. H. Wannier's theory that the energy states available to an electron in a crystal form a series of stark ladders if a uniform electric field is present.

6.6 R. N. Hall, J. H. Racette, and H. Ehrenreich, "Direct Observation of Polarons and Phonons During Tunneling in Group 3-5 Semiconductor Junctions," Phys. Rev. Letters 4, No. 9, 456-457 (May 1960).

Electrical measurements made on Group 3-5 semiconductor junctions at 4.3° K showed a structure on the current vs voltage characteristic. This structure was correlated with the polar electron-phonon coupling constant.

6.7 N. Holonyak, Jr., I. A. Lesk, R. N. Hall, J. J. Tiemann, and H. Ehrenreich, "Direct Observations of Phonons During Tunneling in Narrow Junction Diodes," Phys. Rev. Letters 3, 167-168 (August 1959).

Observation of the current vs voltage characteristics of silicon junction diodes, which exhibit tunneling, at 4.2° K revealed the effect of phonon assistance to the tunneling current. Certain Germanium diodes also exhibited this effect.

6.8 E. O. Kane, "Zener Tunneling in Semiconductors," J. Phys. Chem. Solids 12, No. 2, 181-188 (1960).

A theoretical article which arrives at an expression for the Zener current in a constant field. The results are compared to those obtained by Keldysh (JETP 6, 763 (1958)).

6.9 L. V. Keldysh, "Influence of the Lattice Vibrations of a Crystal on the Production of Electron-Hole Pairs in a Strong Electrical Field," Soviet Phys. JETP 7, (34) No. 4, 665-669 (October 1958).

A theoretical article in which the probability for the production of an electron-hole pair in a semiconductor in a strong electrical field is calculated taking into account the electron-phonon interaction. The calculations show an appreciable temperature dependence at low temperatures.

6.10 L. V. Keldysh, "Behavior of Non-Metallic Crystals in Strong Electric Fields," Soviet Phys. JETP 6 (33) No. 4, 763-770 (April 1958).

A theoretical article in which an expression is obtained for the number of electron-hole pairs generated in a semiconductor by a uniform electric field. An essential fact is that, in the absence of electron-phonon collisions and collisions between electrons, the magnitude of the effective potential barrier is determined not by the width of the forbidden band, but by the lower edge of optical absorption (the interal photoeffect).

6.11 V. S. Kogan and B. Ya Pines, "On the Method of Obtaining Alloys of Varying Concentration," Zhurnal Tekhnicheskoy Fiziki 18, No. 3, 377-382 (1948).

Contains pertinent criticisms of the evaporation method for obtaining varying concentrations of an alloy and practical suggestions for improving the usefulness of the method. (Translation)

6.12 P. T. Landsberg, "Solid State Physics," Nature 182, 567-8 (August 30, 1958).

A resume of the solid state conference at Brussels in June of 1958 is given. Subjects which invoked considerable discussion were 'hot electrons in a lattice, narrow semiconductor junctions with high impurity concentrations, adsorption on semiconductor surfaces, properties of silicon, and properties of tellurides.

6.13 H. Palevsky, D. J. Hughes, W. Kley, and E. Tunkelo, "Lattice Vibrations in Silicon by Scattering of Cold Neutrons," Phys. Rev. Letters 2, No. 6, 258-259 (March 1959).

The use of subthermal neutron scattering indicated peaks the numbers of phonons at 61.5×10^{-3} ev and 20.4×10^{-3} ev which correspond to optical and acoustical respectively. This data is essentially in agreement with Brockhouse's results.

6.14 E. Saur and E. Unger, "Spectro-Analytical Investigation of the Evaporation Process of Binary Alloys," Z. Naturforsh. 13a, No. 2, 72-9 (February 1958).

Samples of several binary alloys were evaporated at constant temperature and condensed onto a number of substrates in succession. From weighing and spectrographic analysis of the films, the decomposition rate during evaporation was found and then compared with that determined theoretically from the known vapor pressure of the components and Raoult's law.

6.15 M. Tsuboyana, "Application of Evaporation in Preparation of Germanium P-N Junction," Inst. Elec. Engrs. Japan--J. 78, No. 840, 1181-6 (September 1958).

Discusses the fabrication of p-n junctions on germanium by evaporation of indium and alloying. In addition, junctions were formed by bombarding a heated sample of n-type Germanium (5Ω cm, 540° C) with 50,000 V electrons obtaining a breakdown voltage of the order of 350 V.

6.16 V. N. Vertsner and L. N. Malahov, "Study of the Microdistribution of Electric Fields by Using Electron Optics," Optika i Spektroskopiya 3, No. 6, 649-652 (1957). (Translation).

A report on studies of the microdistribution of potential on semiconductor surfaces by the shadow electron microscope method.

6.17 G. H. Wannier, "Possibility of a Zener Effect," Phys. Rev. (L) 100, 1227 (1955).

A theoretical discussion which attempted to show that high electric fields modify the band structure of the crystal so that in reality the "Zener" current is due to a metallic conduction - i.e., the gap is closed.

6.18 S. Yamaguchi, "On the Conducting Film of Titanium Dioxide," Nuovo Cimento 11, 876 (March 16, 1959).

Films (~300 Å thick) of TiO_2, formed by evaporation of titanium and subsequent oxidation, were examined by reflection electron diffraction. They exhibited preferred orientation; they have a rutile structure] and they are conducting.

See also: I. 1.1, 1.3, 1.7, 1.9, 1.13, 1.14, 1.18, 1.19, 1.20, 1.23, 2.1, 2.3 2.6, 2.7, 2.8, 2.9, 2.11, 2.12, 2.14, 2.15, 2.16, 5.6, 7.4, 7.5, 7.8.

Sub-Group 7 -- Energy Band Phenomena

7.1 E. N. Adams, "Definition of Energy Bands in the Presence of an External Force Field," Phys. Rev. 107, No. 3, 698-701 (August 1957).

A theoretical calculation of the "physical energy bands" for an electron moving in a periodic potential perturbed by a weak electric field. These bands differ from the energy bands which exist in the absence of external field. The calculations are an extension of Wannier's (Phys. Rev. 100, 1337 (1955) and 101, 1835 (1956)).

7.2 M. Ya. Azbel' and E. A. Kaner, "Cyclotron Resonance in Metals," J. Phys. Chem. Solids 6, No. 2-3, 113-35 (August 1958).

A theoretical analysis of cyclotron resonance in metals shows that the shape of the Fermi surface can be deduced from the form and half-width of the resonance curve and from the anisotropy of the effect. A detailed tabulation is made of the information about a metal which can be obtained from a study of cyclotron resonance.

7.3 William Band, "New Look at the Theory of Electron-Phonon Resonance. II.," Am. J. Phys. 27, 471-477 (1959).

"The perturbation theory of the transitions between electron-phonon resonance states, developed in Part I (Am. J. Phys. 27, 397 (1959)), is here generalized to the many-electron problem, and applied to a discussion of the electrical conductivity of a linear lattice."

7.4 F. Bassani, "Energy Bands in Silicon Crystals," Nuovo Cimento 13, No. 1, 244-5 (July 1959).

Calculation is made of the energy values at two points of the reduced zone, the point, $k = 2_{\pi a}-1$ (1/2, 1/2, 1/2), and the point, $k = 2_{\pi a}-1$ (1/2, 0, 0).

7.5 J. L. Birman, "Electronic Energy Bands in ZnS: Potential in Zincblende and Wurtzite," Phys. Rev. 109, No. 3, 810-17 (February 1, 1958).

A cellular calculation is made on electronic energy bands in zinc sulfide. An effective charge of 1/2 is assumed for zinc and -1/2 for sulfur. This assignment of charge implied approximately 1/3 of the band character to be covalent. Since the zincblende and wurtzite structers are similar many of the linear combination of atomic orbital integrals are identical for the two structures.

7.6 B. N. Brockhouse and A. T. Stewart, "Normal Modes of Aluminum by Neutron Spectrometry," Rev. Modern Phys. 30, No. 1, 236-249 (January 1958).

A review article which describes in detail the neutron spectrometry method of studying lattice vibration.

7.7 H. Brooks and F. S. Ham, "Energy Bands in Solids--The Quantum Defect Method," Phys. Rev. 112, No. 2, 344-61 (October 15, 1958).

A detailed account of the quantum defect method for calculating electron energy bands in solids from spectroscopic data for the corresponding free atom is given. The quantum defect method makes direct use of available tables of coulomb wave functions. Arguments are presented to show that the quantum defect method takes account of correlation and exchange effects in the interaction between a valence electron and the ion cores. The method is advanced as a valuable tool in calculations involving the heavy elements because it includes relativistic effects and spin orbit coupling.

7.8 E. Burstein, G. S. Picus, R. F. Wallis, and F. Blatt, "Zeeman-Type Magneto-Optical Studies of Interband Transitions in Semiconductors," Phys. Rev. 113, No. 1, 15-33 (January 1, 1959).

The effect of a magnetic field on the band structure of a single semiconductor is discussed theoretically in terms of the Landon levels. The Luttinger-Kohn theory is used to obtain selection rules for electronic transitions in the presence of a magnetic field. Room temperature experimental results for the IMO effect in germanium are reported and compared with theory. Experimental criteria for observing well defined absorption in IMO spectra are discussed. These criteria include a consideration of (1) broadening versus peak separation, (2) sample thickness versus absorption constant, (3) instrument resolving power in temp. of band gap and level separation, and (4) carrier concentration in the sample.

7.9 R. R. G. Chambers, "Our Knowledge of the Fermi Surface," Can. J. Phys. 34, 1395 (1956).

A review is presented on magnetoresistance, cyclotron resonance, the anomalous skin effect, and the de Haas-van Alphen effect as related to the Fermi surface.

7.10 Michael J. Harrison, "Magneto-Attenuation of Sound in Semimetals: Longitudinal Waves," Phys. Rev. 119, No. 4, 1260-69 (August 1960).

The calculation of the magnetic field dependence of ultrasonic attenuation in a semimetal is discussed on a simple model of its band structure. The results obtained are analogous to those obtained previously for metals.

7.11 L. Huldt and T. Staflin, "Valence Band Structure of Silicon," Phys. Rev. 1, No. 9, 313-15 (November 1, 1958).

The technique of photogeneration of free carriers was used to excite and observe an absorption spectra in silicon in a wavelength region which is complicated by the lattice vibrations of silicon. The technique may be extended to detection of absorption due to impurity states at room temperature.

7.12 C. Kittel, "Energy Absorption by Charge Carriers of Negative Effective Mass in Crystals," Proc. Nat. Acad. Sci. U.S.A. 45, No. 5, 744-7 (May 1959).

A system of charge carriers all of negative effective mass cannot exist in thermal equilibrium. The electrical resistivity is always positive in thermal equilibrium. The use of the negative resistance characteristics of negative mass regions of wave vector space to construct amplifiers will require auxiliary sources of energy to maintain nonequilibrium carrier distributions.

7.13 T. Kjeldaas, Jr., "Theory of Ultrasonic Cyclotron Resonance in Metals at Low Temperatures," Phys. Rev. 113, No. 6, 1473-8 (March 15, 1959).

Theoretical investigation of the propagation characteristics of circularly polarized acoustic shear waves as a function of a magnetic field applied parallel to the direction of propagation and how it can reveal information about the band structure of metals. Treatment is based on the combined solution of Boltzmann's and Maxwell's equations for a free-electron model.

7.14 W. Kohn, "Image of the Fermi Surface in the Vibration Spectrum of a Metal," Phys. Rev. 2, No. 9, 393-4 (May 1959).

A brief theoretical discussion of the possibility of determining the shape of the Fermi surface from lattice vibration spectra.

7.15 H. Kromer, "The Physical Principles of a Negative-Mass Amplifier," Proc. Inst. Radio Engrs. 47, No. 3, 397-406 (March 1959).

Discussion of the physical properties required of a semiconductor crystal to obtain wave amplification by means of "negative-mass" carriers. An electric field is proposed as the means by which the negative mass is obtained. Some design problems are discussed.

7.16 R. W. Morse, A. Myers and C. T. Walker, "Fermi Surfaces of Gold and Silver From Ultrasonic Attenuation," Phys. Rev. Letters 4, No. 12, 605-607 (June 15, 1960).

Experiments, which made use of the low-temperature magnetic dependence of ultrasonic attenuation, have shown that the Fermi surfaces in gold and silver contact the zone boundary. The size and shape of the contact area were determined in the gold.

7.17 N. F. Mott and K. W. H. Stevens, "The Band Structure of the Transition Metals," Philosophical Magazine 2, 1364-1386 (1957).

This paper proposes a model for the electronic structure of the transition metals with particular emphasis on the difference between the body-centered structure and the close-packed. The relation between the structure and the electrical and magnetic properties is discussed.

7.18 L. G. Parratt, "Electronic Band Structure of Solids by X-Ray Spectroscopy," Rev. Mod. Phys. 31, No. 3, 616-45 (July 1959).

This is a fairly detailed paper on the determination of electronic band structure of all types of solids from x-ray absorption and

emission spectra. Experimental problems are discussed and interpretations of some experimental results are given.

7.19 J. C. Phillips, "Cyclotron Resonance in Metals," Phys. Rev. 3, 327-8 (October 1959).

The purpose of this letter is to elaborate on an idea proposed by Chambers (Can. J. Phys. 34, 1395 (1956)) and Heine (Phys. Rev. 107, 431 (1957)) to explain the results obtained for H nearly parallel to the surface of the metal and to extend this idea to give a qualitative explanation of the masses observed with H normal to the surface of the metal.

7.20 A. B. Pippard, "A Proposal for Determining the Fermi Surface by Magneto-Acoustic Resonance," Philosophical Magazine 2, 1147-1148 (1957).

The proposal is made that the periodic attenuation of ultrasonic sound, which is noted in pure metals at low temperature and in a magnetic field, is a geometrical resonance and as such can give information about the Fermi surface.

7.21 B. W. Roberts, "Magnetoacoustic Oscillations and the Fermi Surface in Aluminum," Phys. Rev. 119, No. 6, 1889-96 (September 1960).

Measurements of magnetoacoustic attenuation in very pure aluminum have been made with 10 to 100 Mc/s longitudinal sound waves in magnetic fields up to 9200 oe at 4.2° K.

7.22 S. Rodriques, "Theory of Cyclotron Resonance in Metals," Phys. Rev. 112, No. 5, 1616-20 (December 1, 1958).

The Boltzmann transport equation in conjunction with Maxwell's equations for the microwave field is solved. The electrons are assumed to have an isotropic effective mass and to constitute a degenerate Fermi gas. In the extreme anomalous skin region, the surface impedances for longitudinal and transverse cyclotron resonance are the same.

7.23 A. C. Rose-Innes, "Observation by Cyclotron Resonance of the Effect of Strain on Germanium and Silicon," Proc. Phys. Soc. 72, Pt. 4, 514-22 (October 1958).

Cyclotron resonance is used to investigate the effect of a non-isotropic strain on the conduction band edges in germanium and silicon. The results are in agreement with Herring's interpretation of piezoresistance measurements. The minima of the conduction band which lie on a direction in momentum space parallel to the elongation of the crystal are raised in energy and those in a direction of compression are lowered.

7.24 V. P. Shirokovskii, "Electron States in Crystals," Fiz. Metal. i Metalloved., Akad. Nauk SSSR, Ural. Fibal 6, No. 1, 3-14 (1958). (Translation)

Generalized group theory arguments are used to determine those properties of the electron energy spectrum which result directly from the space symmetry of the periodic potential alone. The spectrum and electron states in one and two dimensional lattices are investigated in detail.

7.25 V. Sergiescu, "A Statistical Proof of the Cyclic Conditions in the Zone Theory of Crystals," Acad. rep. populare Romîne, Inst. fiz., Studii cercetari fiz. 9, No. 4, 459-463 (1958). (Translation)

A statistical mechanical justification for the use of the cyclic boundary conditions.

7.26 George E. Smith, "Anomalous Skin Effect in Bismuth," Phys. Rev. 115, 1561-1568 (September 1959).

High frequency (23.5 KMc/s) surface resistance measurements have been made on plane surfaces of single-crystal bismuth at 2° K as a function of orientation. It was ascertained that extreme anomalous skin effect conditions were present which allowed details of the Fermi surface to be deduced from Pippard's theory.

7.27 S. Zwerdling, B. Lax, L. M. Roth and K. J. Button, "Exciton and Magneto-Absorption of the Direct and Indirect Transitions in Germanium," Phys. Rev. 114, No. 1, 80-9 (April 1, 1959).

Low temperature, high resolution experiments on magneto-absorption effects in germanium revealed fine structure in the interband transitions. A magnetic field of 38.9 kilogauss was used.

7.28 E. M. Conwell, "Properties of Silicon and Germanium: II," Proc. I.R.E. 46, No. 6, 1281-1300 (June 1958).

A review article which discusses some of the more recent findings in the study of silicon and Germanium. This article includes a very extensive bibliography.

7.29 V. Glaser and B. Jakšic, "On the Methods of Solution of the Block Integral Equation at Low Temperatures," Glasnick Mat. Fiz. i. Astr. 12, No. 4, 257-266 (1957). (Translation).

7.30 R. R. Haering, "Band Structure of Rhombohedral Graphite," Canad. J. Phys. 36, No. 3, 352-62 (March 1958).

The nearest neighbor tight binding approximation was used to determine the band structure of rhombohedral graphite. Measurements of the de Haas-van Alphen effect as a function of orientation of the magnetic field is required for more detailed interpretation of the results.

See also: I - 1.7, 1.10, 6.5; II - 3.3.

Sub-Group 1 -- Mechanical Effects

1.1 F. P. Burns and A. A. Fleischer, "Piezoresistive Effect in Indium Antimonide," Phys. Rev. 107, 1281-2 (September 1, 1957).

Room-temperature measurements on the variation of resistivity of pure InSb with hydrostatic and uniaxial stress were made to determine the piezoresistive and elastoresistive coefficients.

1.2 V. Gh. Neaga and V. I. Antonescu, "A New Method for the Measurement of Vacuum, the Electroacoustic Vacuum Gauge," Analele stient univ. "Al. I. Cuza" Iasi, Sect. I, 3 No. 1-2, 281-286 (1957). (Translation).

A description of an acoustic vacuum gauge for the range from atmospheric pressure down to 5 mm Hg.

Sub-Group 2 -- Electrical Effects

2.1 R. Bersohn, "Electric Field Gradients in Ionic Crystals. I. Nuclear Quadrupole Coupling Constants," J. Chem. Phys. 29, No. 2, 326-33 (August 1958).

In ionic crystals and metals the coupling constant of a quadrupolar nucleus can often be written in the simplified form $eQ(\Delta\epsilon)(1-\gamma_\infty)$. The polarization factors $(1-\gamma_\infty)$ were calculated previously. When Q is known by other means, information about the distribution of charges in crystals may be obtained. The agreement between experimental and observed coupling constants proves that the field gradients in ionic crystals and metals are of long-range origin in contrast to molecular crystals.

2.2 S. D. Chatterjee and S. K. Sen, "Induced Conductivity at the Surface of Contact Between Metals," Phil. Mag. 3, 839-52 (August 1958).

Properties of alkali metals in contact with metals such as aluminum are investigated. Experiments on the electrical properties of the contact are in agreement with the production of an intermediate oxide layer.

2.3 J. J. Hopfield, "Theory of the Contribution of Excitons to the Complex Dielectric Constant of Crystals," Phys. Rev. 112, No. 5, 1555-67 (December 1, 1958).

A quantum-electrodynamical formalism is applied to the calculation of the contribution of excitons to the complex dielectric constant of crystals. The fundamental absorption process is considered as an exciton forming an intermediate state between the photon and the final energy absorbing states. More information on exciton wave functions and the exciton-lattice interaction is necessary to make satisfying calculations on the basis of the theory.

3.1 R. H. Bube, "Optc-Electronic Properties of Mercuric Iodide," Phys. Rev. 106, 703-17 (May 15, 1957).

The effect of the phase transformation of HgI_2 from tetragonal to orthorhombic on the optical, photoelectric and other properties is described.

3.2 K. J. Button, L. M. Roth, W. H. Kleiner, S. Zwerdling and B. Lax, "Fine Structure in the Zeeman Effect of Excitons in Germanium," Phys. Rev. Letters 2, No. 4. 161-2 (February 15, 1959).

Exciton formation observed in the study of indirect transitions in Ge produced two strong absorption edges at zero magnetic field and .75 ev photon energy. The application of magnetic field shifted the peaks up in energy and also produced a number of superimposed lines.

3.3 W. P. Dumke, "Indirect Transitions at the Center of the Brillouin Zone with Application to InSb and a Possible New Effect," Phys. Rev. 108, 1419-25 (December 25, 1957).

The theory of indirect optical transitions is extended to the case where both the valence and conduction band extrema occur at the center of the Brillouin zone. A new effect is predicted involving the modulation of the indirect absorption constant by the selective excitation of the long wavelength optical modes.

3.4 R. J. Elliott, T. P. McLean and G. G. Macfarlane, "Theory of the Effect of a Magnetic Field on the Absorption Edge in Semiconductors," Proc. Phys. Soc. 72, Pt. 4, 553-65 (October 1958).

Selection rules are found for direct transitions in the presence of a magnetic field for spherical bands. The effect of degeneracy is investigated. Indirect transitions are found to give rise to a series of steps in the absorption. Between each step the absorption is roughly a constant and proportional to the square of the magnetic field.

3.5 V. N. Filimonov, "Electronic Absorption Bands of ZnO and TiO_2 in the Infrared Region of the Spectrum," Optika i Spektroskopiya 5, No. 6, 709-711 (1958). (Translation)

Irradiation of zinc oxide and titanium dioxide in the intrinsic absorption region or heating in vacuum causes the appearance of an absorption band in the infrared. These effects are said to be due to changes in the amount of surface-adsorbed oxygen and corresponding changes in the electron concentrations in the bulk.

3.6 V. L. German and E. A. Kaner, "Optical Activity with Account Being Taken of the Nonlinear 'Saturation' Effect," Optika i Spektroskopiya 3, No. 1, 68-72 (1957). (Translation).

The nonlinear "saturation" effect in radio spectroscopy refers to the rapid variation of the microwave absorption coefficient with incident intensity near resonance and to the fact that the absorbed energy does not change above certain high levels of intensity. The effect is present in the optical frequency range also. In addition similar nonlinear effects should occur for optical activity and circular dichroism. This paper is a contribution to the theory of these effects.

3.7 N. M. Gudris and I. N. Shul'ts, "Optical Absorption by $PbCl_2$ with a Stoichiometric Excess of Metal or Halogen," Optika i Spektroskopiya 3, No. 3, 246-250 (1957). (Translation)

The results of an investigation on the optical absorption by $PbCl_2$ films heated in vapors of various metals and chlorine or irradiated with x-rays. New absorption bands appear.

3.8 L. Huldt and T. Staflin, "Optical Constants of Evaporated Films of Zinc Sulphide and Germanium in Infra-Red," Optical Acta 6, No. 1, 27-36 (January 1959).

Optical constants of evaporated films of ZnS and Ge were determined from transmission, reflectance, and brewster angle measurements. The optical constants are found to be fundamentally changed by the addition of oxygen.

3.9 M. A. Jeppesen, "Some Optical, Thermo-Optical, and Piezo-Optical Properties of Synthetic Sapphire," J. Opt. Soc. Amer. 48, No. 9, 629-32 (September 1958).

The ordinary and extraordinary refractive indexes of Al_2O_3 were determined by the method of minimum deviation. The temperature dependence of the refractive index and the temperature coefficient of birefringence were determined.

3.10 W. F. Koehler, F. K. Odencrantz and W. C. White, "Optical Constants of Evaporated Selenium Films by Successive Approximations," J. Opt. Soc. Amer. 49, No.2, 109-115 (February 1959).

Precise measurements of the absorption constant and the refractive index were made on evaporated selenium films in the wavelength range of 0.24 to 2.5 microns. Uniformity of the thickness of the films was a result of rotating the optically flat substrates during evaporation and floating chips of fused quartz on the liquid selenium surface to prevent the bursting of large bubbles.

3.11 V. K. Miloslavskii, "Optical Properties of Thin Layers of Cadmium Oxide in the Infrared Region of the Spectrum," Optika i Spektroskopiya 3, No. 3, 251-257 (1957). (Translation).

Cadmium oxide films formed by reactive sputtering were studied to relate electrical conductivity to optical absorption. Comparison of the results with the free electron theory was made.

3.12 P. Srivastava, "Renninger Effect in Naphthazarin," Indian J. Phys. 33, 123-6 (March 1959).

The Renninger Effect (Zeit f'. Kristallogr. 97, 1957) which is a double reflection was noted in the study of the space group in naphthazarin. Both graphical and analytical analyses are given. It (the double reflection) is ascribed to double reflection from three pairs of strong planes. This was a study made by x-ray diffraction.

3.13 M. J. Stephen and A. B. Lidard, "The Faraday Effect in Semiconductors," J. Phys. Chem. Solids 9, 43-7 (1959).

A theoretical paper in which a general expression for the Faraday rotation as a function of frequency and magnetic field strength is derived.

3.14 E. Toma, I. Teodorescu, and G. Hollos, "Optical and Electron-Diffraction Study of Gold-Tin Alloys Deposited by Simultaneous Evaporation," Acad. rep. populare Romine, Inst. fiz., Studii cercetare fiz. 10, No. 1, 63-73 (1959). (Translation)

By simultaneous evaporation from a pair of filaments separated from each other a range of concentrations of gold and tin was obtained on a microscope slide. From the reduced optical reflectivity at certain concentrations one can deduce the presence of intermetallic compounds which have a nonmetallic character.

Sub-Group 4 -- Transport Phenomena

4.1 S. A. Moskalenko, "Mott Exciton Theory in Alkali Halide Crystals," Optika i Spektroskopiya 5, No. 2, 147-155 (1958). (Translation).

A theoretical paper on Mott's many-electron exciton theory in alkali halide crystals.

See also: I - 2.2.

GROUP III

Sub-Group 1 -- Resonance Effects

1.1 V. A. Arkhangel'skaya and P. P. Feofilon, "Zeeman Effect of Anisotropic Centers in a Cubic Crystal Lattice," Optika i Spektroskopiya 4, No. 5, 602-619 (1958). (Translation)

Magnetic splitting of spectral lines due to trivalent rare earth metal ions introduced into a synthetic fluorite crystal was investigated. An investigation of this sort enables one to establish the

orientation of the separate anisotropic centers with respect to the symmetry axes of the crystal.

1.2 G. M. Androes and W. D. Knight, "Nuclear Magnetic Resonance in Superconducting Tin," Phys. Rev. Letters 2, No. 9, 386-7 (May 1959).

NMR measurements were made on samples of very small particles (or platelets) 40 Å thick and 140 Å diameter, at temperatures and magnetic fields below the critical ones for superconductivity.

1.3 L. Liebermann, "Acoustical Absorption Arising from Molecular Resonance in Solids," Phys. Rev. 113, No. 4, 1052-5 (February 15, 1959).

Resonance phenomena resulting in anomalously high acoustic absorption can occur whenever lattice and internal molecular vibrational frequencies overlap. Significant effects are predicted at all acoustic frequencies, without restriction to the resonance region.

1.4 M. H. Seavey, Jr. and P. E. Tannenwald, "Direct Observation of Spin-Wave Resonance," Phys. Rev. Letters 1, No. 5, 168-9 (Sept. 1, 1958).

The microwave absorption spectrum at 8890 Mc/sec for a 80% - 20% permalloy film of 5600 Å thickness is given. The spectrum agrees with the theoretical results for spin wave resonance.

1.5 S. Yatsiv, "Multiple Quantum Transitions in Nuclear Magnetic Resonance," Phys. Rev. 113, No. 6, 1522-38 (March 15, 1959).

The theory of Bloch and Wangsness for nuclear magnetic resonance signals is applied to multiple-quantum transitions. A method of enhancing multiple transitions by audio-modulating the rf field is described. Other references: Anderson, W. A., Phys. Rev. 104, 850 (1956). Kaplan, J. I. and Meiboom, S., Phys. Rev. 106, 499 (1957). Hughes, V. W. and Geiger, J. S., Phys. Rev. 99, 1845, (1954).

See also: IV - 1.1.

Sub-Group 2 -- Devices

2.1 N. Bloembergen, "Solid State Infrared Quantum Counters," Phys. Rev. 2, No. 3, 84-5 (February 1, 1959).

This letter compares the infrared quantum-mechanical amplifier with the maser. It shows the similarities and the differences. The model for the solid counter was proposed by Weber (Phys. Rev. 108, 537).

2.2 R. H. Hoskins, "Two-Level Maser Materials," J. Appl. Phys. 30, 797 (May 1959).

Experiments with two-level masers using paramagnetic ions in ionic crystals show that the spin-lattice relaxation time is the same as obtained by CW saturation methods. A two level ruby maser was operated at X band at liquid helium temperatures. It is suggested that the crystalline field splitting of the magnetic energy levels inherent in ionic crystals might be used to lessen the magnetic field requirements of two level solid state maser. An alternate scheme using multiple energy level materials is proposed to overcome the limitation on the repetition rate of two-level masers.

2.3 A. L. Schawlow and C. H. Townes, "Infrared and Optical Masers," Phys. Rev. 112, No. 6, 1940-9 (December 15, 1958).

A fairly detailed discussion of the possibility of obtaining masers which operate at optical frequencies. The use of multimode cavities is discussed. An illustrative example is developed using potassium vapor. Solid state applications and high frequency limits are discussed.

2.4 S. Yatsiv, "Role of Double-Quantum Transitions in Masers," Phys. Rev. 113, No. 6, 1538-40 (March 15, 1959).

A generalized discussion of a three-level maser is treated. Advantage lies in the fact that population inversion is not as difficult to achieve. Certain requirements limit its use at microwave frequencies. The frequency of operation is also temperature sensitive.

GROUP IV

Miscellaneous Techniques

1.1 S. S. Charmatti, K. J. Sundara Rao, and R. Vijayaraghavan, "Construction and Working of a Wide Line Nuclear Magnetic Resonance Spectrometer and the Measurements of Some Chemical Shifts," Nuovo Cimento 11, 656-69 (March 1, 1959).

The chemical shifts of O^{17} resonance in several compounds was measured. The results were interpreted in terms of CO bond character in various groups of organic compounds.

See also: I - 5.5, 5.9, 5.13, 5.15, 6.12, 6.14, 6.15, 6.16; II - 1.2.

☆ U.S. GOVERNMENT PRINTING OFFICE: 1961 O - 608607